

## TECHNICAL REPORT STANDARD PAGE

<b>1. Report No.</b> <b>FHWA/LA.03/380</b>	<b>2. Government Accession No.</b>	<b>3. Recipient's Catalog No.</b>
<b>4. Title and Subtitle</b> Evaluation of Interaction Properties of Geosynthetics in Cohesive Soils: Lab and Field Pullout Tests	<b>5. Report Date</b> January 2004	
	<b>6. Performing Organization Code</b>	
<b>7. Author(s)</b> Khalid Farrag, Ph.D., P.E. & Mark Morvant, P.E.	<b>8. Performing Organization Report No.</b> 380	
<b>9. Performing Organization Name and Address</b> Louisiana Transportation Research Center 4101 Gourrier Ave. Baton Rouge, LA 70808	<b>10. Work Unit No.</b>	
	<b>11. Contract or Grant No.</b> State Project No. 736-99-0658	
<b>12. Sponsoring Agency Name and Address</b> Louisiana Department of Transportation and Development Louisiana Transportation Research Center 4101 Gourrier Ave. Baton Rouge, LA 70808	<b>13. Type of Report and Period Covered</b> Final Report July 1997 – December 2003	
	<b>14. Sponsoring Agency Code</b> 92-4GT	
<b>15. Supplementary Notes</b> <b>Conducted in Cooperation with the U.S. Department of Transportation, Federal Highway Administration</b>		
<b>16. Abstract</b> <p>The considerable increase of using geosynthetics in mechanically stabilized earth (MSE) walls has raised the need to evaluate their interface shear strength and pullout properties in various types of backfills. This report investigates the use of a marginal silty-clay soil of medium plasticity as a suitable backfill in MSE walls. The interface parameters between the geosynthetics and the soil were evaluated in pullout tests. The testing program included performing laboratory and field pullout tests on four types of geogrids and three types of geotextiles. Laboratory pullout tests were carried out using the large pullout testing equipment at the Louisiana Transportation Research Center (LTRC). Field pullout tests were performed in a test section of the LTRC full-scale reinforced test wall. The pullout test section contained geogrid and geotextile specimens at various wall elevations.</p> <p>The testing program evaluated the effect of reinforcement type, length, and confining pressure on the pullout resistance. Laboratory and field tests were performed using the same type of soil at a similar density and moisture content. Laboratory and field results compared well for the extensible reinforcements of medium to low stiffness modulus. However, field pullout results were significantly higher than laboratory results for the rigid geogrids.</p> <p>The pullout resistance factor (<math>F^*</math>) and the scale effect correction factor (<math>\alpha</math>) were established for the geogrid and geotextile specimens. These values can be used to determine the pullout resistance of these types of geosynthetics at various confining pressures and specimen lengths.</p>		
<b>17. Key Words</b> Geosynthetics, Geogrids, full-scale pullout tests, mechanically stabilized earth wall, reinforcements, marginal soils	<b>18. Distribution Statement</b> <b>Unrestricted. This document is available through the National Technical Information Service, Springfield, VA 21161.</b>	
<b>19. Security Classif. (of this report)</b> None	<b>20. Security Classif. (of this page)</b>	<b>21. No. of Pages</b> 95
		<b>22. Price</b>

## **Project Review Committee**

Each research project will have an advisory committee appointed by the LTRC Director. The Project Review Committee is responsible for assisting the LTRC Administrator or Manager in the development of acceptable research problem statements, requests for proposals, review of research proposals, oversight of approved research projects, and implementation of findings.

LTRC appreciates the dedication of the following Project Review Committee Members in guiding this research study to fruition.

### ***LTRC Administrator/ Manager***

Mark J. Morvant  
Pavement & Geotechnical Administrator

### ***Members***

Doug Hood, DOTD  
Kim Martindale, DOTD  
Mike J. Boudreaux, DOTD  
Mike B. Boudreaux, LTRC  
Zhongjie “Doc” Zhang, Ph.D., LTRC  
Murad Abu-Farsakh, Ph.D., LTRC/LSU

### ***Directorate Implementation Sponsor***

William T. Temple, DOTD Chief Engineer

# **Evaluation of Interaction Properties of Geosynthetics in Cohesive Soils: Lab and Field Pullout Tests**

By

Khalid Farrag, Ph.D., P.E.

And

Mark J. Morvant, P.E.

LTRC Project No. 92-4GT  
State Project No. 736-99-0658

conducted for

Louisiana Department of Transportation and Development  
Louisiana Transportation Research Center

The contents of this report reflect the views of the author/principal investigator who is responsible for the facts and the accuracy of the data presented herein. The contents do not necessarily reflect the views or policies of the Louisiana Department of Transportation and Development, the Federal Highway Administration, or the Louisiana Transportation Research Center. This report does not constitute a standard, specification, or regulation.

January 2004



## ABSTRACT

The considerable increase of using geosynthetics in mechanically stabilized earth (MSE) walls has raised the need to evaluate their interface shear strength and pullout properties in various types of backfills. This report investigates the use of a marginal silty-clay soil of medium plasticity as a suitable backfill in MSE walls. The interface parameters between the geosynthetics and the soil were evaluated in pullout tests. The testing program included performing laboratory and field pullout tests on four types of geogrids and three types of geotextiles. Laboratory pullout tests were carried out using the large pullout testing equipment at the Louisiana Transportation Research Center (LTRC). Field pullout tests were performed in a test section of the LTRC full-scale reinforced test wall. The pullout test section contained geogrid and geotextile specimens at various wall elevations.

The testing program evaluated the effect of reinforcement type, length, and confining pressure on the pullout resistance. Laboratory and field tests were performed using the same type of soil at a similar density and moisture content. Laboratory and field results compared well for the extensible reinforcements of medium to low stiffness modulus. However, field pullout results were significantly higher than laboratory results for the rigid geogrids.

The pullout resistance factor ( $F^*$ ) and the scale effect correction factor ( $\alpha$ ) were established for the geogrid and geotextile specimens. These values can be used to determine the pullout resistance of these types of geosynthetics at various confining pressures and specimen lengths.



## **ACKNOWLEDGMENTS**

The research program was funded by the Louisiana Department of Transportation and Development (LA DOTD) and the Louisiana Transportation Research Center (LTRC) under State Project Number 736-99-0658 and LTRC Research Project Number 92-4GT. The support and cooperation provided by these agencies are gratefully acknowledged.

The assistance of student interns Travis Richards, Matthew Olson, and Heath Williams, in the laboratory and field pullout tests is highly appreciated.

Appreciation is also extended to Tensar Corp. for donating the geogrids and the non-woven geotextiles, to Stratagrid Systems for donating the geogrids, and to Synthetic Industries for donating the woven geotextile used in the laboratory and field pullout tests.



## IMPLEMENTATION STATEMENT

The pullout tests were performed on geosynthetic specimens in marginal silty-clay soil with a low plasticity index of 15. The results of the pullout tests can be used to determine the pullout design parameters for geogrids and geotextiles in cohesive soils. The test conditions in the lab should replicate field conditions as the interface parameters depend on soil confining pressure, moisture, and density. The comparison between the laboratory and field pullout test results provided the means of evaluating of the effect of these parameters on the pullout resistance of the geosynthetics.

The results of the testing program provided the interface parameters (pullout coefficient of interaction ( $F^*$ ) and the scale effect correction factor ( $\alpha$ )) used to determine the stability of reinforced soil structures against pullout, according to the FHWA design procedures. Charts were provided to determine the effect of the change of specimen length from the 3-ft. laboratory specimen size to the longer field specimens.



# TABLE OF CONTENTS

ABSTRACT .....	iii
ACKNOWLEDGMENTS .....	v
IMPLEMENTATION STATEMENT .....	vii
TABLE OF CONTENTS .....	ix
LIST OF TABLES .....	xi
LIST OF FIGURES .....	xiii
INTRODUCTION .....	1
OBJECTIVES .....	3
SCOPE.....	5
METHODOLOGY .....	7
Review of Geosynthetics Testing in Cohesive Soils .....	7
Testing Equipment .....	8
Soil Properties.....	11
Testing Procedures .....	14
Pullout Testing Program.....	15
Soil Properties.....	15
Geosynthetics Material Properties .....	17
Laboratory Pullout Tests.....	29
Pullout Testing Equipment .....	29
Laboratory Pullout Test Program.....	31
Field Pullout Tests .....	33
Pullout Test Section.....	33
Pullout Testing Program.....	37
DISCUSSION OF RESULTS .....	43
Pullout Tests on the Clamping Plates .....	43
Laboratory Pullout Tests.....	43
Field Pullout Tests .....	43

Pullout Tests on Tensar UX-750.....	45
Laboratory Pullout Test .....	45
Field Pullout Tests .....	46
Comparison between Lab and Field Pullout Tests .....	49
Pullout Tests on Tensar UX-1500.....	51
Laboratory Pullout Test .....	51
Field Pullout Tests .....	51
Comparison between Lab and Field Pullout Tests .....	56
Pullout Tests on Tensar UX-1700.....	58
Laboratory Pullout Test .....	58
Field Pullout Test.....	58
Comparison between Lab and Field Pullout Tests .....	61
Pullout Tests on the Stratagrid-500.....	62
Laboratory Pullout Tests.....	62
Field Pullout Tests .....	62
Comparison between Lab and Field Pullout Tests .....	66
Pullout Tests on the Woven Geotextile .....	67
Laboratory Pullout Tests.....	67
Field Pullout Tests .....	67
Pullout Tests on the Nonwoven Geotextile .....	72
Field Pullout Tests .....	72
Analysis of Pullout Test Results .....	74
Evaluation of Pullout Coefficients .....	74
Effect of Confining Pressure.....	76
Effect of Specimen Length .....	80
Effect of Reinforcement Extensibility .....	84
CONCLUSIONS .....	89
RECOMMENDATIONS.....	91
REFERENCES .....	93

## LIST OF TABLES

Table 1 - Review of pullout and direct shear tests of geosynthetics in clay.....	9
Table 2 - Clay-geotextiles interface friction at various water contents [8].....	13
Table 3 - Properties of the soil backfill.....	15
Table 4 - Material properties of the geogrid UX-750SB .....	18
Table 5 - Material properties of the geogrid UX-1500HS .....	20
Table 6 - Material properties of the geogrid UX-1700HS .....	22
Table 7 - Material properties of the geogrid Strata-500.....	24
Table 8 - Material properties of the woven geotextiles .....	26
Table 9 - List of the laboratory pullout tests .....	32
Table 10 - List of the pullout tests in the field .....	40
Table 11 - Pullout test results on the clamping plates .....	45
Table 12 - Field pullout test results on the UX750 geogrid.....	46
Table 13 - Field pullout test results on the UX1500 geogrid.....	52
Table 14 - Field pullout test results on the UX1700 geogrid.....	58
Table 15 - Field pullout test results on the Strata-500 geogrid .....	63
Table 16 - Field pullout test results on the Geotex-4x4 geotextile .....	68
Table 17 - Field pullout test results on the Geotex-6x6 geotextile .....	70
Table 18 - Field pullout test results on the nonwoven geotextile .....	72



## LIST OF FIGURES

Figure 1 - Laboratory tests for determining in-soil geosynthetics properties .....	8
Figure 2 - Pullout test results of geogrid at different moisture contents.....	13
Figure 3 - Pore water pressure at the front of the specimen in saturated soil during pullout .	14
Figure 4 - Moisture-density relationship of the silty-clay soil.....	16
Figure 5 - Field measurements of soil dry density along the height of the test wall .....	16
Figure 6 - Unconfined extension tests on the UX-750 geogrid .....	18
Figure 7 - Calibration of the strain gauges in UX-750 geogrid .....	19
Figure 8 - Results of wide-sidth test on the UX-1500 geogrid .....	20
Figure 9 - View of the instrumented geogrid specimen in the extension test.....	21
Figure 10 - Results of the strain gauge calibration in the UX-1500 geogrid.....	21
Figure 11 - Unconfined extension test on the UX-1700 geogrid .....	23
Figure 12 - Extension test on the Strata-500 geogrid .....	24
Figure 13 - Results of the calibration of strain gauges in the Strata-500 geogrid .....	25
Figure 14 - Calibration of strain gauges in the woven geotextiles .....	26
Figure 15 - Calibration of strain gauges in woven geotextile Geotex 4x4 .....	27
Figure 16 - Extension tests on the non-woven geotextile TG-700 .....	28
Figure 17 - Schematic of the pullout box.....	30
Figure 18 - Loading the pullout box inside the hydraulic loading frame .....	30
Figure 19 - View of the geogrid specimen in the pullout box .....	31
Figure 20 - Plan and elevation of the LTRC test wall .....	33
Figure 21 - View of the pullout boxes at the vertical facing of the wall .....	34
Figure 22 - Cross section of the pullout section of the wall .....	34
Figure 23 - View of the first layer of pullout boxes during construction .....	35
Figure 24 - View of the pullout boxes inside the test wall .....	36
Figure 25 - The loading frame during pullout testing.....	36
Figure 26 - Schematic of the locations of pullout tests in the wall.....	38
Figure 27 - View of the instrumentation in geogrid UX-1500 .....	41
Figure 28 - View of the instrumentation in geogrid Stratagrid-500 .....	41
Figure 29 - Schematic of the instrumentation in the 3-ft. and 4-ft. geogrid specimens .....	42

Figure 30 - Results of lab pullout tests on the clamping plates .....	44
Figure 31 - Field pullout test results on the clamping plates .....	44
Figure 32 - Lab pullout test results on the UX-750 geogrid .....	45
Figure 33 - Field results on the UX-750 geogrid at confining pressure 3.2 psi.....	47
Figure 34 - Field results on the UX-750 geogrid at confining pressure 6 psi.....	47
Figure 35 - Locations of strain gauge in UX-750 geogrid .....	48
Figure 36 - Strain distribution along the specimen in test UX750-E5.....	49
Figure 37 - Lab and field pullout resistance for the 3-ft geogrid UX-750.....	50
Figure 38 - Lab and field pullout loads for the 3-ft. geogrid UX-750.....	50
Figure 39 - Displacements in the lab and field geogrids UX-750 .....	51
Figure 40 - Lab pullout test results on the UX-1500 geogrid .....	53
Figure 41 - Field pullout tests on the UX-1500 geogrid, length 3 ft. ....	53
Figure 42 - Field pullout results of UX-1500 at confining pressure 3.2 psi.....	54
Figure 43 - Field pullout results of UX-1500 at confining pressure 6 psi .....	54
Figure 44 - Effect of specimen length on pullout resistance .....	55
Figure 45 - Locations of strain gauges in the UX-1500 geogrid .....	55
Figure 46 - Strain along the geogrid specimen in test UX1500-E4.....	56
Figure 47 - Lab and field pullout test results at various confining pressures .....	57
Figure 48 - Measurements of front strains in field and lab pullout for UX-1500.....	57
Figure 49 - Lab pullout test results of the UX-1700 geogrid.....	59
Figure 50 - Field pullout on geogrid UX-1700 for specimen length 3 ft.....	59
Figure 51 - Pullout tests on UX1700 at confining pressure 11.3 psi.....	60
Figure 52 - Pullout tests on UX-1700 at confining pressure 13 psi.....	60
Figure 53 - Lab and field pullout tests on the geogrid UX-1700.....	61
Figure 54 - Displacement at front and Node-1 in lab and field tests for UX-1700 .....	62
Figure 55 - Lab pullout test results on the Stratagrid-500 .....	63
Figure 56 - Field pullout results on the 3-ft Stratagrid-500 .....	64
Figure 57 - Field pullout test results on the 5-ft Stratagrid-500 .....	64
Figure 58 - Field pullout results on the Stratagrid-500.....	65
Figure 59 - Strain distribution in the field along the 4-ft Stratagrid-500.....	66
Figure 60 - Comparison between lab and field pullout.....	67

Figure 61 - Lab pullout tests on the woven geotextiles Geotex-4x4 .....	68
Figure 62 - Field pullout results on Geotex-4x4 at confining pressure 3.2 psi .....	69
Figure 63 - Field pullout results on Geotex-4x4 at confining pressure 6 psi .....	69
Figure 64 - Field pullout results on the Geotex-6x6 geotextile .....	71
Figure 65 - Filed pullout results on the Geotex-6x6 geotextile .....	71
Figure 66 - Field pullout tests of the nonwoven of length 3 ft. ....	73
Figure 67 - Field pullout tests of the nonwoven of length 4 ft. ....	73
Figure 68 - The mechanism of pullout in geogrid specimen .....	75
Figure 69 - Pullout coefficient ( $F^*$ : <b>a</b> ) for the Tensar UX-750 .....	77
Figure 70 - Pullout coefficient ( $F^*$ : <b>a</b> ) for the Tensar UX-1500 .....	77
Figure 71 - Pullout coefficient ( $F^*$ : <b>a</b> ) for the Tensar UX-1700 .....	78
Figure 72 - Pullout coefficient ( $F^*$ : <b>a</b> ) for the Stratagrid-500 .....	78
Figure 73 - Pullout coefficient ( $F^*$ : <b>a</b> ) for the Woven 4 x4 .....	79
Figure 74 - Pullout coefficient ( $F^*$ : <b>a</b> ) for the Woven 6x6 .....	79
Figure 75 - Pullout coefficient ( $F^*$ : <b>a</b> ) for the Nonwoven geotextile .....	80
Figure 76 - Pullout coefficient ( $F^*$ : <b>a</b> ) for the UX-750 .....	81
Figure 77 - Pullout coefficient ( $F^*$ : <b>a</b> ) for the UX-1500 .....	81
Figure 78 - Pullout coefficient ( $F^*$ : <b>a</b> ) for the UX-1700 .....	82
Figure 79 - Pullout coefficient ( $F^*$ : <b>a</b> ) for the Stratagrid-500 .....	82
Figure 80 - Pullout coefficient ( $F^*$ : <b>a</b> ) for the woven 4x4 .....	83
Figure 81 - Pullout coefficient ( $F^*$ : <b>a</b> ) for the woven 6x6 .....	83
Figure 82 - Schematic of the forces at the first element .....	84
Figure 83 - Confined extension modulus of the UX-750 .....	85
Figure 84 - Confined extension modulus of the UX-1500 .....	85
Figure 85 - Confined extension modulus of the UX-1700 .....	86
Figure 86 - Confined extension modulus of the Stratagrid-500 .....	86
Figure 87 - Confined extension modulus of the woven Geotex 4x4 .....	87



## INTRODUCTION

The increasing use of geosynthetics to reinforce walls and slopes has raised the need to evaluate the reinforcement interaction parameters (i.e. pullout resistance and shear stress-strain characteristics) in a wide range of soil types, including cohesive soils and low-quality backfills. In determining the geosynthetics' interaction parameters in such soils, many factors can influence the measured properties. These factors are related to the testing equipment and the associated boundary effects, soil properties and compaction procedures, geosynthetic type and geometry, and confining pressure.

In order to evaluate the behavior of reinforced soil walls constructed with low-quality backfill, the Louisiana Transportation Research Center (LTRC) has constructed a reinforced test wall with silty-clay soil backfill. The primary objectives of the test wall were to assess the effect of reinforcement properties on the deformation and stress distribution in the wall and to investigate the soil-geosynthetic interface mechanism through a comparison of laboratory and field pullout tests. The first objective of the test wall was addressed in a separate report [1]. The second objective is addressed in this report. It details the research program and presents the analysis of the laboratory and field pullout tests in the silty-clay soil.

The soil-geosynthetic reinforcement interaction mechanism is complex and raises difficulties in interpreting the pullout test results. The confined stress-strain of the geosynthetic during pullout is significantly affected by its geometry, length, extensibility, and the amount of soil confinement. Pullout resistance of geotextile reinforcement is provided mainly by friction resistance along the soil-geotextile interface. On the other hand, the pullout resistance of a geogrid is mainly due to soil frictional resistance and passive bearing resistance against its transverse members. Furthermore, non-uniform shear stress-strain distribution is developed along the geosynthetic specimen during pullout due to the coupled effect of its elongation and interface shear. Various theoretical and empirical procedures have been developed in order to model the soil-geosynthetic interface mechanism during pullout [2, 3, 4, 5]. These models varied in their assumptions with respect to the constitutive material properties, the

load transfer mechanism at the interface, and the shape of the load-strain curve during pullout.

The design procedures recommended by the Federal Highway Administration (FHWA) for the evaluation of pullout resistance included the pullout design factors  $F^*$  and  $\mathbf{a}$ , which incorporate the effects of the geosynthetic friction-bearing interaction and its extensibility [6, 7]. These factors can be obtained experimentally from pullout tests on reinforcements with different lengths and at various confining pressures.

To determine the pullout design factors in silty-clay soils, laboratory pullout tests were performed on various types of geogrids and geotextiles. The field tests were performed on various types of geogrid and geotextile reinforcements in a test section in the LTRC reinforced-soil wall. The results of laboratory pullout tests were compared with field pullout test results.

## OBJECTIVES

The performance of reinforced-soil walls constructed with marginal backfill silty-clay soils was evaluated at the LTRC test wall. The two major objectives of the test wall were to:

1. Evaluate the effect of reinforcement type, strength, and design configuration on the state of deformations and stresses in the wall sections.
2. Evaluate the pullout performance of geogrids and geotextiles in silty-clay soils.

The first objective of the research program was addressed in a separate report [1]. The laboratory and field pullout testing programs are presented in this report. The results were correlated for various types of geogrid and geotextile reinforcements and the report presents an evaluation of the pullout resistance parameters for this type of soil.



## SCOPE

Field pullout tests were performed on geogrid and geotextile specimens placed between the main reinforcement layers in one section of the test wall. The geogrids used in the testing program included: Tensar UX750, UX1500, UX1700, and Stratagrid 500. The geotextiles tested were Synthetic Industries woven Geotex 4x4, Geotex 6x6, and Evergreen nonwoven TG700. These materials included weak and strong reinforcement types and covered a wide stiffness modulus range.

Laboratory tests were performed on the geosynthetic specimens in the same type of silty-clay soil used in the test wall and at comparable confining pressures. The hydraulic testing equipment used in the laboratory tests was also used in the field tests in order to provide the same control and pullout rates. In both tests, the soil was compacted to 90 percent of its modified proctor density at optimum moisture content. Various length specimens from 3 ft. to 5 ft. were tested in the field while the laboratory tests were performed only on 3-ft. long specimens.

The analysis of test results included a comparison of laboratory and field tests. The analysis focused on evaluating the pullout design factors,  $C_i$ ,  $F^*$ , and  $\alpha$ , according to the FHWA design procedures.



# METHODOLOGY

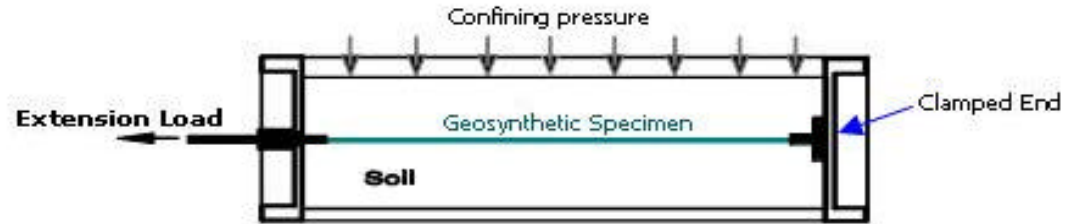
## Review of Geosynthetics Testing in Cohesive Soils

The characteristics and mechanical properties of confined geosynthetics can be experimentally modeled by monitoring:

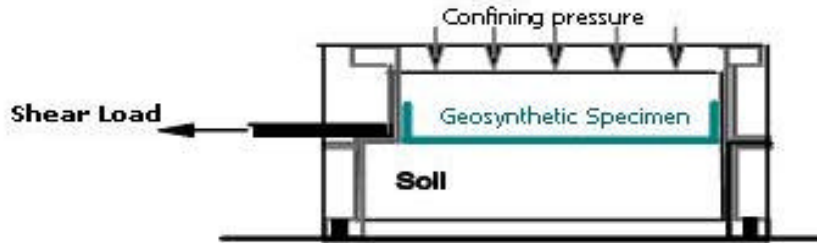
1. The in-soil mechanical properties of geosynthetics in confined extension tests. In these tests, one end of the specimen is clamped to the box while the other end is subjected to an extension force (figure 1-a). The test provides the confined stress-strain properties of the geosynthetic.
2. The soil-geosynthetic interface shear characteristics in direct shear tests. In the direct shear box, tests are usually performed in accordance with the conventional procedure for testing un-reinforced soil samples (figure 1-b). The results provide the soil-geosynthetic interface friction properties.
3. The soil-geosynthetic interface properties in a pullout box. In this test, one end of the specimen is free inside the soil, while the other end is subjected to a pullout load (figure 1-c). Pullout tests provide the load-displacement relationship of the geosynthetic and its maximum pullout resistance. Pullout displacement is a result of the coupled effect of material confined elongation and shear displacement at the interface.

Limited research relevant to the evaluation of geosynthetic interaction parameters in cohesive soils has been done. Moreover, this limited research has been conducted using various equipment and testing procedures, making it difficult to consistently compare the performance of geosynthetics in clays.

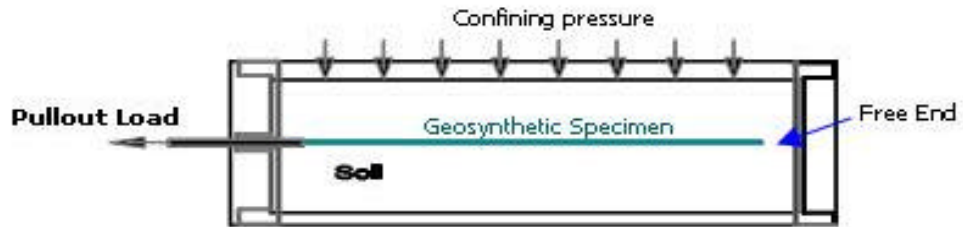
A summarized literature review of test equipment and procedures used in determining the clay-geosynthetic interface parameters is shown in table 1. The review focused on evaluating testing equipment, soil properties, and testing procedures.



**(a) Confined Extension Test**



**(b) Direct Shear Test**



**(c) Pullout Test**

**Figure 1**  
**Laboratory tests for determining in-soil geosynthetics properties**

### Testing Equipment

Direct shear tests and pullout tests are associated with different testing procedures, loading paths, and boundary conditions. The fundamental difference between the two tests is that the direct shear test provides uniform interface friction properties at one surface along the geosynthetic specimen. However, the interface friction along both sides of the specimen in the pullout test is coupled with reinforcement extension, resulting in a non-uniform shear distribution along the specimen length. These differences result in different interpretation procedures for test results when they are implemented in the design and analysis of reinforced structures.

**Table 1**  
**Review of pullout and direct shear tests of geosynthetics in clay**

Ref.	Test	Soil Properties	Reinforcement Type	Notes <sup>(1)</sup>
[8]	Direct shear test, box: 6 in. x 6 in.	Plastic clay,  LL = 56, PI = 30, w/c = 25,40,60	- Needle-punched non-woven geotextile  - Woven geotextile	s = 50 -150 kPa
[9]	Pullout Test, Box: 12 in. x12 in., Specimen 10 in. x 10 in.	Smectite clay,  Wyoming Bentonite, LL = 515, PI = 470, w/c = 10.	Tensar SS2, SR2, SR3 TT1 and TT2 geogrid	Rate 0.1 mm/min s = 11.79 & 47.9 kPa
[10]	Direct Shear Test , Box: 12 in. x12 in.	- Ottawa sand and 5% Bentonite, LL= 38, PI = 20.  - Ottawa sand and 10% Bentonite, LL= 47, PI = 20  - Gulf clay (CL) LL = 42, PI=14	- Non-woven geotextile - Woven geotextile - PVC membrane - HDPE membrane	Rate 0.3 mm/min s = 0-100 kPa
[11]	Direct shear test, Box: 10 in. x10 in.  Soil: 0.5-3.0 in. thick.	Sandy clay: 45% Ottawa sand,  50% Kaolinite, 5% Bentonite, PI = 28, w/c = 16	- Woven geotextile - Non-woven geotextile	Rate 0.7 mm/min s = 72-288 kPa
[12]	Direct shear test, Box: 12 in. x 12 in.	Clayey sand	- Geotextile - PVC membrane	s = 0.2, 0.35, 0.6 and 0.9 kPa.
[13]	Direct shear and Pullout tests, Box: 2.5 in. x 2.5 in.	Silty Clay (CL), LL = 27, PI = 13 w/c = 15-17-19	- Non-woven geotextile - Woven geotextile - Netlon geogrid	Rate 0.9 mm/min (undrained), .003 mm/min (drained).

<sup>(1)</sup> Notes:      rate = pullout/shear rate (1 mm/min = 0.04 in/min)  
                    s = Applied confining pressure (1 kPa = 0.145 psi)

Table 1 - [Continued]

Ref.	Test	Soil Properties	Reinforcement Type	Notes
[14]	Direct shear test, Box: 10 in. x10 in.	Silty clay, LL= 40.8, PL= 20.6 w/c = 23	- Paragrid 50S - TNX-5001 geogrid - Tensar SR2, SS2 geogrid	Rate 3 mm/min. s = 5-250 kPa
[15]	Direct shear test, Box: 6 in. x 6 in.  Pullout test, Box: 31 in. x 40 in. x 12 in.	Clayey sand (SC), PL =12.2, PI =18.3 w/c = 15  Weathered clay(CH) PL = 25 , PI = 35 w/c= 23.5	- Tensar SR2 geogrid - Bamboo grids.	Rate 1.2 mm/min
[16], [17]	Direct Shear test, Box: 2.5 in. x 2.5 in.  Pullout test, Box: 11 in. x 20 in. x 12 in.	Kaolin clay, LL = 60, PL= 35, w/c = 35.	- Metallic plates and grids - Polyethylene grid	Rate = 2% min.
[18]	Pullout test, Box: 36 in. x 54 in. x 18 in.	Silty clay (ML) 50% passing #200	- Bar-mats - Wire mesh	
[19]	Pullout test, Box: 30 in. x 50 in. x 20 in.	Weathered clay 83% passing #200 PI= 24, w/c = 23.	Wire mesh	
[20]	Pullout test, Box: 35 in. x 60 in. x 47 in.	Silty clay c = 7.5 kPa	Tensar UX1600 geogrid	s= 13.3,21.6 kPa
[21]	Pullout test, Box 28 in. x 30 in. x 24 in.	CL clay, dry and saturated	Rigid HDPE geogrid	s= 28.7 kPa
[22], [23]	Pullout test, Box 36 in. x 60 in. x 36 in.	Silty-Clay, PI=6  Clayey-Silty, PI = 24	Tensar SR2	s= 7 psi w/c = 15, 20, 40 %

For reinforced embankments over soft foundations, the transfer of shear stresses at the soil-geosynthetic interface is usually modeled in the direct shear box. Meanwhile, the development of the interface shear resistance in reinforced walls and slopes is more appropriately modeled in the pullout box.

A review of direct shear tests in table 1 shows that box dimensions range from the conventional interface area of 2.5 in. by 2.5 in. [13,16, 17] to larger boxes of 12 in. by 12 in. [9, 10]. The advantages of using larger boxes are to minimize the effect of box boundaries on the results and to permit testing of larger representative geosynthetic specimens.

The literature review showed that few testing programs were conducted for evaluating pullout interaction mechanism in cohesive soils. In these tests, pullout box dimensions ranged from small sizes of 1ft. by 1 ft. [9] to larger boxes of 3 ft. wide, 4.5 ft. long, and 3.5 ft. high [20].

### **Soil Properties**

The cohesive soils evaluated in the direct shear tests have a wide range of plasticity indices. Soils ranged from silty clay with a plasticity index of 6 percent [22, 23] to a highly expansive clay [9]. Most of the cohesive soils tested were natural soils with at least 50 percent clay content. Synthesized soils at various clay contents were also tested with geosynthetics in the direct shear box [11].

Various soil properties affect geogrid interaction in clay (e.g., soil plasticity, density, and water content) which makes it difficult to compare between pullout resistances in various soils. Pullout test results on geogrids in low quality backfills [19, 20] showed lower coefficients of sliding than those tested in granular soils at similar confining pressure. This was mainly due to higher particle interlocking of the granular soils within the geogrid opening.

Tests were conducted on cohesive soil samples at optimum moisture contents [9, 11, 13], and in fully saturated soils [16, 21]. Results of direct shear tests on the clay-geotextile at various water contents [8] are shown in table 2. The results show a decrease of interface shear with increasing soil water content. Pullout test results on geogrid in clay also showed that saturated soils yield only about 80 percent resistance of the un-saturated soil [21]. However, higher reduction in the pullout resistance was observed when the geogrid was tested in saturated sand.

Previous pullout tests performed at LTRC on geogrid reinforcement in cohesive soils also showed that increased moisture content resulted in decreased pullout resistance. This effect was mainly due to reduction of frictional resistance at the interface and to the development of pore water pressure in saturated soil [22, 23].

Figure 2 shows the results of two sets of pullout tests performed on geogrids in silty clay soil of  $PI = 24$ . The first set was compacted at the optimum moisture content of 18 percent. In the second set, soil was initially compacted at the optimum moisture and water was added to reach a near saturation water content of 40 percent. Three tests were repeated in each set at identical testing conditions. The results show a significant drop of the geogrid pullout resistance in wet soil. Measurements of pore water pressure at the front of the geogrid specimens during pullout are shown in figure 3 for two tests at water content of 40 percent. The figure shows an increase in pore water pressure at the early stages of pullout, resulting in a decrease in the effective shear resistance at the interface.

**Table 2**  
**Clay-geotextile interface friction at various water contents [8]**

Soil-Geotextile Properties	Water Content (%)	Adherence Angle (d) <sup>o</sup>	tan d/ tan f
Plastic clay-woven	25	22	0.59
	40	21	0.61
	60	15	0.47
Plastic clay-thin non-woven	25	37	1.09
	40	33	1.03
	60	29	0.98
Plastic clay- thick non-woven	25	39	1.15
	40	34	1.09
	60	28	0.94

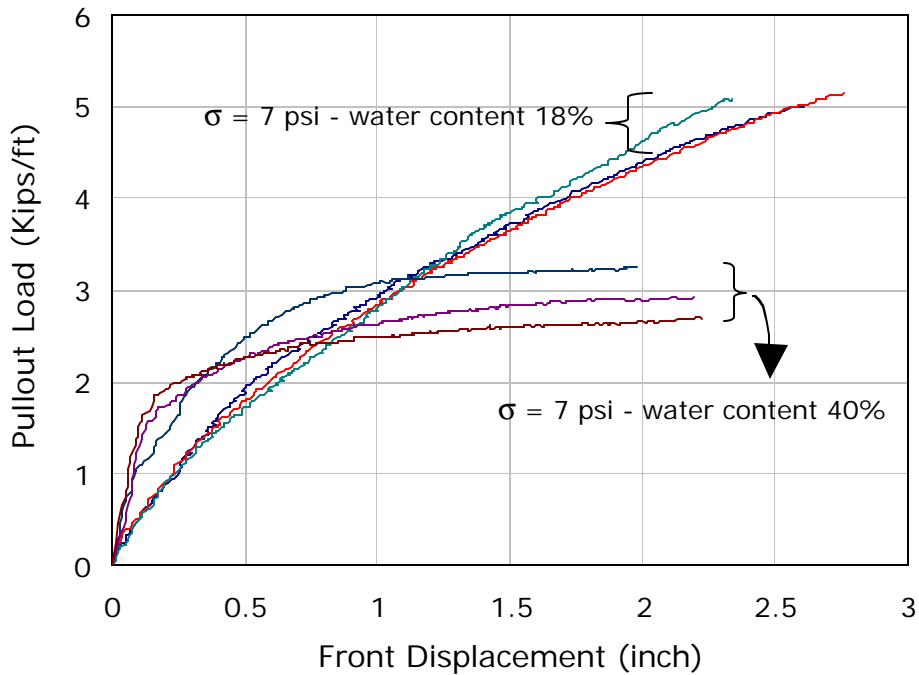


**Figure 2**  
**Pullout test results of geogrid in soil at different moisture contents**

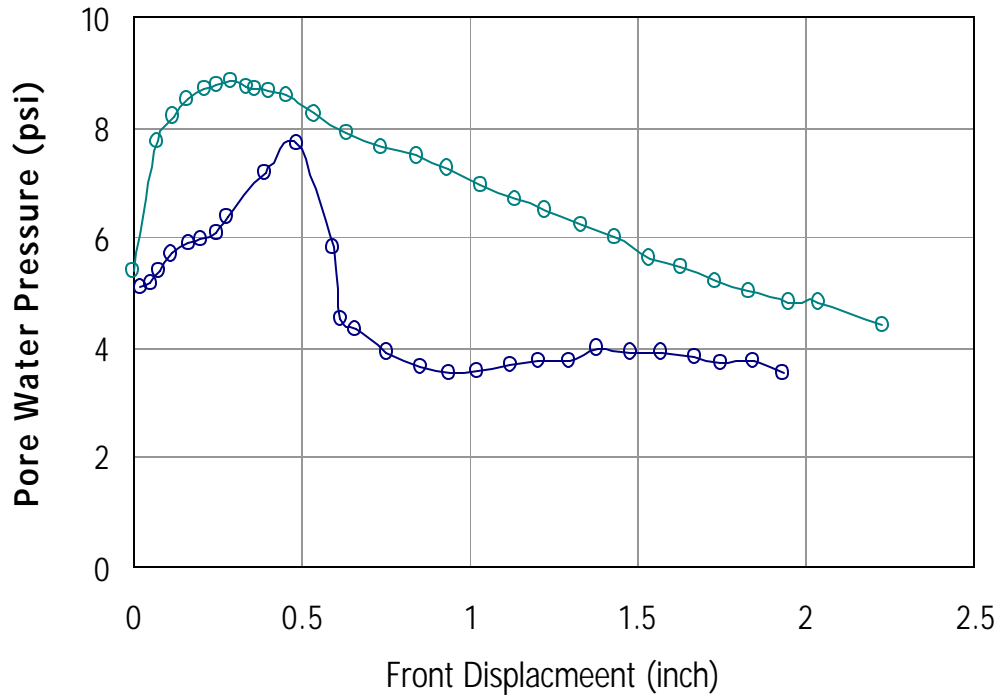


**Figure 3**  
**Pore water pressure at the front of the specimen in saturated soil during pullout**

**Testing Procedures**

Most of the direct shear and pullout tests were conducted on the cohesive soils at undrained testing conditions. Direct shear tests were performed at the same rates as in the conventional direct shear testing procedures (2%/min) [16], and at shearing rates ranging from 0.1 to 1.2 mm/min [9, 11, 13,15]. In the few tests performed in drained testing conditions, shear rates ranged from 0.003 mm/min [3] to 0.024 mm/min [8]. The results of direct shear tests showed that the drained shear resistance of geotextiles was lower than the undrained shear resistance. This reduction was mainly attributed to the relaxation of the geotextiles [13].

## Pullout Testing Program

### Soil Properties

The soil used in field and laboratory pullout tests was silty-clay soil type A-4 with the properties shown in table 3. The shear strength parameters were obtained from the direct shear tests according to ASTM D-6528. Maximum soil dry density and optimum moisture content were determined from the Standard Proctor test according to AASHTO T-99. Figure 4 shows the moisture-density relationship obtained from the compaction test.

The soil was compacted in the test wall to 8-in. lifts (equals the height of the modular block facing). Measurements of soil densities and moistures were performed at each compacted layer using the nuclear density gauge. Figure 5 shows the results of field measurements of soil dry density in the pullout test-section of the wall. The figure shows the average density at each soil lift and at the locations of the pullout tests (layers A to E). Measurements of soil density averaged 102 pcf, which was about 98 percent of the Standard Proctor results. The figure shows uniform soil density along the height of the wall with the exception of the soil density in layer B, which averaged 105 pcf.

Laboratory pullout tests were performed at the completion of the test wall construction and soil density was controlled at 102 pcf in these tests.

**Table 3**  
**Properties of the soil backfill**

% Silt	% Clay	PI	$\phi$ (degree)	Cohesion C (psf)	Optimum Moisture (%)	$\gamma_{d \max}$ (pcf)
72	19	15	24	30	18.5	104

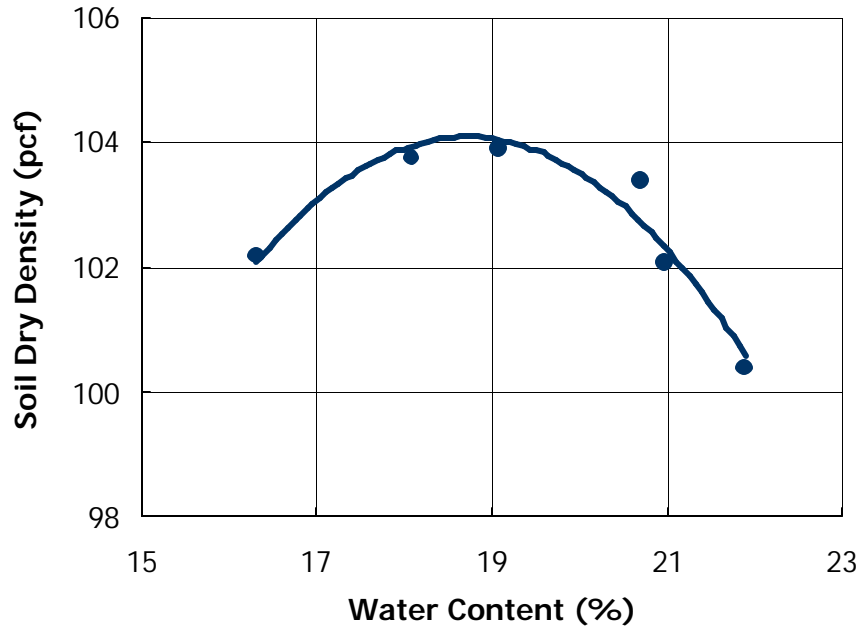


**Figure 4 Moisture-density relationship of the silty-clay soil**

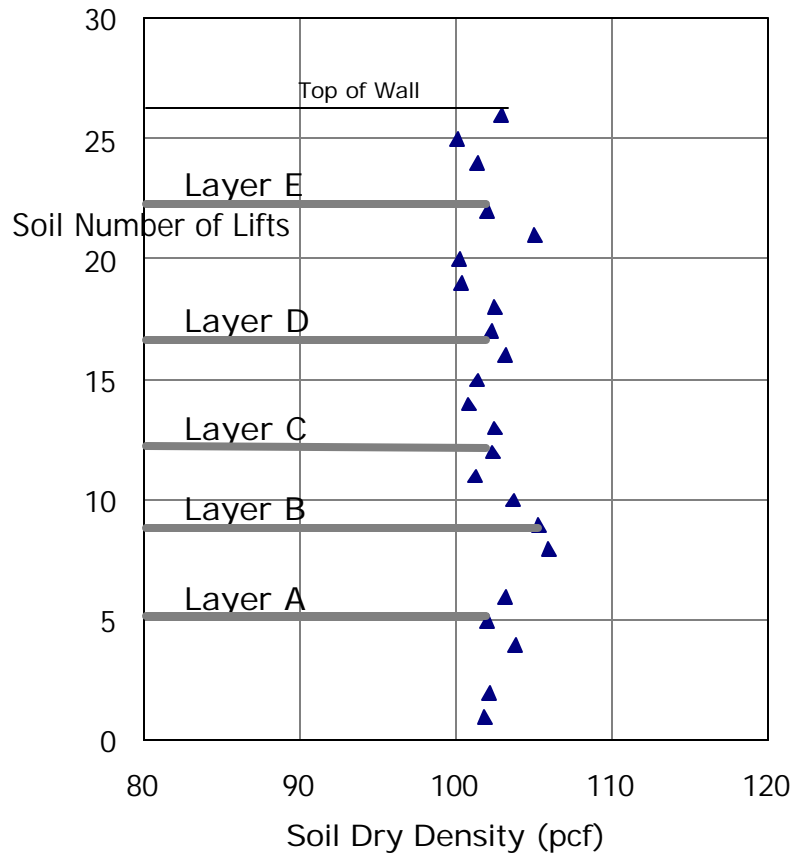


**Figure 5 Field measurements of soil dry density along the height of the test wall**

## **Geosynthetic Material Properties**

Pullout tests were performed on four types of geogrids (Tensar UX-750, Tensar UX-1500, Tensar UX-1700, and Stratagrid-500), two types of woven geotextiles (Geotex 4x4 and Geotex 6x6), and one nonwoven geotextile (Evergreen TG700). Unconfined extension tests were performed on these materials to determine their tensile strength properties. These tests were modified from the ASTM D4595 standard for the tensile properties of geotextiles by the wide-width strip method. The standard was modified to test larger size specimens of the geogrids and geotextiles and was run at an extension rate of 2.5 percent/min, which was lower than the 10 percent/min value specified in the standard. Test results and material properties are presented in the following sections.

### **Tensar Geogrid UX-750**

The Tensar UX-750 is a high-density polyethylene (HDPE) uniaxial geogrid with relatively low tensile modulus and strength. The geogrid was used in the test wall section of “weak geogrid- minimum spacing” reinforcement. The properties of the geogrid are shown in table 4. Unconfined extension tests were performed at an extension rate of 2.5 percent/min on the geogrid and the results are shown in figure 6. The tests were performed on 8-in. wide specimens (nine strands) and three longitudinal units in the machine direction with a total length of 18.75 in. Micro Measurements EP40-250BF-350 strain gauges were installed on the middle unit of the specimen in some tests to calibrate strain gauge readings with specimen extension. Details of the installation procedure and calibration of strain gauges are presented in another report [1]. The calibration results are shown in figure 7 and they show a gauge calibration factor of 0.8.

**Table 4**  
**Material properties of the geogrid UX-750**

Property	Value	Unit
Aperture size:		
Machine Direction (MD)	6.00	inch
Cross-Machine Direction (CMD)	0.66	inch
Open Area	60	%
Thickness:		
Ribs	0.018	inch
Junction	0.072	inch
Ultimate Strength – MD	2,200	lb/ft
Tensile Modulus	27	Kips/ft

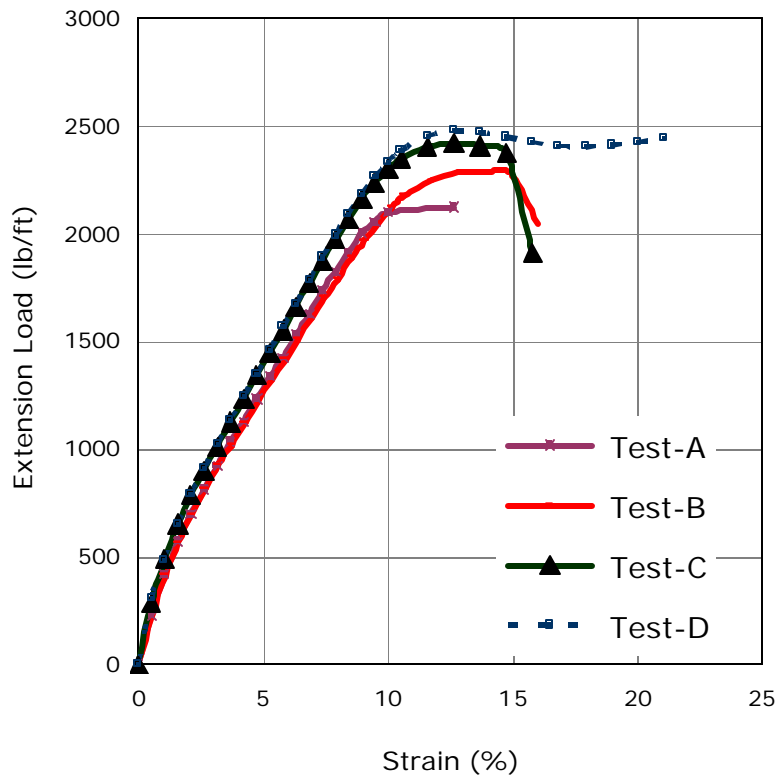


**Figure 6**  
**Unconfined extension tests on the UX-750 geogrid**

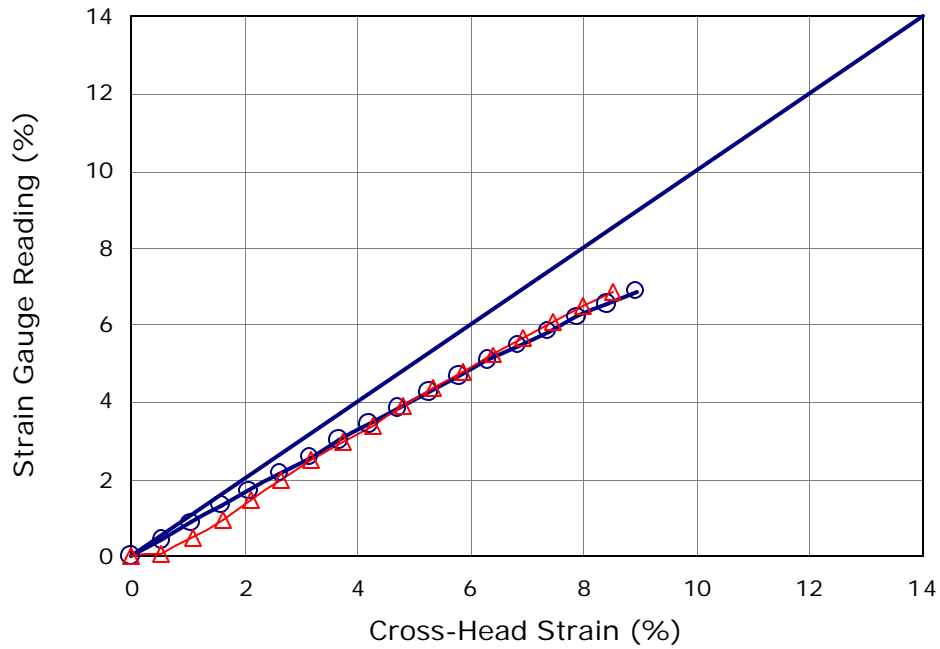


**Figure 7**  
**Calibration of the strain gauges in UX-750 geogrid**

### **Tensar Geogrid UX-1500**

The Tensar UX-1500 is also a uniaxial HDPE geogrid. Table 5 shows the properties of the geogrid and figure 8 shows the results of unconfined extension tests. The tests were performed on 8-in. wide specimens (seven strands) with three longitudinal units, at an extension rate of 1 percent/min. Strain gauges and extensometers were installed and calibrated during the tests. Figure 9 shows the instrumented geogrid specimen during the test. Results of the calibration of the strain gauges are shown in figure 10. A calibration factor of 0.85 was used to calculate strains from the measurements of the strain gauges in the pullout tests.

**Table 5**  
**Material properties of the geogrid UX-1500**

Property	Value	Unit
Aperture size: Machine Direction (MD)	14.5	inch
Cross-Machine Direction (CMD)	0.66	inch
Open Area	68	%
Thickness		
Ribs	0.065	inch
Junction	0.0167	inch
Ultimate Strength – MD	7,800	lb/ft
Tensile Modulus	90 –100	Kips/ft

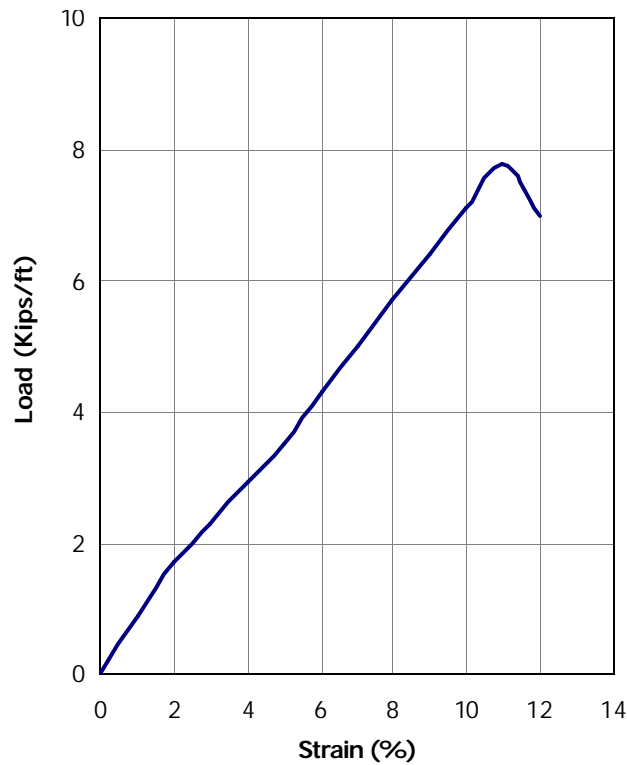


**Figure 8**  
**Results of wide-width test on the UX-1500 geogrid**

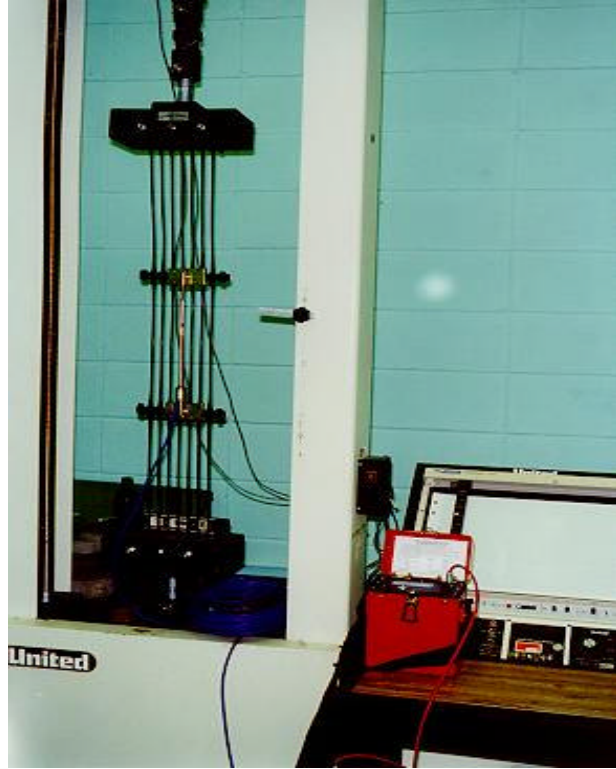


**Figure 9**  
**View of the instrumented geogrid specimen in the extension test**

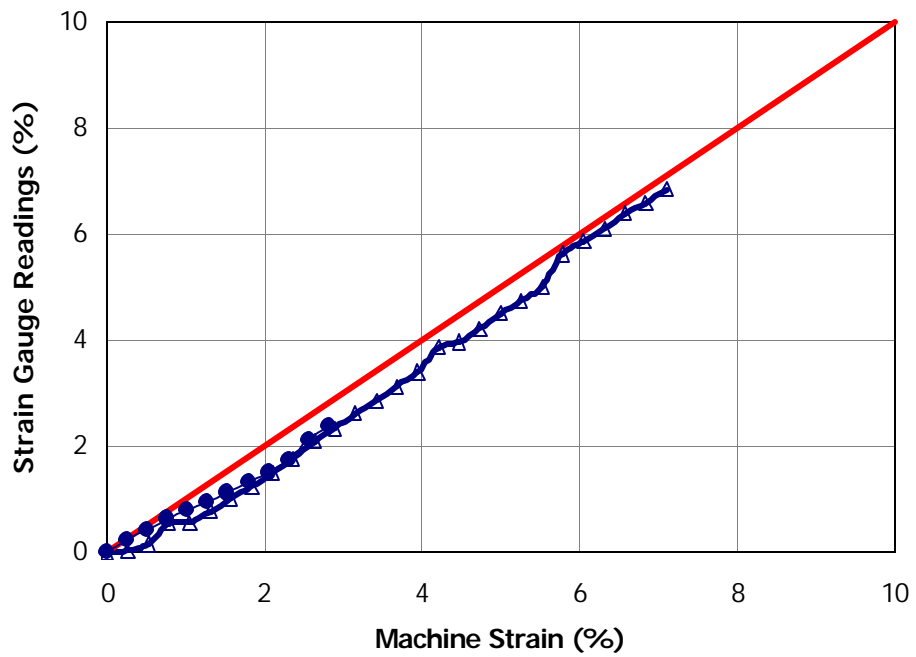


**Figure 10**  
**Results of the strain gauge calibration in the UX-1500 geogrid**

### **Tensar Geogrid UX-1700**

The Tensar UX-1700 is identical to the UX-1500 in aperture size. The UX-1700 has thicker ribs, which results in a higher strength and modulus. Table 6 shows the properties of the geogrid and figure 11 shows the results of wide-width tests. The strain gauge calibration value of the UX-1500 (0.85) was also used for this geogrid.

**Table 6**  
**Material properties of the geogrid UX-1700**

Property	Value	Unit
Aperture size: Machine Direction (MD)	14.5	inch
Cross-Machine Direction (CMD)	0.66	inch
Open Area	68	%
Thickness		
Ribs	0.125	inch
Junction	0.283	inch
Ultimate Strength – MD	11,900	lb/ft
Tensile Modulus	160	Kips/ft

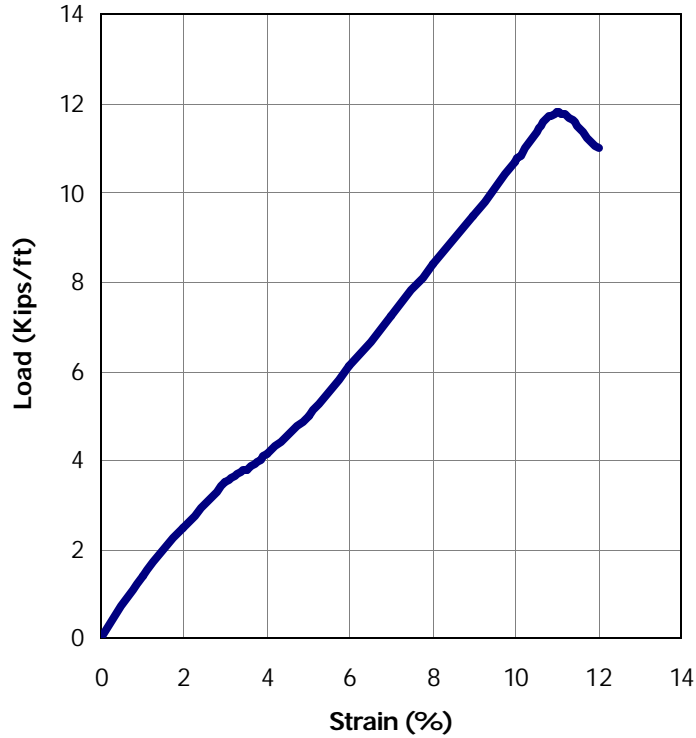


**Figure 11**  
**Unconfined extension test on the UX-1700 geogrid**

**Stratagrid-500**

This Stratagrid geogrid is a PVC-coated polyester yarn. Table 7 shows the properties of the geogrid. Unconfined extension tests were performed on 8-in. wide, 22-in. long specimens (six strands). Figure 12 shows the results of the extension test. It should be noted that the test in this figure did not run until failure. Micro Measurements EP08-110BE-120 strain gauges were installed and calibrated on the geogrid. The results of the strain gauges' calibration are shown in figure 13; a calibration factor of 0.75 was used to analyze strain gauge readings during pullout tests.

**Table 7**  
**Material properties of the Stratagrid-500**

Property	Value	Unit
Aperture size:		
Machine Direction (MD)	2.3	inch
Cross-Machine Direction (CMD)	1.0	inch
Open Area	55	%
Thickness		
Ribs	0.05	inch
Junction	0.06	inch
Ultimate Strength – MD	4,600	lb/ft
Tensile Modulus	22	Kips/ft

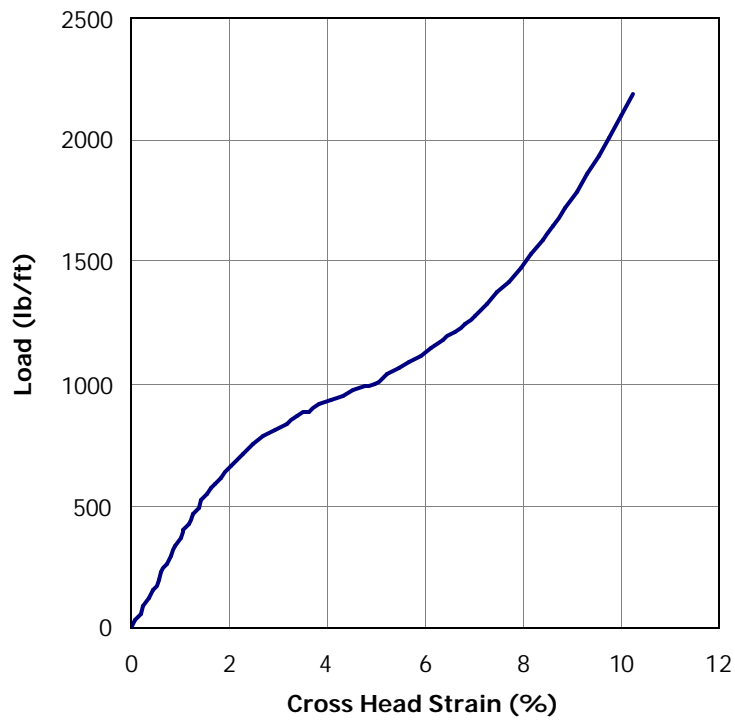


**Figure 12**  
**Extension test on the Stratagrid-500**

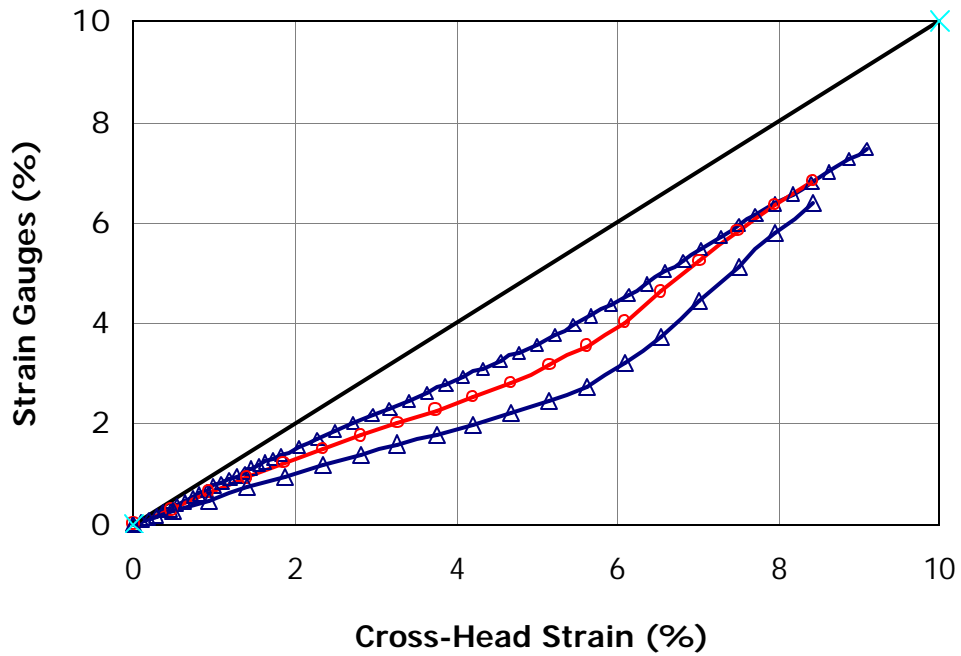


**Figure 13**  
**Results of the calibration of strain gauges in the Stratagrid-500**

### **Woven Geotextiles**

Two types of woven geotextiles were tested, Geotex 4x4 and Geotex 6x6. They are polypropylene (PP) woven geotextiles manufactured by “Synthetic Industries.” Table 8 shows the properties of these geotextiles. Micro Measurement EP08-10CBE-120 strain gauges were installed on the geotextiles. Figure 14 shows the calibration of the gauges in an extension test. The results of the calibration test are shown in figure 15.

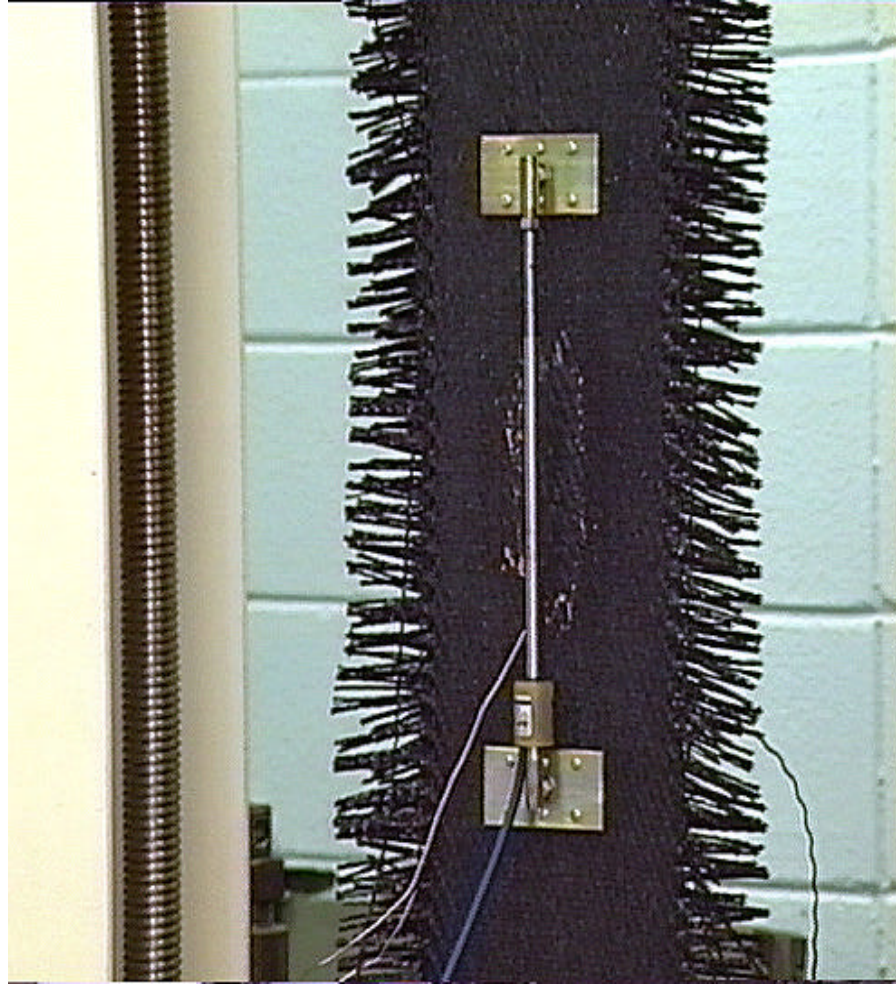


**Figure 14**  
**Calibration of strain gauges in the woven geotextiles**

**Table 8**  
**Material properties of the woven geotextiles**

Property	Geotex 4x4	Geotex 6x6	units
Mass/unit area	13	13.5	oz/yd <sup>2</sup>
Wide Width Strength- MD	4,800	7,200	lb/ft
Strength at 5% strain- MD	2,400	2,100	lb/ft

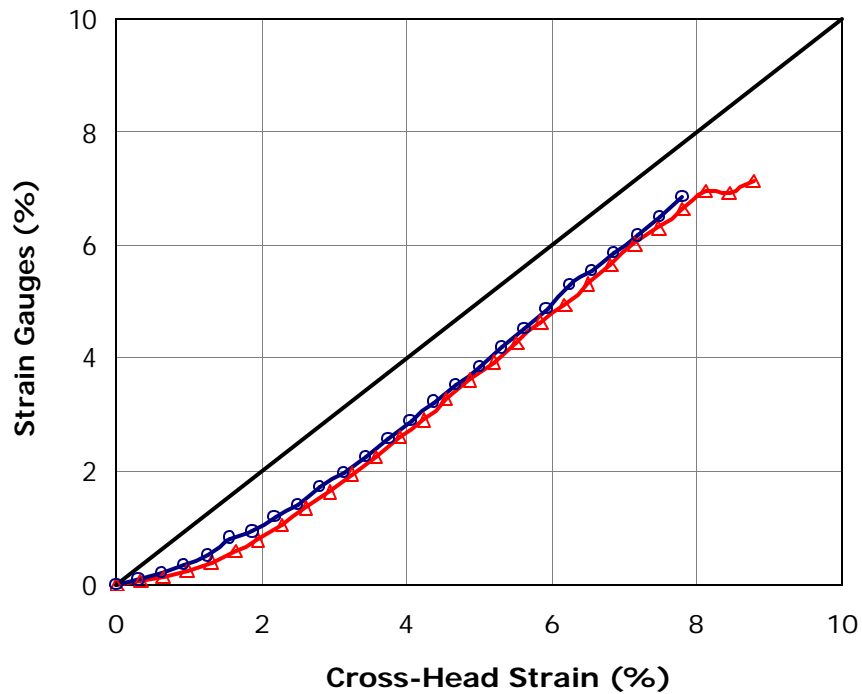


**Figure 15**  
**Calibration of strain gauges in woven geotextile Geotex 4x4**

### **Nonwoven Geotextile**

Field pullout tests were performed on a nonwoven geotextile, Evergreen TG700. The geotextile is a polypropylene (PP) fabric with mass/unit area of 8 oz/yd<sup>2</sup>. The geotextile was also used in the reinforcement of one of the slope sections in the LTRC test wall. No laboratory pullout tests were performed on this geotextile.

Figure 16 shows results of extension tests on 8-in. wide, 20-in. long specimens. The installation of strain gauges on the non-woven geotextile was unsuccessful and the calibration results had a weak relationship, mainly due to the difficulty in installing the gauge on the surface of the fabric. Furthermore, the high permittivity of the fabric resulted in moisture damage to the gauge.

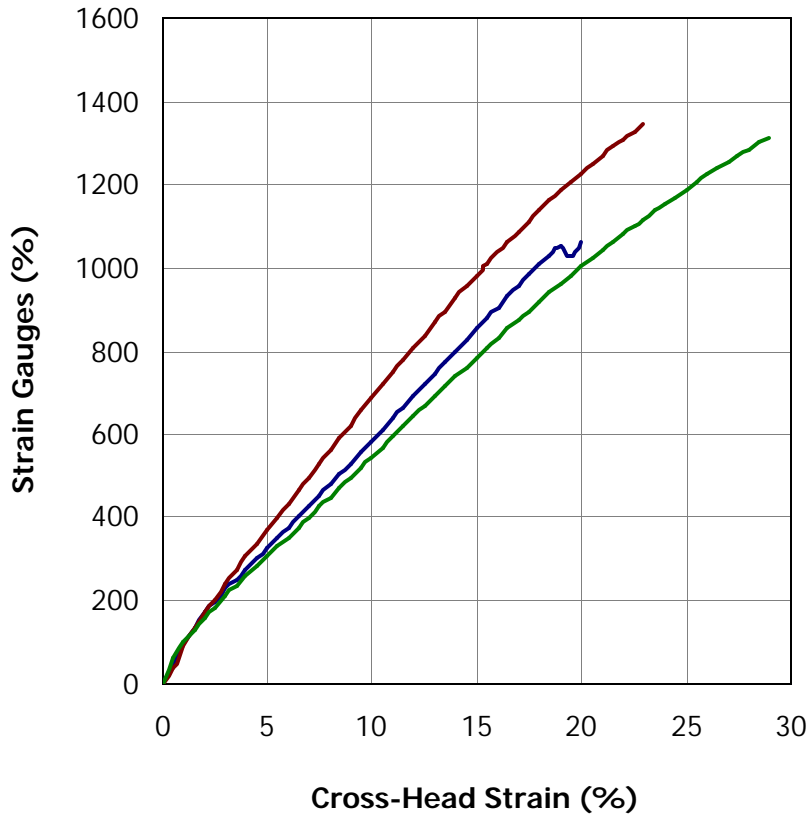


**Figure 16**  
**Extension tests on the non-woven Evergreen TG-700**

## **Laboratory Pullout Tests**

### **Pullout Testing Equipment**

Laboratory pullout tests were performed using the pullout testing equipment at LTRC. The pullout box dimensions are 48 in. long x 24 in. wide x 18 in. tall. Figure 17 shows a schematic diagram of the pullout box. Sleeve plates of 6 inches length were placed at the front wall slot to minimize load transfer to the rigid front facing. The geosynthetic specimens were bolted between two clamping plates that extended inside the soil to insure that the specimen remained confined during the test. A confined air bag applied vertical pressure to the top of the soil specimen. The pullout box was movable to facilitate loading and unloading of soil and to allow compaction and moisture control of the silty-clay soil. Mounted on a loading frame, the hydraulic loading system operates at a constant displacement rate of 0.06 in./min in these tests. Figure 18 shows the placement of the pullout box inside the loading frame of the hydraulic system.

Pullout loads and the front displacements were monitored using a load cell and a linear variable differential transformer (LVDT) mounted on the loading frame. Displacements along the length of the specimens were monitored using tell-tails connected to the LVDTs at the back of the pullout box. A detailed description of the pullout testing equipment and procedure was presented in a previous report [24].

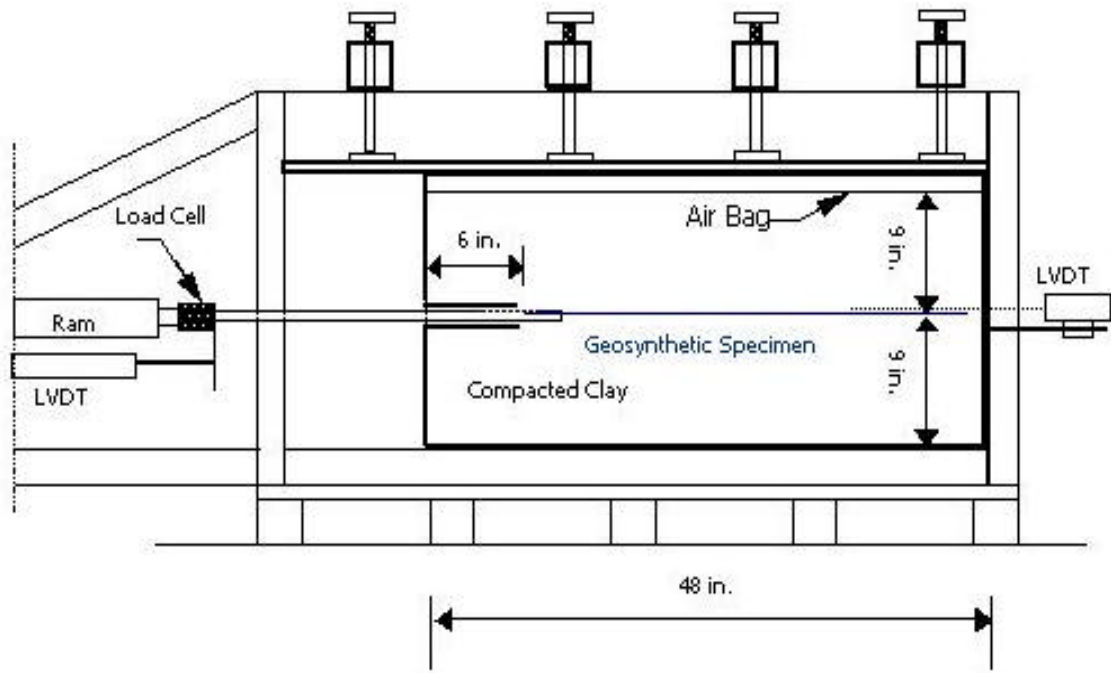


**Figure 17**  
Schematic of the pullout box



**Figure 18**  
Loading the pullout box inside the hydraulic loading frame

### **Laboratory Pullout Test Program**

Pullout tests were performed on the four types of geogrids (Tensar UX-750, UX-1500, UX-1700, and Stratagrid500), and one woven geotextile (Geotex 4x4). Table 9 shows a list of the pullout tests performed in the lab. The geosynthetic specimens were 1 ft. wide x 3 ft. long. Tests were performed at soil densities of 102 pcf and at the optimum moisture content of 17 percent. The soil was prepared to the target moisture content and was placed in two lifts of 4.5 in. thickness each. The geosynthetic specimen was placed on the top of the second layer and was covered by two soil layers. Figure 19 shows a view of the geogrid specimen inside the pullout box.

Pullout tests on the clamping plates were also performed at various confining pressures in order to determine the shear resistance of the clamping plates. The resistance of the plates was subtracted from the results of pullout tests on the geosynthetics.



**Figure 19**  
**View of the geogrid specimen in the pullout box**

**Table 9**  
**List of the laboratory pullout tests**

Material	Test ID	Confining pressure (psi)
Clamping plates	Plate-3a	3
	Plate-5a	5
	Plate-7a	7
Tensar UX-750	UX750-3a	3
	UX750-3b	3
	UX750-5a	5
	UX750-7a	7
Tensar UX-1500	UX1500-3a	3
	UX1500-5a	5
	UX1500-7a	7
	UX1500-10a	10
	UX1500-15a	15
Tensar UX-1700	UX1700-7a	7
	UX1700-10a	10
	UX1700-12a	12
Stratagrid 500	Strata-6a	6
	Strata-8a	8
	Strata-10a	10
Woven Geotextile 4x4	Wov-3a	3
	Wov-4a	4
	Wov-6a	6
	Wov-8b	8

## Field Pullout Tests

### Pullout Test Section

Field pullout tests were done in the pullout section of the LTRC test wall. The pullout section was one of three test sections at the vertical side of the wall. The plan and elevation of the test wall are shown in Figure 20. The pullout section was 30 ft. long, and it contained the pullout specimens inside wooden boxes that replaced the modular block facing. Figure 21 shows the pullout boxes in the vertical facing of the wall, and Figure 22 shows a cross-section of the pullout section of the wall. Pullout tests were also performed in the 3-to-1 slope at the vertical facing. The details of the reinforcement and construction of the test wall are presented in another report [1].

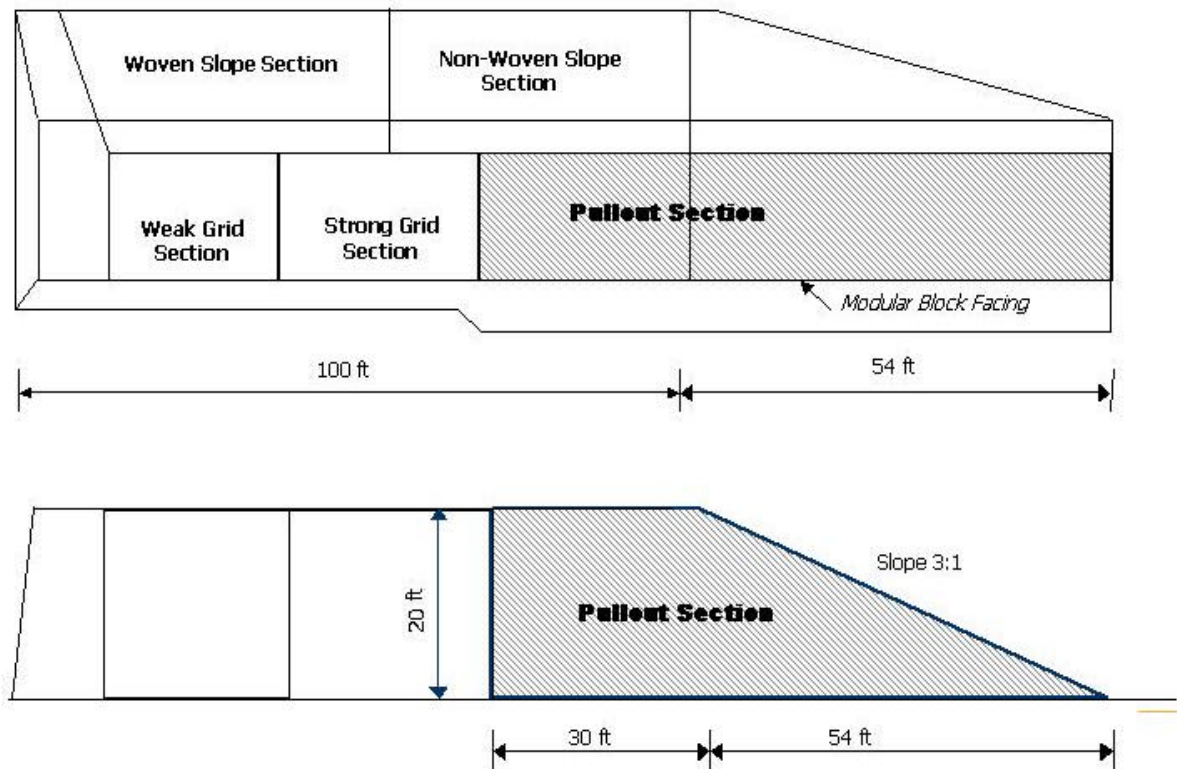


**Figure 20**  
**Plan and elevation of the LTRC test wall**



**Figure 21**  
View of the pullout boxes at the vertical facing of the wall

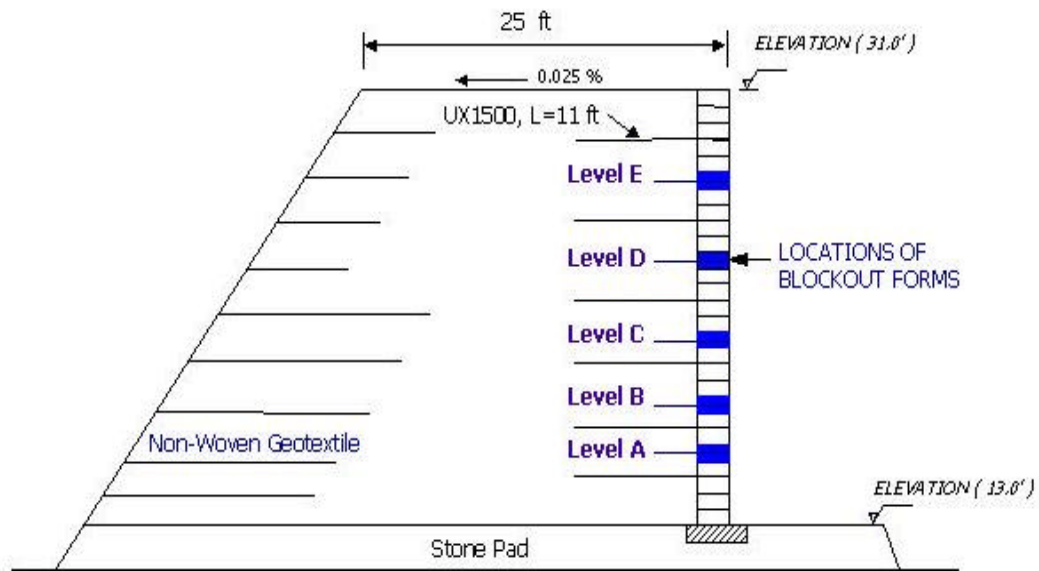


**Figure 22**  
Cross section of the pullout section of the wall

The pullout specimens were placed at elevations between the main reinforcement of the test sections in five levels (levels A to E) as shows in figure 22. The geosynthetic specimens were connected to 1-ft.-wide metal plates that extended through the modular block facing of the wall via wooden boxes that were 18 in. wide, 8 in. high, and 3 ft. long. The metal plates extended 1 foot inside the soil to keep the geosynthetic specimens confined during the pullout tests. Figures 23 and 24 show the metal plates, wooden boxes, and the geosynthetic specimen inside the soil.

Pullout tests were performed using the same pullout equipment that was used in the laboratory tests. A loading frame was constructed and placed against the wall facing in order to perform the tests at the various locations. Figure 25 shows a view of the pullout loading frame.



**Figure 23**  
**View of the first layer of pullout boxes during construction**



**Figure 24**  
**View of the pullout boxes inside the test wall**



**Figure 25**  
**The loading frame during pullout testing**

## **Pullout Testing Program**

Figure 26 shows a schematic of the pullout test section in the LTRC wall and the locations of pullout specimens. The tests are identified by their elevation in the wall (layers A to E) and their location in each layer (1 to 12). A total of 55 tests were performed in the test section on various types of geogrid and geotextile reinforcements. The specimens had a constant width of 1 ft. and various lengths from 3 ft. to 5 ft. A list of the pullout tests is shown in table 10. The table identifies the geosynthetic type, length, and confining pressure for each test.

Pullout loads and displacements at the front of the specimens were measured using a load cell and an LVDT mounted on the pullout hydraulic system, respectively. The displacements of the specimens at a distance of 1 ft. from the front were also monitored using tell-tail metal rods which extended through the wooden blocks and connected to an LVDT at the loading frame. Strain gauges were installed on some geogrids and woven geotextiles at various locations along the specimen. Figures 27 and 28 show the locations of displacement and strain measurements in the geogrid specimens. A schematic of the strain gauge locations along the geogrid specimens is shown in figure 29.

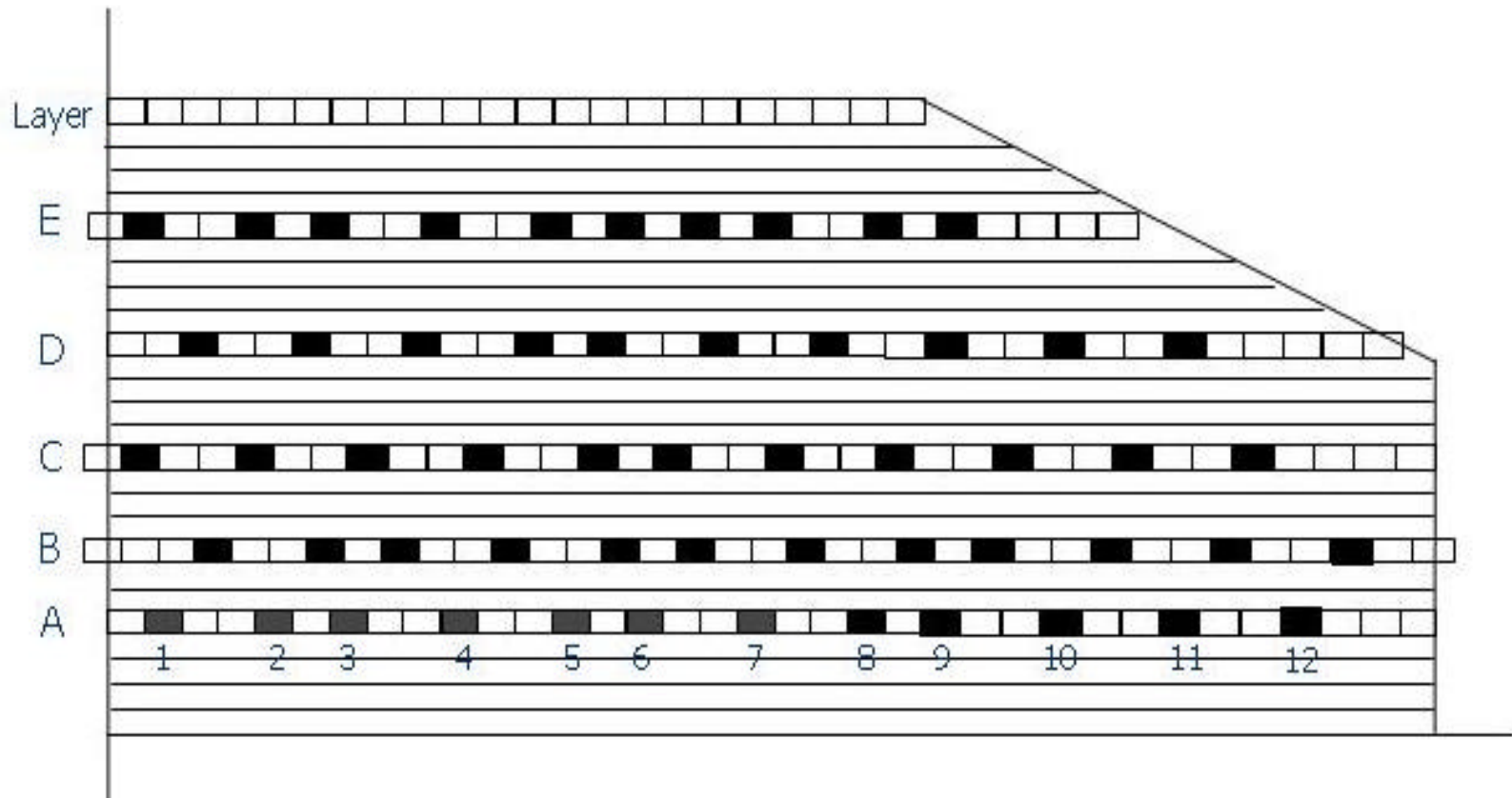


**Figure 26**  
**Schematic of the locations of pullout tests in the wall**

**Table 10**  
**List of the pullout tests in the field**

Layer	Location	Material	Length (ft)	No. of blocks above specimen	Overburden Pressure (psi)
A	A-1	UX-1700	3	22.5	13
	A-2	UX-1700	4	22.5	13
	A-3	UX-1700	5	22.5	13
	A-4	Stratagrid-500	3	22.5	13
	A-5	Stratagrid-500	4	22.5	13
	A-6	Stratagrid-500	5	22.5	13
	A-7	Woven-6x6	3	22.5	13
	A-8	Woven-6x6	4	22.5	13
	A-9	Woven-4x4	3	22.5	13
	A-10	Nonwoven	3	20	11.5
	A-11	Nonwoven	4	18	10.5
	A-12	Plate A	1	14	8
B	B-1	UX-1700	3	19.5	11.3
	B-2	UX-1700	4	19.5	11.3
	B-3	UX-1500	3	19.5	11.5
	B-4	Stratagrid-500	3	19.5	11.5
	B-5	Stratagrid-500	4	19.5	11.5
	B-6	Stratagrid-500	5	19.5	11.5
	B-7	Woven-6x6	3	19.5	11.5
	B-8	Woven-6x6	4	19.5	11.5
	B-9	Woven-4x4	3	18	10.5
	B-10	Nonwoven	3	14	8
	B-11	Nonwoven	4	12	7
	B-12	Plate B	1	10	6
C	C-1	UX-1700	3	15.5	9
	C-2	UX-1500	3	15.5	9
	C-3	UX-1500	4	15.5	9
	C-4	Stratagrid-500	3	15.5	9
	C-5	Stratagrid-500	4	15.5	9
	C-6	Stratagrid-500	5	15.5	9
	C-7	Woven-6x6	3	15.5	9
	C-7	Woven-4x4 (C1)	3	15.5	9
	C-9	Woven-4x4 (C2)	3	14	8
	C-10	Nonwoven	3	11.5	6.6
	C-11	Plate-C	1	8.5	5

(Continued)

**Table 10**  
**List of the pullout tests in the field (continued)**

Layer	Location	Test Name	Length (ft)	No. of blocks above specimen	Overburden Pressure (psi)
D	D-1	UX1500	3	10.5	6
	D-2	UX1500	4	10.5	6
	D-3	UX1500	5	10.5	6
	D-4	UX750	3	10.5	6
	D-5	UX750	4	10.5	6
	D-6	Woven 6x6	3	10.5	6
	D-7	Woven 4x4	3	10.5	6
	D-8	Woven 4x4	4	10.5	6
	D-9	Woven 4x4	5	9	5.2
	D-10	Nonwoven	4	5.5	3.2
E	E-1	UX1500	3	5.5	3.2
	E-2	UX1500	4	5.5	3.2
	E-3	UX1500	5	5.5	3.2
	E-4	UX750	3	5.5	3.2
	E-5	UX750	4	5.5	3.2
	E-6	UX750	5	5.5	3.2
	E-7	Woven 4x4	3	5.5	3.2
	E-8	Woven 4x4	3	5.5	3.2
	E-9	Woven 4x4	4	5.5	3.2
	E-10	Woven 4x4	5	4.5	2.7



**Figure 27**  
**View of the instrumentation in geogrid UX-1500**



**Figure 28**  
**View of the instrumentation in geogrid Stratagrid-500**

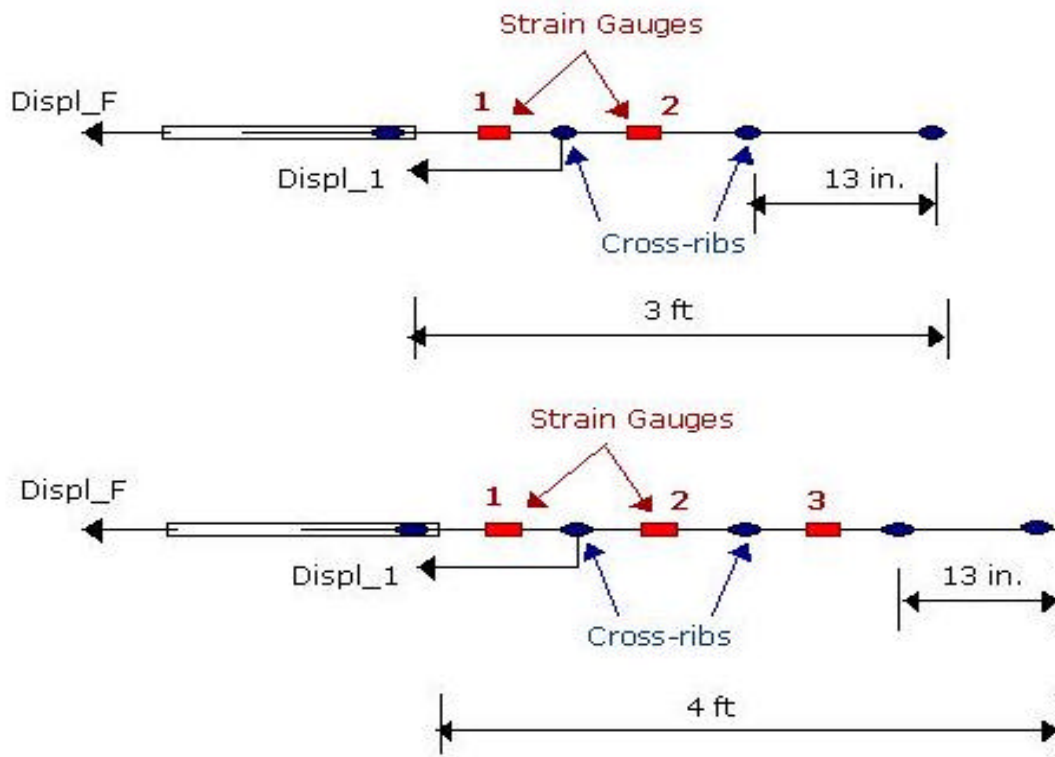


**Figure 29**  
**Schematic of the instrumentation in the 3 ft. and 4 ft. geogrid specimens**

## DISCUSSION OF RESULTS

### Pullout Tests on the Clamping Plates

#### Laboratory Pullout Tests

Pullout tests were conducted on the clamping plates without the geosynthetics to determine their frictional resistance. The plates were 1 ft. wide and extended 6 in. inside the soil. The clamps were tested at confining pressures of 3, 5, and 7 psi. The results of the pullout tests on the clamping plates are shown in figure 30. The pullout loads of the plates were subtracted from the results of laboratory pullout tests on the geosynthetics. The resistance of the plate was represented by the best fit equation in the form:

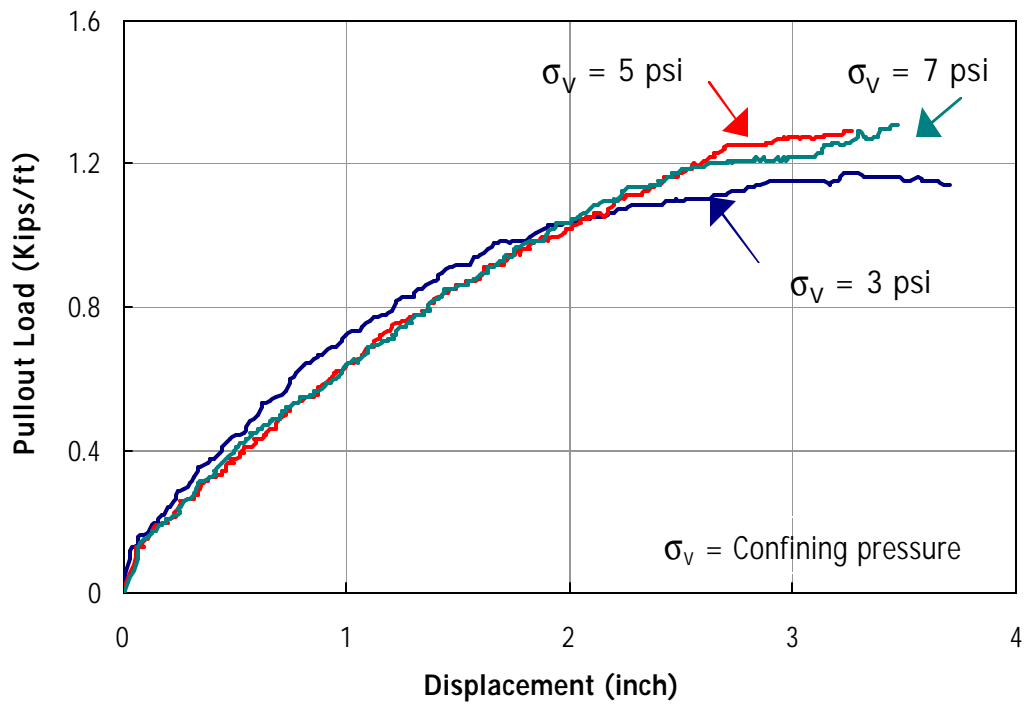
$$y = a x^2 + b x \quad (1)$$

Table 11 shows the plates' pullout resistance and the best fit parameters "a" and "b" of the best fit curves. The average values of -0.125 and 0.787 were used for "a" and "b" for all the ranges of confining pressures.

#### Field Pullout Tests

In the field tests, the clamping plates were 1 ft. wide and extended 9 in. inside the soil. The results of the field tests are shown in figure 31. The pullout curves of the plates were not significantly dependent on the confining pressure and were linear up to a pullout resistance of 0.8 Kips/ft at a plate displacement of 0.5 in. The resistance remained approximately constant at larger displacements.

In subsequent sections of the report, the results of pullout tests are presented after subtraction of the plates' frictional resistance.



**Figure 30**  
**Lab pullout test results on the clamping plates**

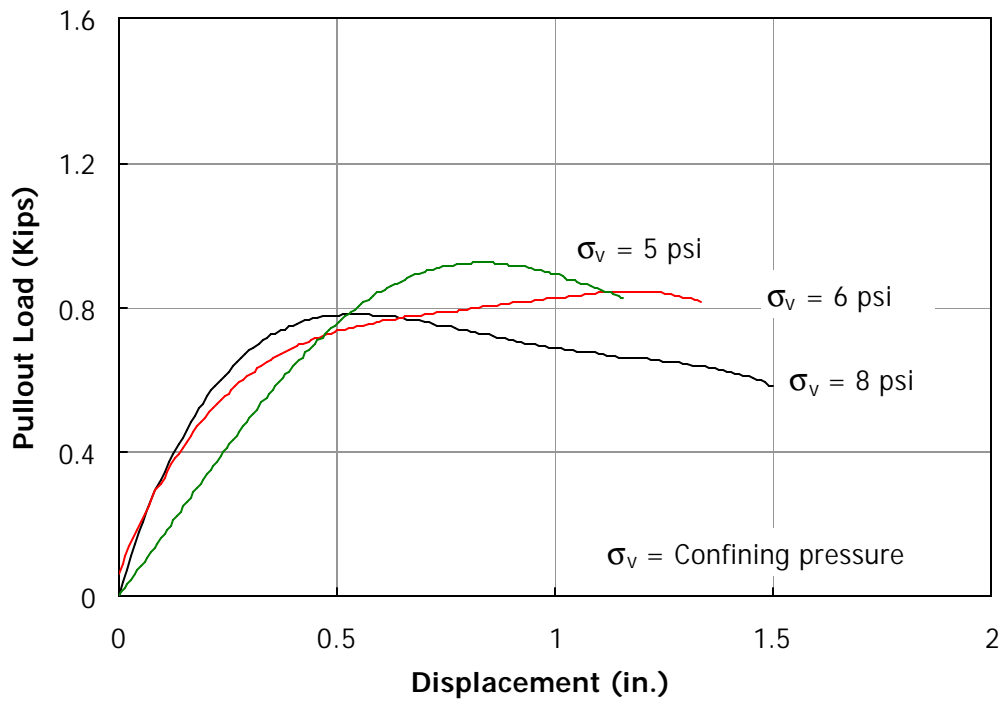


**Figure 31**  
**Field pullout test results on the clamping plates**

**Table 11**  
**Pullout test results on the clamping plates**

Test	Confining pressure (psi)	Pullout Resistance (Kips/ft)	a	b
1	3	1.1	-0.1465	0.8293
2	5	1.26	-0.1112	0.7542
3	7	1.28	-0.12	0.7761
Average			-0.125	0.787

**Pullout Tests on Tensar UX-750**

**Laboratory Pullout Test**

The results of the pullout tests on the UX-750 geogrid at confining pressures of 3, 5, and 7 psi are shown in figure 32.

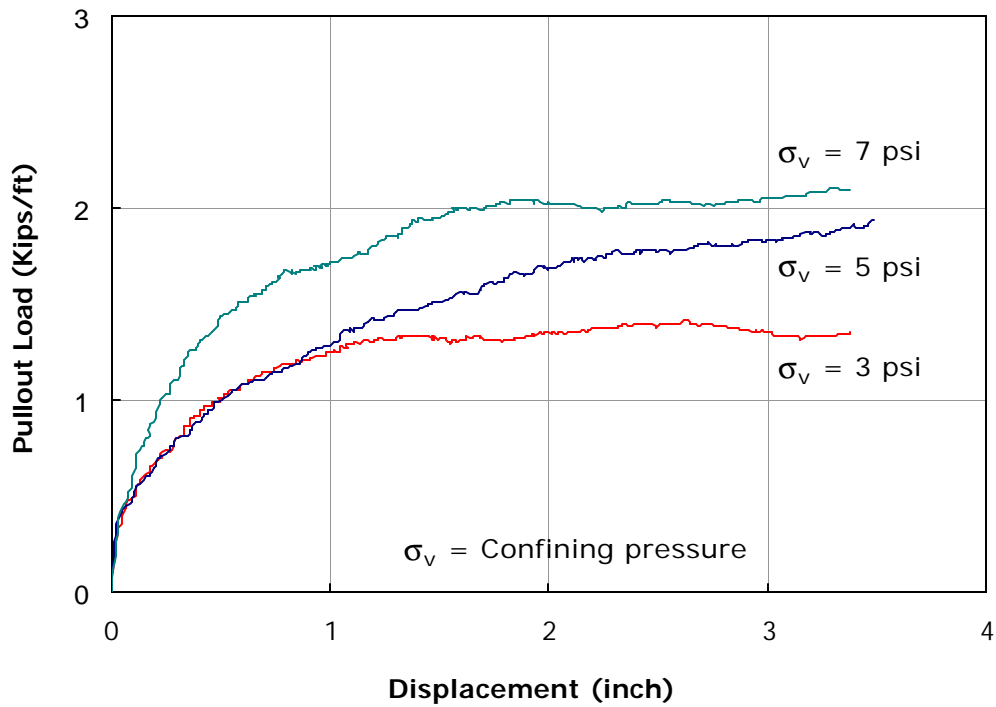


**Figure 32**  
**Lab pullout test results on the UX-750 geogrid**

### Field Pullout Tests

Table 12 shows the results of the pullout tests on the UX750 geogrid in the field. Tests are identified in the table by their layer number and the length of the specimen. Refer to table 10 for the location of the specimens in the wall. The results of pullout load versus front displacement are shown in figures 33 and 34 for confining pressures of 3.2 psi and 6 psi, respectively. It should be noted that the breakage load of the geogrid specimen UX750-D4 was comparable to the geogrid unconfined strength of the material (2,200 lb/ft).

**Table 12**  
**Field pullout test results on the UX750 geogrid**

Test	No. of blocks	Overburden Pressure (psi)	Length (ft)	Pullout Resistance (Kips/ft)	Failure Mode
UX750-D3	10.5	6	3	2	Pullout
UX750-D4	10.5	6	4	2.26	Breakage
UX750-E3	5.5	3.2	3	1.74	Pullout
UX750-E4	5.5	3.2	4	2	Pullout
UX750-E5	5.5	3.2	5	1.8	Pullout

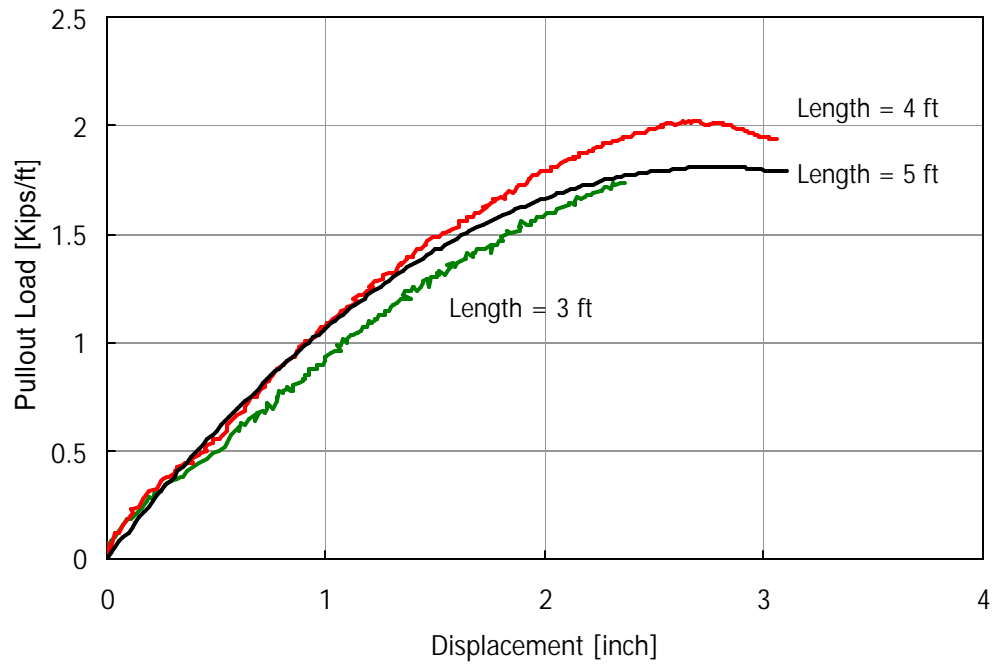


**Figure 33**  
Field results on the UX750 geogrid at confining pressure 3.2 psi

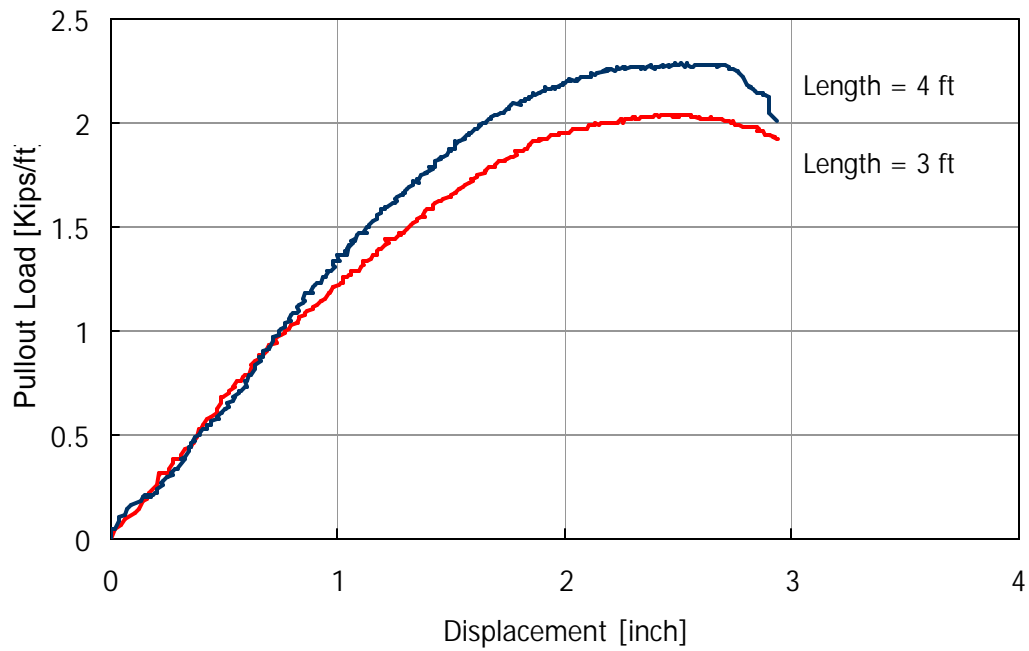


**Figure 34**  
Field results on the UX750 geogrid at confining pressure 6 psi

The location of strain gauges in the 3 ft. and 4 ft.-long UX-750 specimens is shown in figure 35. The results of strain measurements were used to determine the strain distribution along the length of the specimen during the test. The distribution of strains along the specimen length is plotted in figure 36 for test UX750-E5. The figure shows strain curves at various levels of front displacement of 0.5, 1.0, and 1.5 inches. The strain in the first element is the average strain at the front element and it was calculated from the displacement measurements in the relationship:

$$\varepsilon_{(1)} = [\text{Displ}_F - \text{Displ}_1] * 100 / \Delta L \quad (2)$$

where,  $\text{Displ}_F$  and  $\text{Displ}_1$  are the measured displacements at the front cross rib and at a node located 1 ft. from the front, respectively, and  $\Delta L$  is the distance between the two nodes (1 ft). The strains at nodes 3, 5 and 7 are measured by strain gauges. The results show that pullout resistance developed before the shear strength was fully mobilized along the whole length of the specimen.

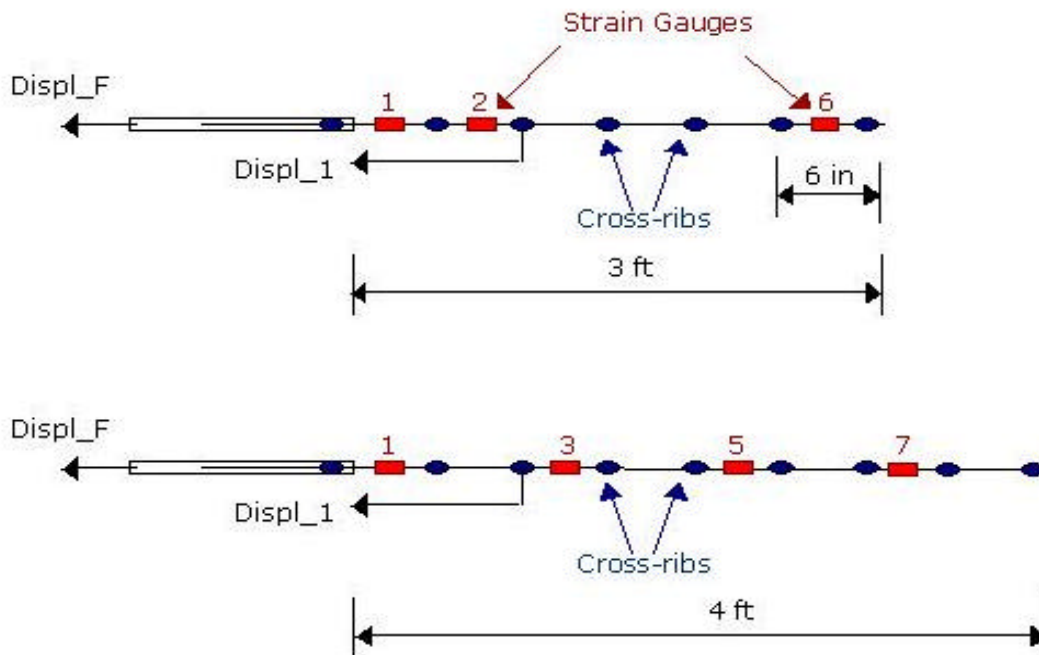


**Figure 35**  
**Location of strain gauges in UX-750 geogrid**

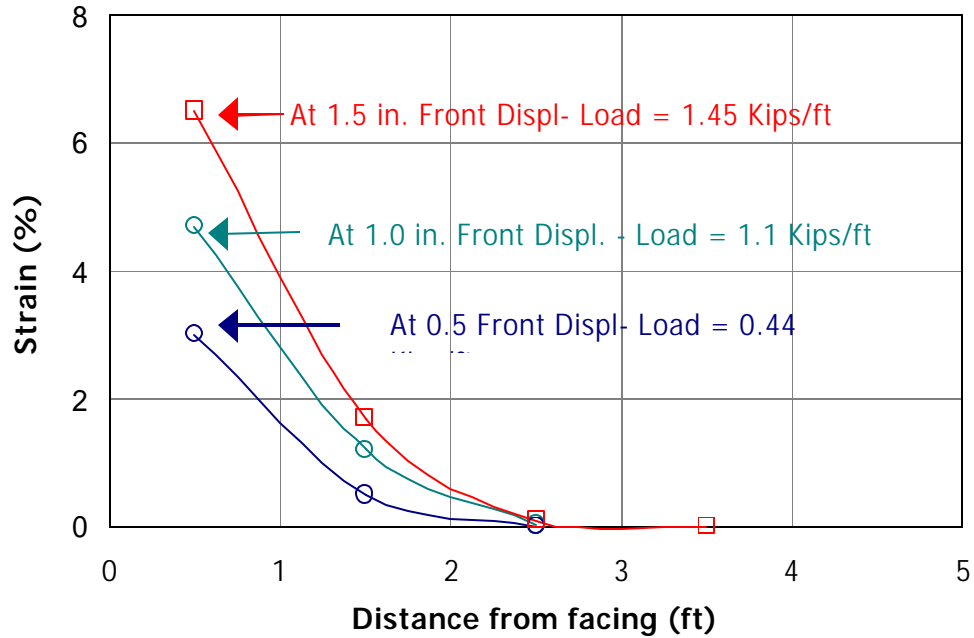


**Figure 36**  
**Strain distribution along the specimen in test UX750-E5**

### Comparison between Lab and Field Pullout Tests

The comparison between the lab and field pullout resistance results for the tests on the 3-ft.-long UX-750 geogrid is shown in figure 37. Although the results look comparable at various confining pressures, the shape of the field and lab pullout load curves were different, as shown in figure 38. Figure 39 shows the displacement at various locations in both tests. In the figure, the displacement measurements at the front and at ‘Disp1-1’ location are plotted for lab and field tests. The figure shows that the front displacements were comparable for both tests. However, the displacement at 1 ft. from the front was significantly lower in the field test; indicating a higher elongation of the front element in the field specimen.

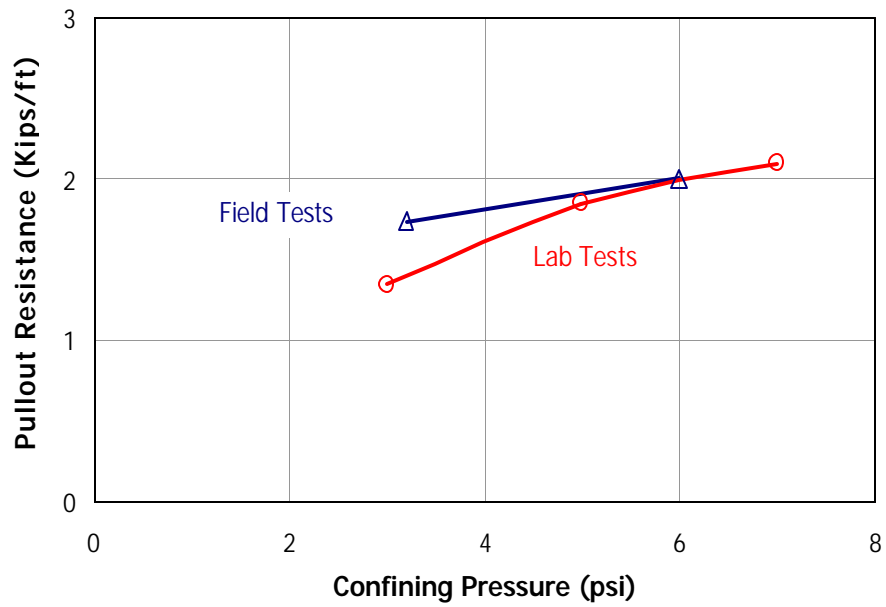


**Figure 37**  
**Lab and Field pullout resistance for the 3-ft. geogrid UX-750**

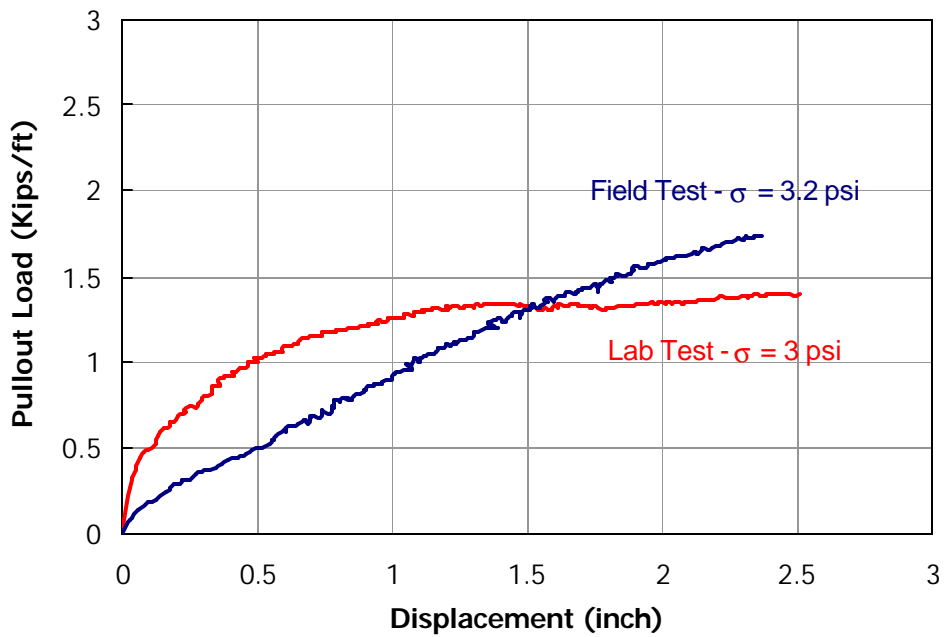


**Figure 38**  
**Lab and Field pullout loads for the 3-ft. geogrid UX-750**

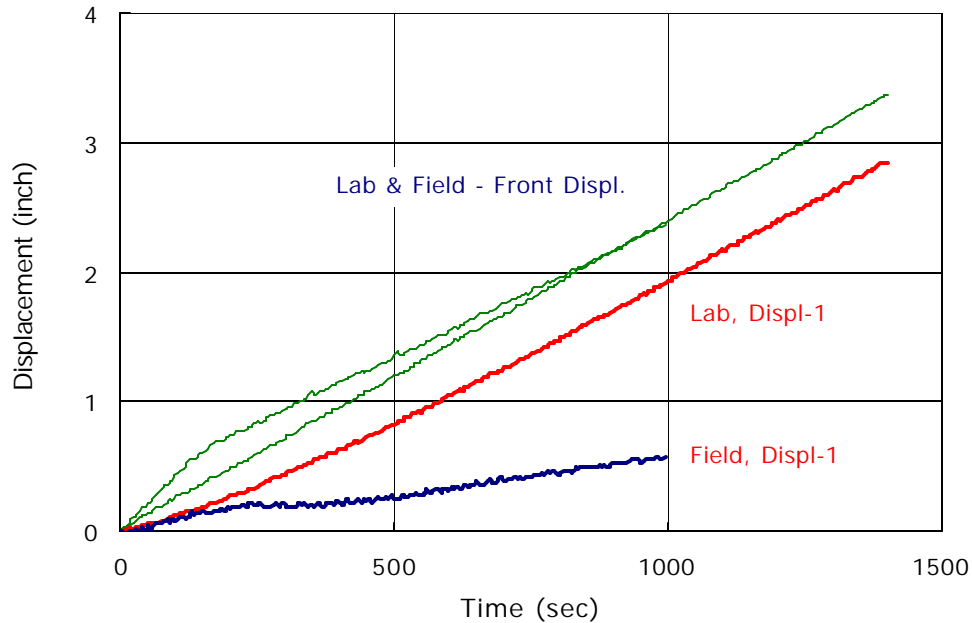


**Figure 39**  
**Displacements in the lab and field geogrids UX-750**

### **Pullout Tests on Tensar UX-1500**

#### **Laboratory Pullout Test**

The results of the lab pullout tests on the UX-1500 geogrid are shown in figure 40.

#### **Field Pullout Tests**

Tensar UX-1500 was tested in the field at various confining pressures and specimen lengths. Table 13 shows the testing parameters and pullout resistance from the field tests. The results of tests on the 3-ft.-long specimens are shown in figure 41. Pullout resistance commonly increases with an increase of confining pressure. However, the geogrid at level C had lower pullout resistance. Many factors may have caused the low pullout resistance in this test such as low soil density and higher moisture contents.

The results of pullout tests at various specimen lengths are shown in figures 42 and 43 for confining pressures of 3.2 and 6 psi, respectively. The increase in specimen length resulted in an increase in pullout resistance. However, the specimen length had small effect on pullout

resistance at the early stages of pullout. Figure 44 shows the effect of specimen length on the pullout resistance.

The location of the strain gauges in the UX1500 specimens is shown in figure 45. The measurements of strain along the geogrid specimen in test UX1500-E4 is shown in figure 46. The results show that the strains were mobilized along the full length of the specimen at the low confining pressure of 3.2 psi.

**Table 13**  
**Field pullout test results on the UX1500 geogrid**

Test	No. of blocks	Overburden Pressure (psi)	Length(ft)	Pullout Resistance (Kips/ft)
UX1500-B3	19.5	11.3	3	4.7
UX1500-C3	15.5	9	3	3.2
UX1500-C4	15.5	9	4	3.6
UX1500-D3	10.5	6	3	4.1
UX1500-D4	10.5	6	4	5.3
UX1500-D5	10.5	6	5	5.9
UX1500-E3	5.5	3.2	3	3.8
UX1500-E4	5.5	3.2	4	4.7
UX1500-E5	5.5	3.2	5	5.4

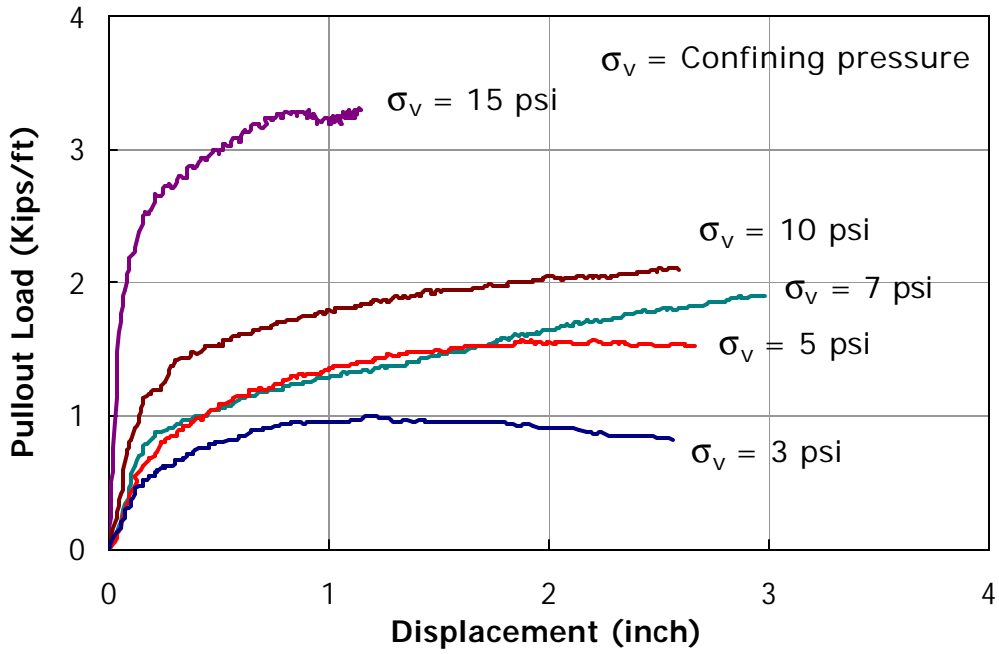


**Figure 40**  
**Lab pullout test results on the UX-1500 geogrid**

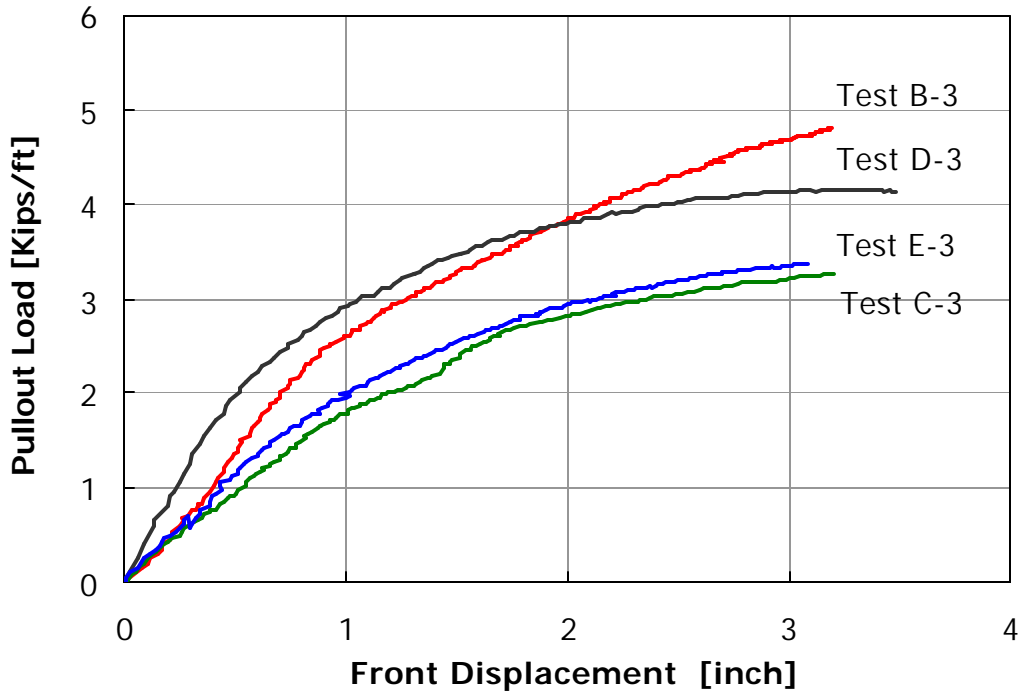


**Figure 41**  
**Field pullout tests on the UX-1500 geogrid, length 3 ft.**

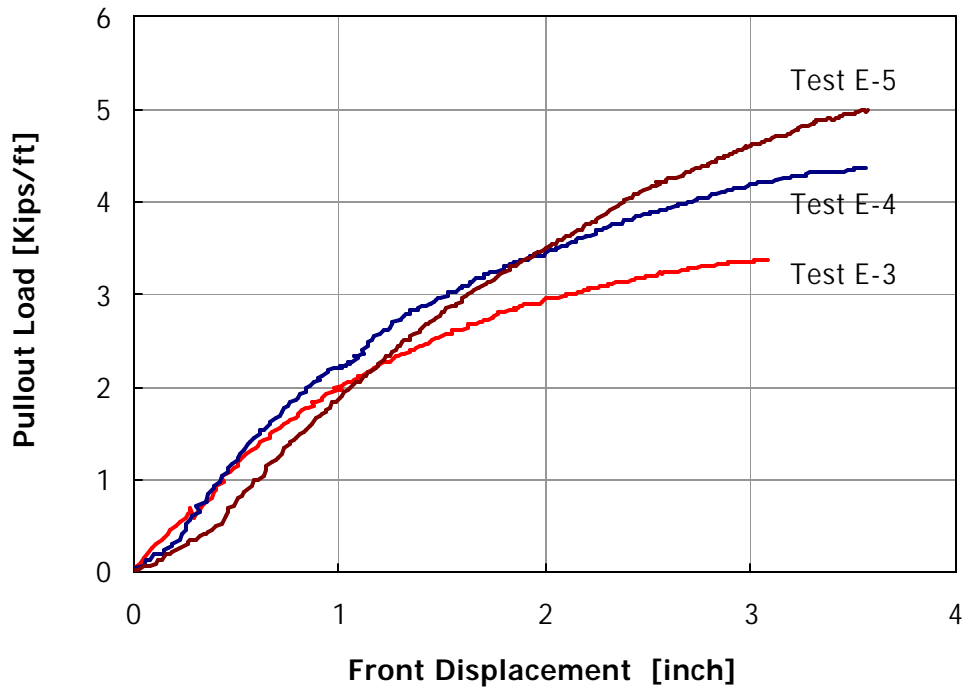


**Figure 42**  
Field pullout results of UX-1500 at confining pressure 3.2 psi

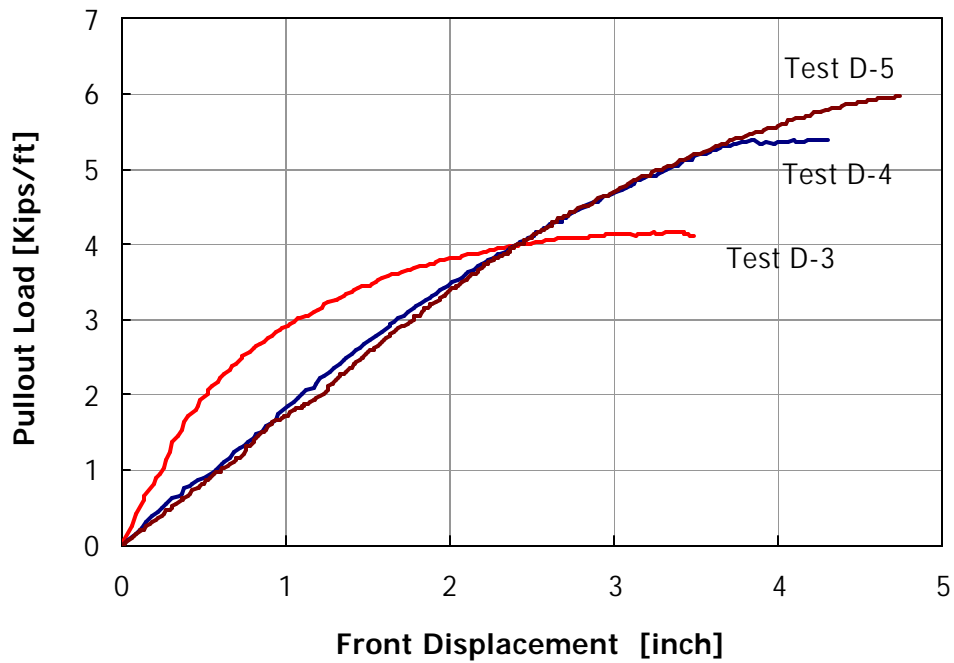


**Figure 43**  
Field pullout results of UX-1500 at confining pressure 6 psi

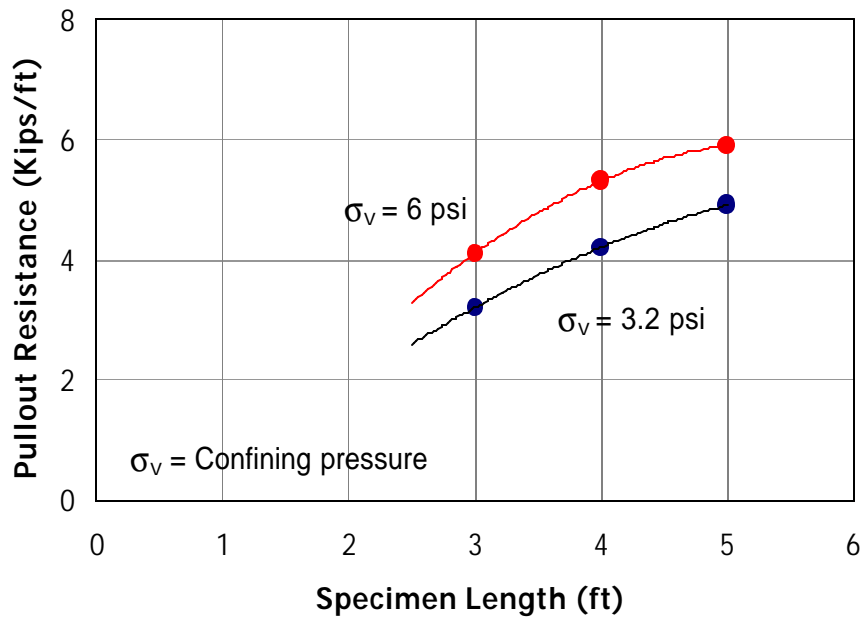


**Figure 44**  
Effect of specimen length on pullout resistance

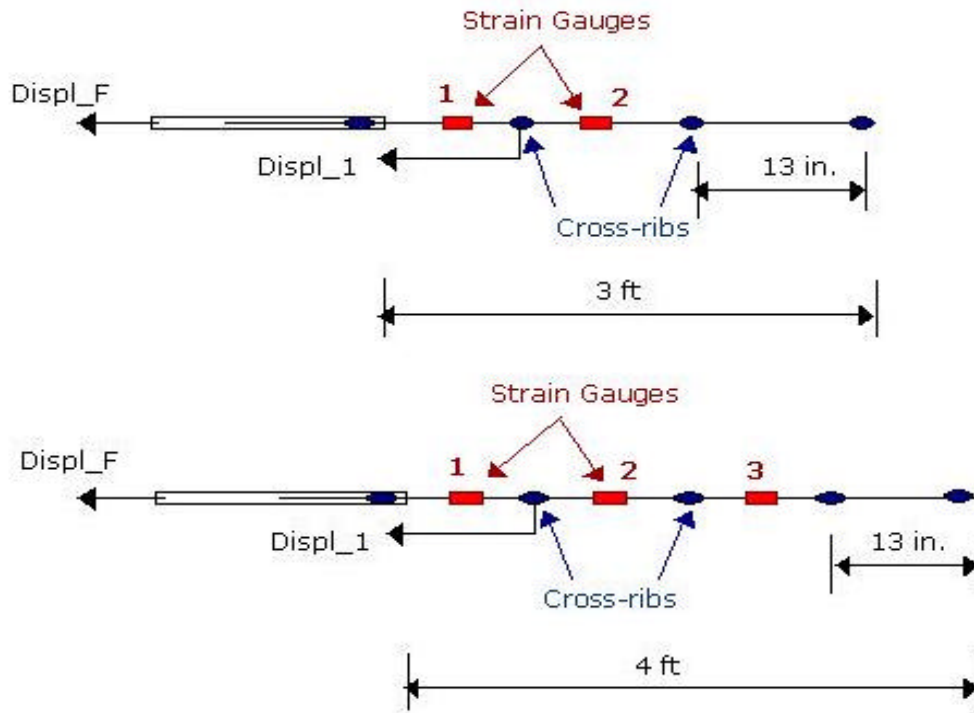


**Figure 45**  
Location of strain gauges in the UX1500 geogrid

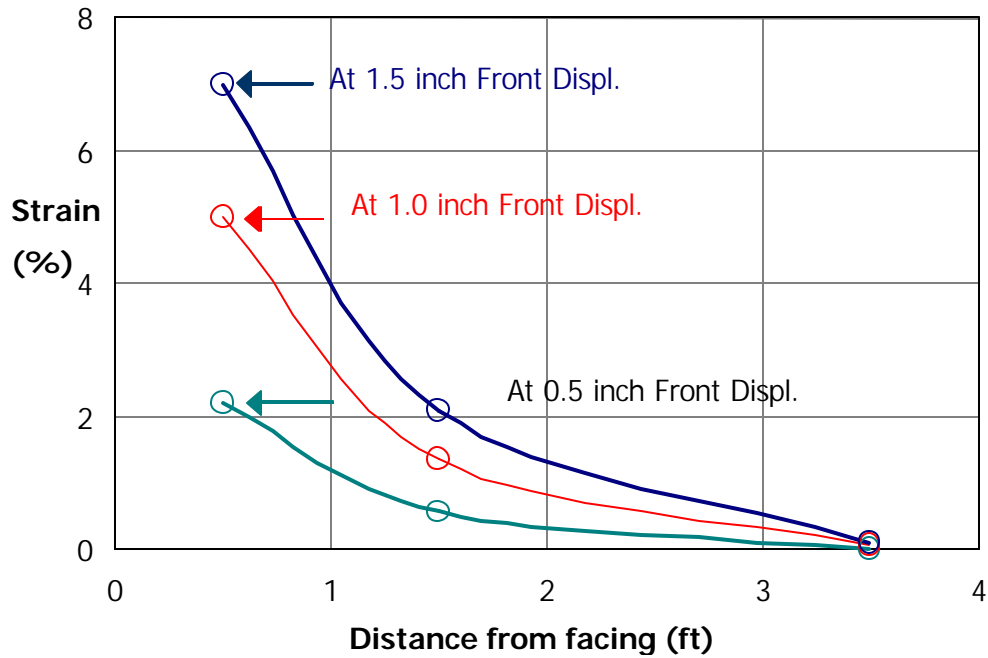


**Figure 46**  
**Strain along the geogrid specimen in test UX1500-E4**

**Comparison between Lab and Field Pullout Tests**

The results of lab and field pullout tests on the 3-ft.-long geogrids are plotted in figure 47 for various confining pressures. The figure shows that field tests had significantly higher pullout resistance than the ones in the lab. In order to further analyze geogrid pullout in the lab and field tests, the strains at the front elements of the specimens at confining pressure 3 psi were plotted in Figure 48. The strains were calculated from the LVDT measurements at the first elements of the specimens using equation (2). The figure shows a significantly higher elongation of the first element in the field specimen. The results suggest that soil confinement, or density, may be higher in the field than in the lab due to wall settlement or soil consolidation.

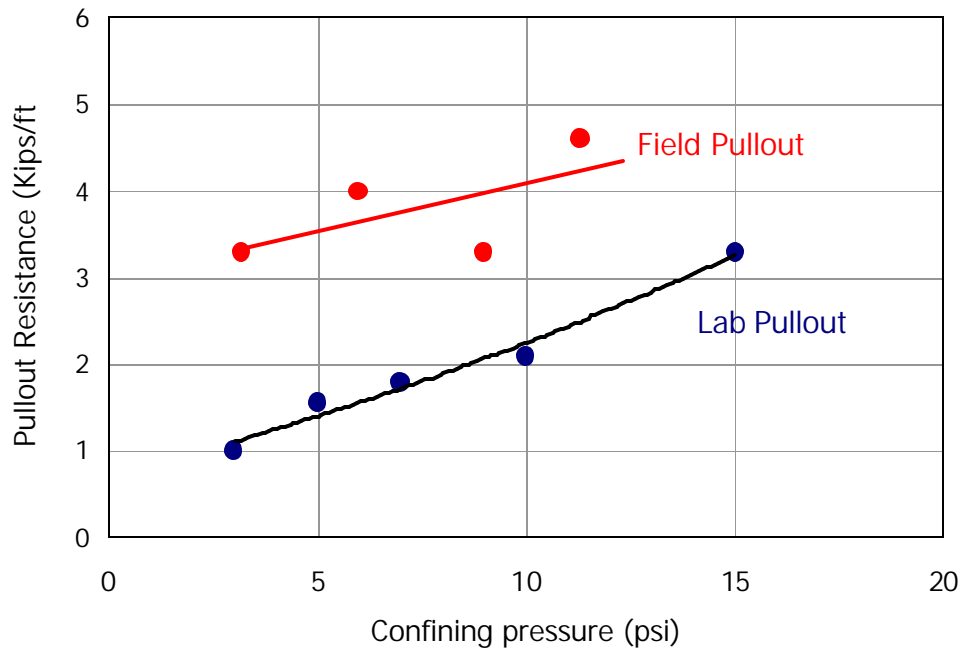


**Figure 47**  
**Lab and field pullout test results at various confining pressures**

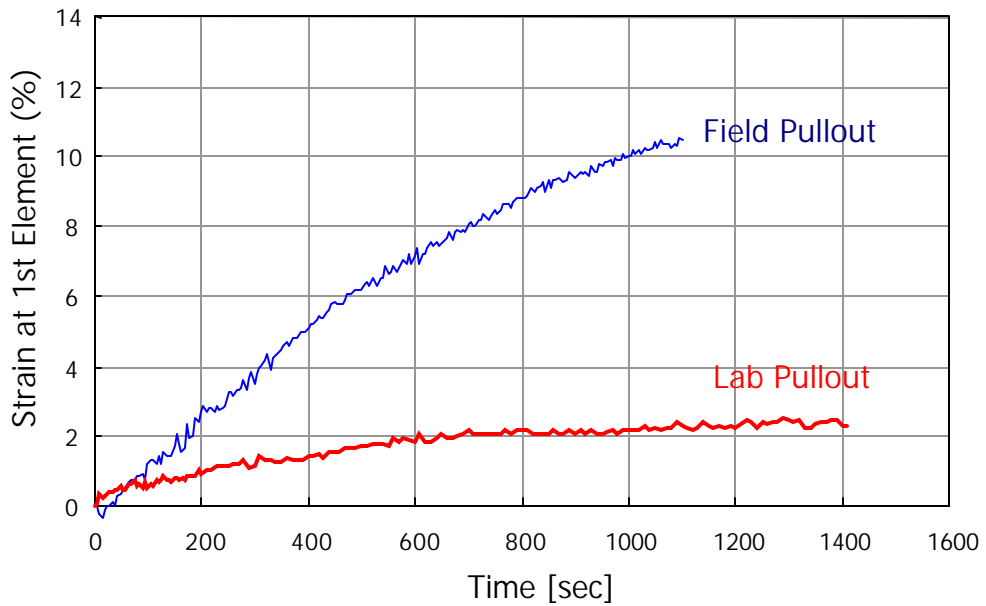


**Figure 48**  
**Measurements of front strains in field and lab pullout for UX-1500**

## Pullout Tests on Tensar UX-1700

### Laboratory Pullout Test

The results of the pullout tests on the geogrid at various confining pressures are shown in figure 49. The high-strength Tensar UX-1700 geogrid was tested at high confining pressures in the lab and the field.

### Field Pullout Test

Field pullout tests on this geogrid are shown in table 14. Pullout results on the 3-ft.-long specimens are shown in figure 50 for various confining pressures. Pullout loads at various specimen lengths are shown in figures 51 and 52 for confining pressures of 11.3 psi and 13 psi, respectively. Similar to the results on the geogrid UX-1500, the length of the specimen has a small effect on the pullout load until the specimen is fully mobilized at later stages of pullout loading.

**Table 14**  
**Field pullout test results on the UX-1700 geogrid**

Test	No. of blocks	Overburden Pressure (psi)	Length(ft)	Pullout Resistance(Kips/ft)
UX1700-A3	22.5	13	3	4.6
UX1700-A4	22.5	13	5	5.8
UX1700-A5	22.5	13	5	5.8
UX1700-B3	19.5	11.3	3	5.5
UX1700-B4	19.5	11.3	4	6.7
UX1700-C3	15.5	9	5	5

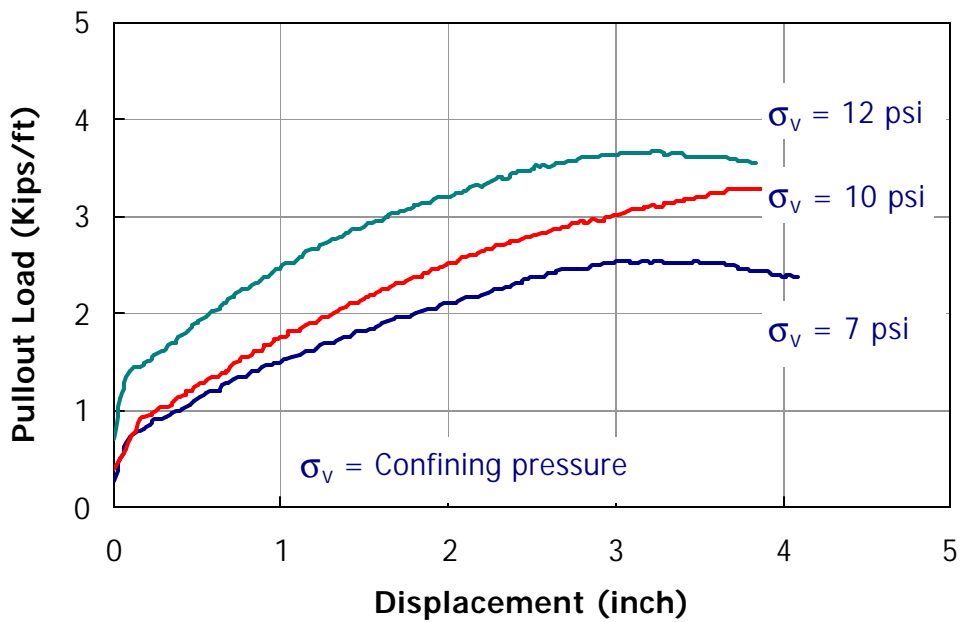


**Figure 49**  
**Lab pullout test results of the UX-1700 geogrid**

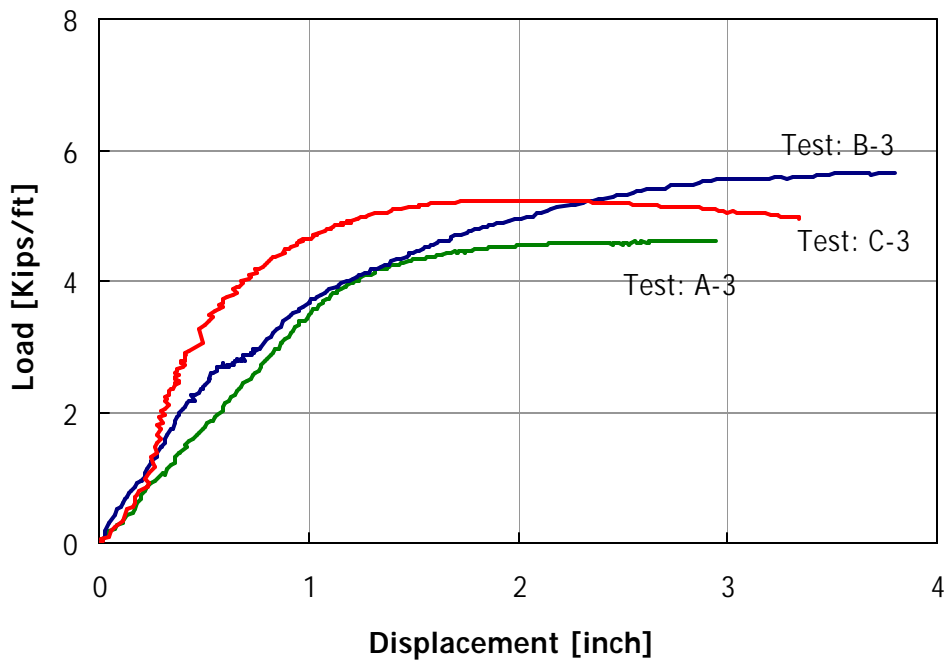


**Figure 50**  
**Field pullout on geogrid UX-1700 for specimen length 3 ft.**

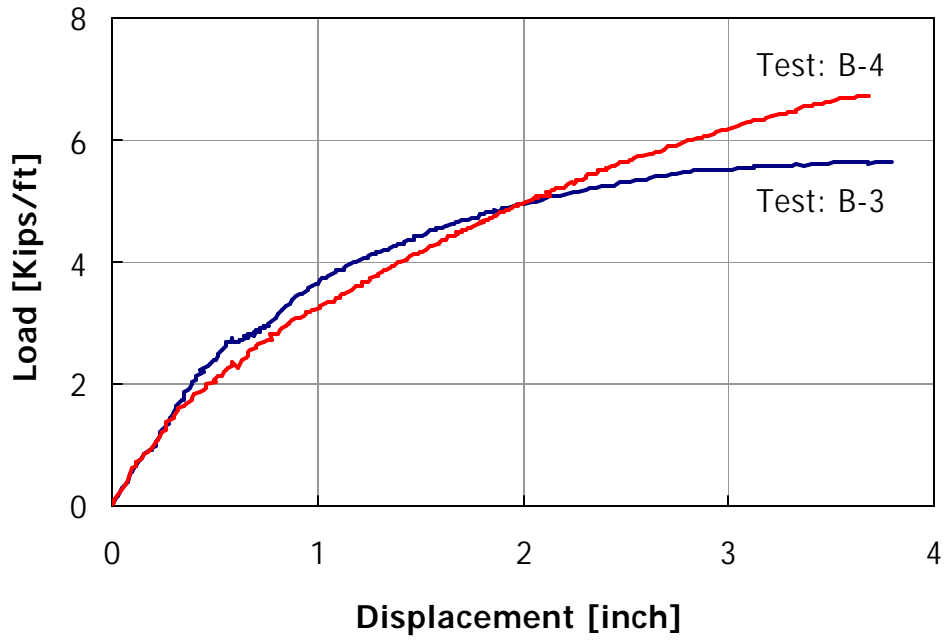


**Figure 51**  
**Pullout tests on UX-1700 at confining pressure 11.3 psi**

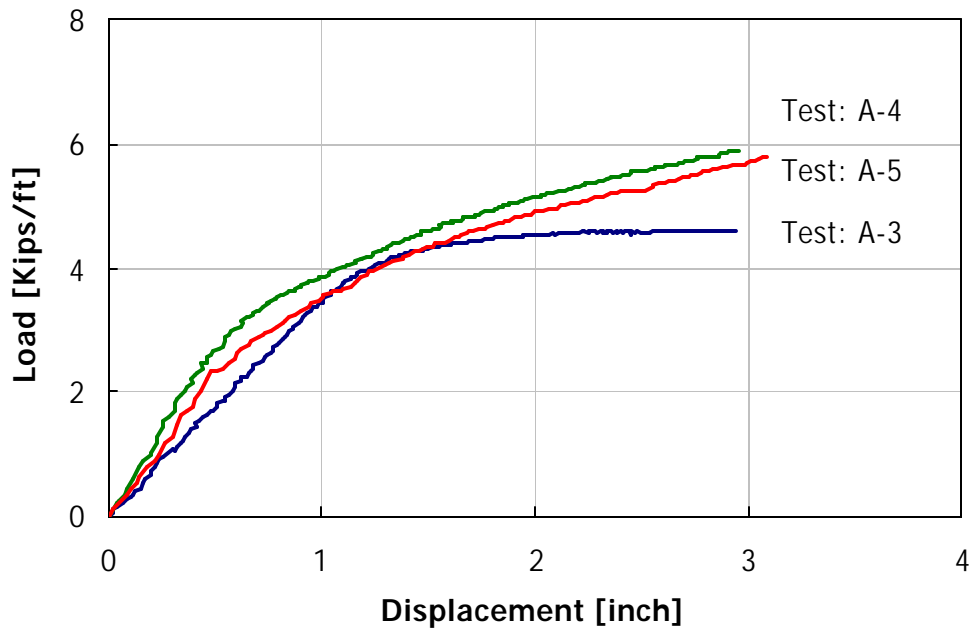


**Figure 52**  
**Pullout tests on UX-1700 at confining pressure 13 psi**

### Comparison between Lab and Field Pullout Tests

The comparison between the lab and field pullout resistance of the UX-1700 geogrid is similar to that of the UX-1500 geogrid. Field results were significantly higher than lab results as shown in figure 53 for a 3-ft. specimen length. Displacement measurements are also characterized by higher elongation at the front element in field specimens in comparison to lab tests. The displacement at the front and at the first cross-rib of the geogrid (Displ\_1) for both lab and field tests are shown in figure 54. The front displacement rates in both tests were almost identical. However, the figure shows much lower movement in the first cross-rib in the field test, and, consequently, higher elongation at the front geogrid element.

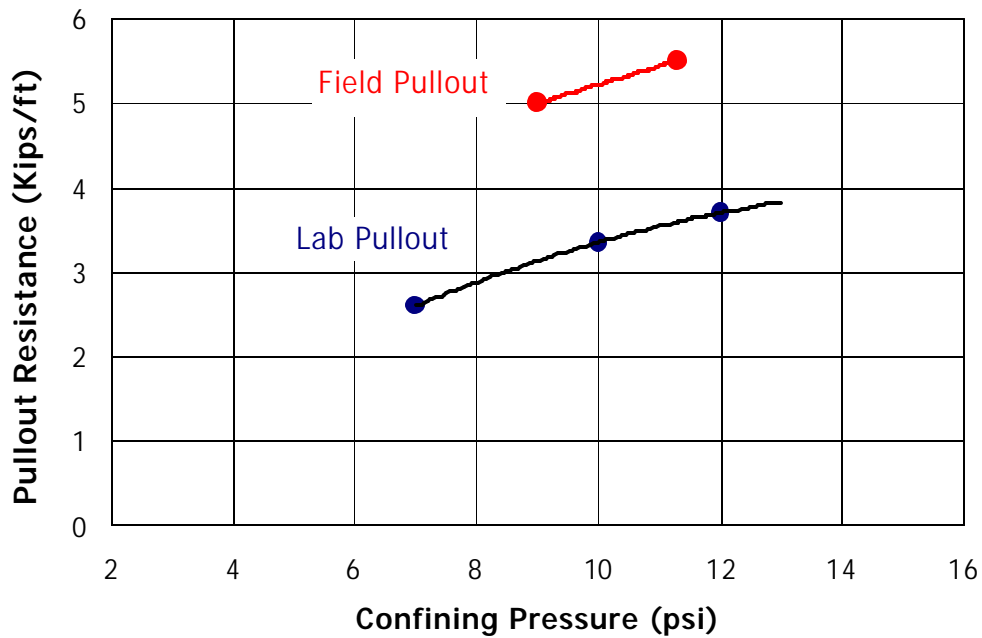


**Figure 53**  
**Lab and field pullout tests on the geogrid UX-1700**

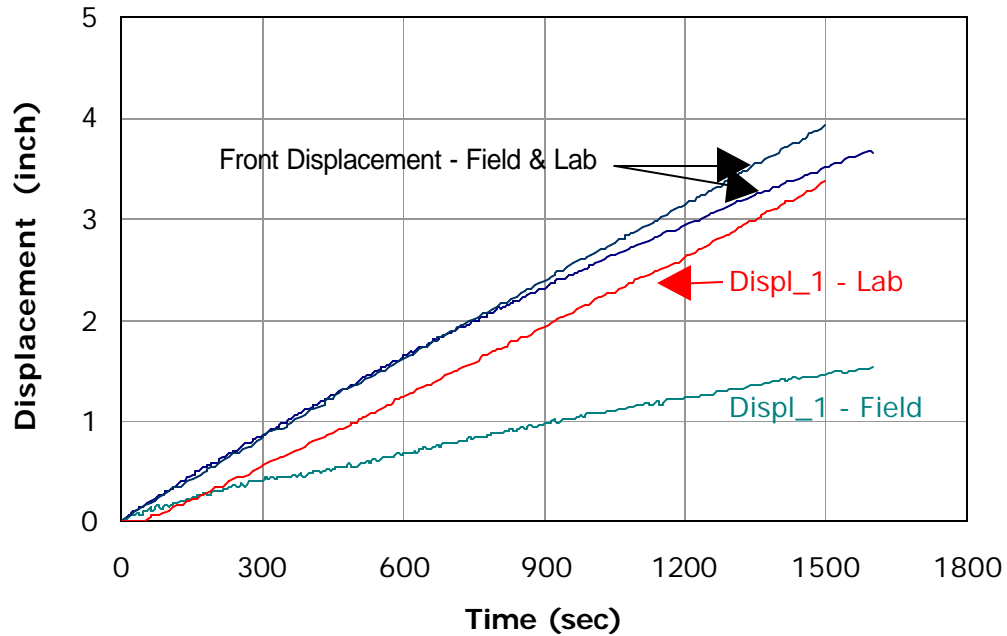


**Figure 54**  
**Displacement at front and node-1 in lab and field tests for UX-1700**

### **Pullout Tests on the Stratagrid-500**

#### **Laboratory Pullout Tests**

The results of the lab pullout tests on the Stratagrid are shown in figure 55.

#### **Field Pullout Tests**

The field tests on the Stratagrid 500 are shown in table 15. Most of the specimens ruptured at the high confining pressures of the field tests. However, the tests illustrate the pullout behavior before breakage, and test results for 3 ft. and 5 ft. specimens are shown in figures 56 and 57, respectively. Figure 58 shows the results of pullout tests at various confining pressures for a 3-ft.-long specimen.

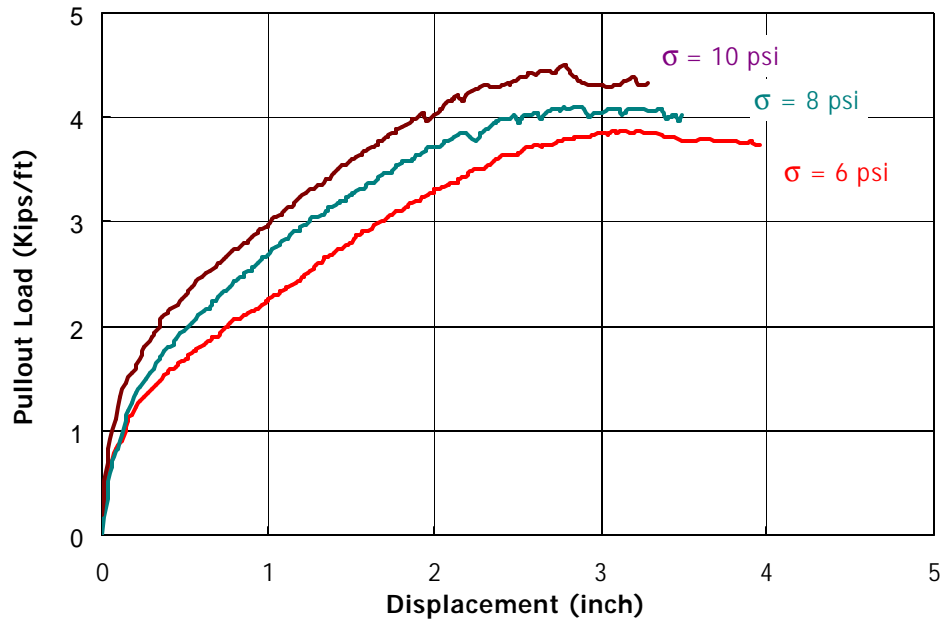


**Figure 55**  
**Lab pullout test results on the Stratagrid-500**

**Table 15**  
**Field pullout test results on the Strata-500 geogrid**

Test	No. of blocks	Overburden Pressure(psi)	Length(ft)	Pullout Resistance (Kips/ft)	Failure Mode
Strata-A3	22.5	13	3	5	Breakage
Strata-A4	22.5	13	4	4.4	Breakage
Strata-A5	22.5	13	5	5	Breakage
Strata-B3	19.5	11.3	3	4.8	Breakage
Strata-B4	19.5	11.3	4	3.3	Test stopped at 3.3 Kips/ft
Strata-B5	19.5	11.3	5	5	Breakage
Strata-C3	15.5	9	3	4	Pullout
Strata-C4	15.5	9	4	4.4	Breakage
Strata-C5	15.5	9	5	4.8	Breakage

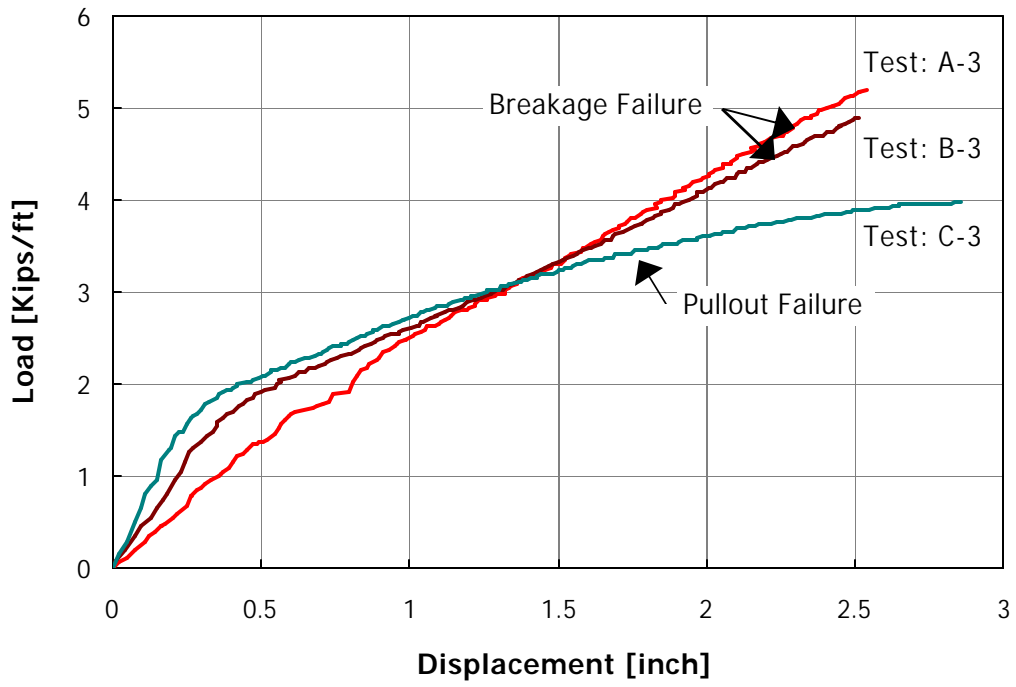


**Figure 56**  
**Field pullout test results on the 3-ft Stratagrid-500**

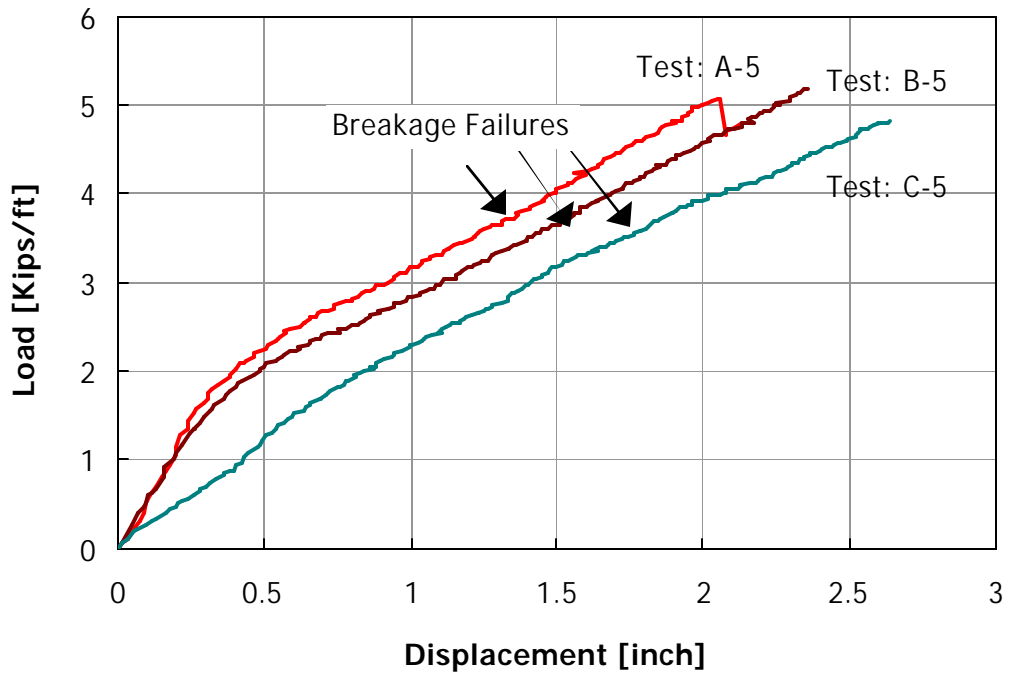


**Figure 57**  
**Field pullout test results on the 5-ft Stratagrid-500**

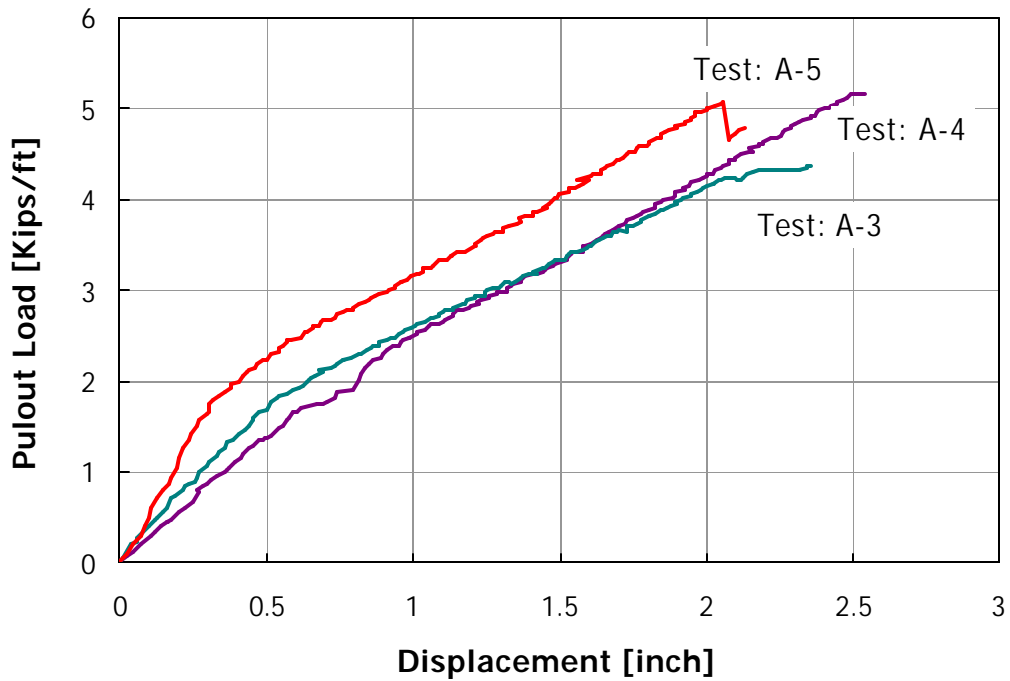


**Figure 58**  
**Field pullout results on the Stratagrid-500**

The strain distribution along the length of the specimen is shown in figure 59 during a pullout test on the 4-ft. specimen. The figure shows the strain distributions when the front displacements were at 0.5, 0.75, and 1.0 in. The figure shows that the strains were mobilized at the front half of the specimen during most of the pullout test.

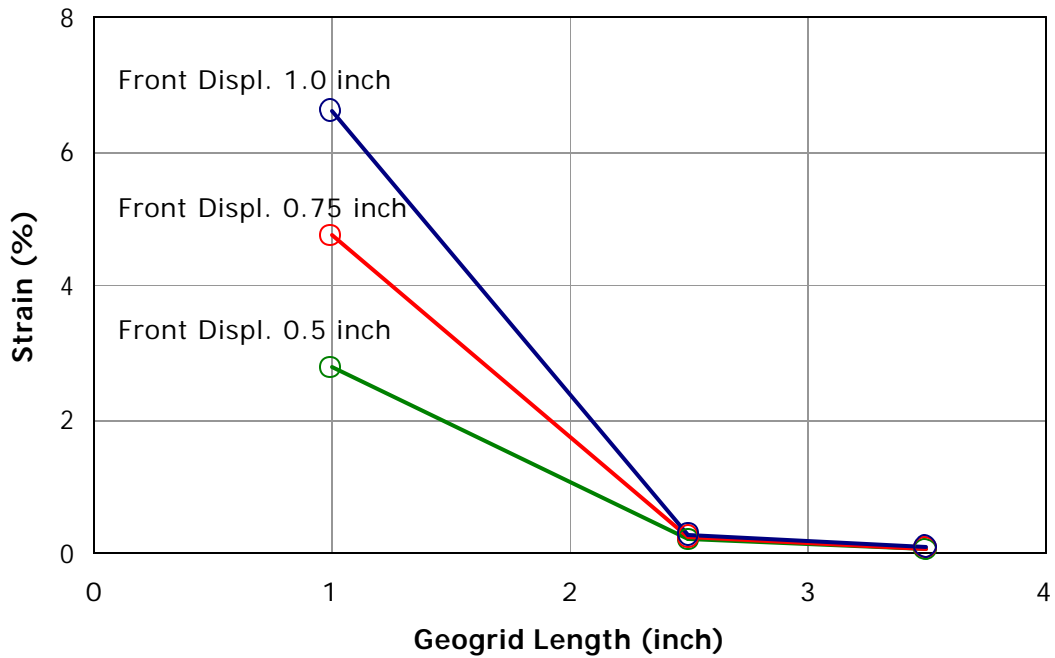


**Figure 59**  
**Strain distribution in the field along the 4-ft. Stratagrid-500**

**Comparison between Lab and Field Pullout Tests**

The field tests performed at confining pressures higher than 9 psi resulted in breakage of the specimens. The breakage load of the geogrid was near its unconfined tensile strength of 4,400 lb/ft.

The results of the lab and field pullout tests for 3-ft.-long specimens at various confining pressures are shown in figure 60. The figure shows that lab and field test results compared well for this geogrid.

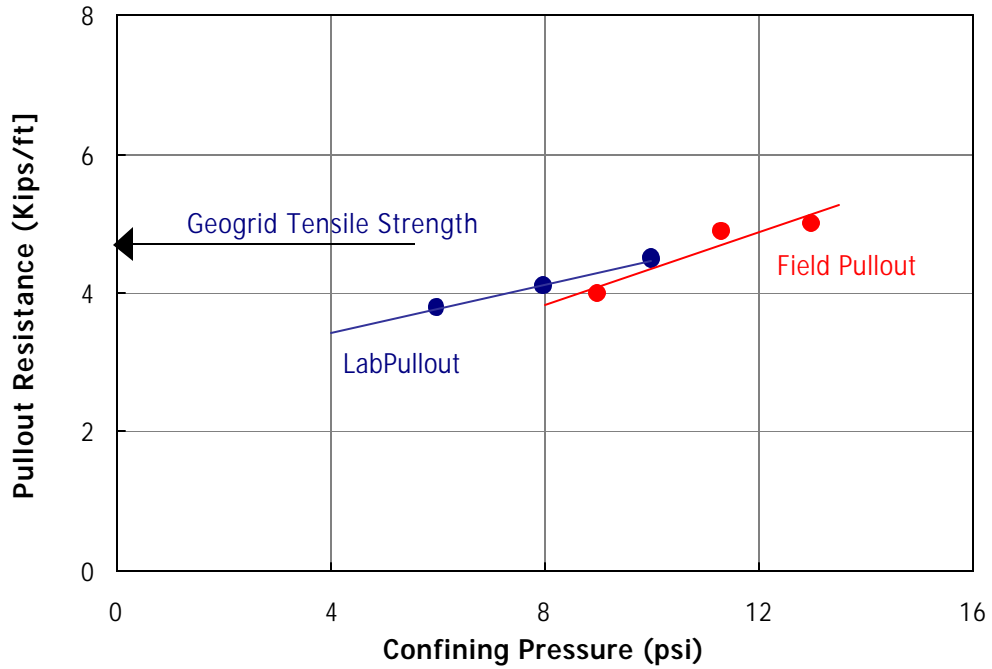


**Figure 60**  
**Comparison between lab and field pullout results for Statagrid-500**

### **Pullout Tests on the Woven Geotextile**

#### **Laboratory Pullout Tests**

The results of the lab pullout tests on the woven geotextile Geotex-4x4 are shown in figure 61.

#### **Field Pullout Tests**

The results of field pullout tests on the woven geotextile Geotex-4x4 are shown in table 16. The results of the tests for confining pressures 3.2 psi and 6 psi are shown in figure 62 and 63, respectively. Similar to the test results on the geogrid, the effect of specimen length is only measurable near the peak load at the late stage of pullout.

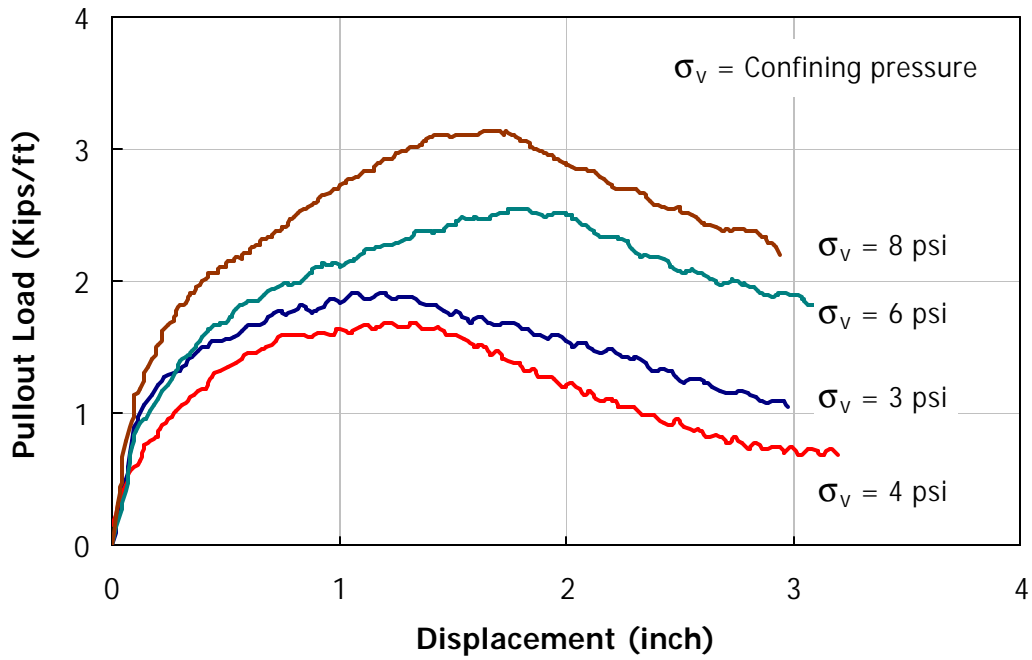


**Figure 61**  
**Lab pullout tests on the woven geotextile Geotex 4x4**

**Table 16**  
**Field pullout test results on the Geotex 4x4 geotextile**

Test	No. of blocks	Overburden Pressure (psi)	Length (ft)	Pullout Resistance (Kips/ft)	Failure Mode
Wov4x4-A3	22.5	13	3	3.6	Breakage
Wov4x4-D4	10.5	6	4	2.6	Pullout
Wov4x4-D5	9	5.2	5	3.5	Breakage
Wov4x4-E3	5.5	3.2	3	2.6	Pullout
Wov4x4-E4	5.5	3.2	4	2.5	Pullout
Wov4x4-E5	4.5	2.7	5	3.0	Pullout

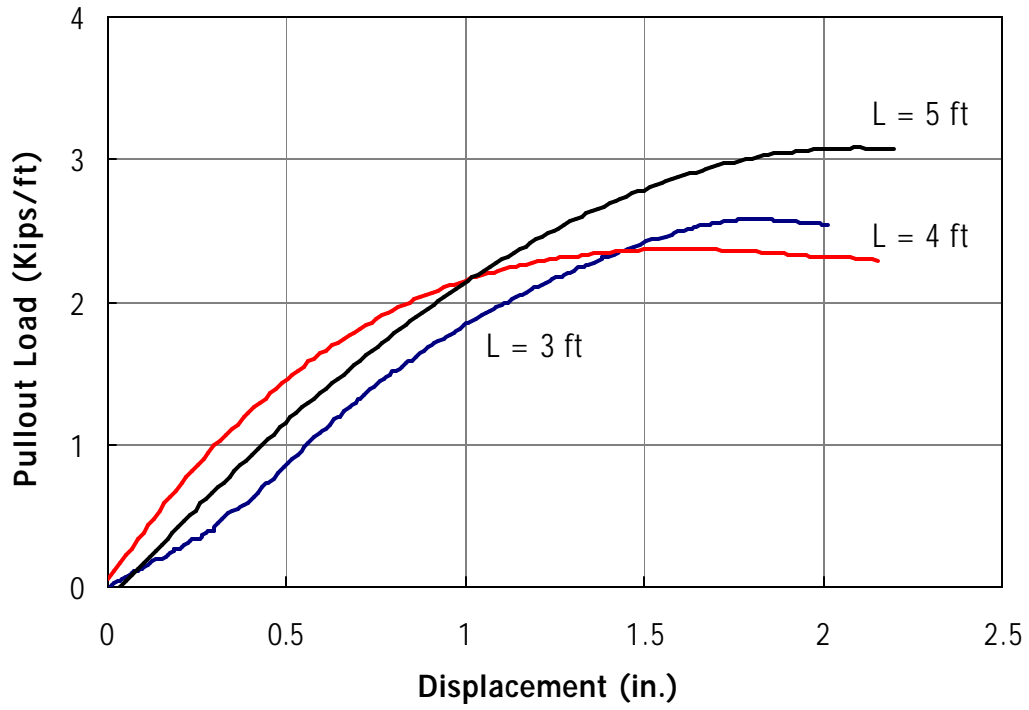


**Figure 62**  
Field pullout results on Geotex-4x4 at confining pressure 3.2 psi

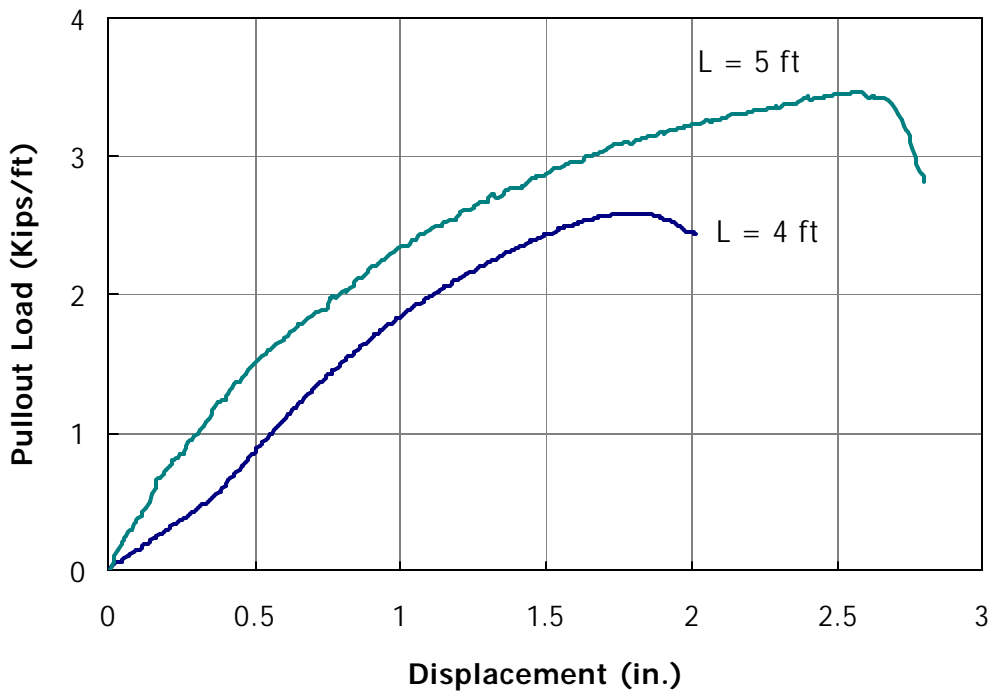


**Figure 63**  
Field pullout results on Geotex-4x4 at confining pressure 6 psi

The results of field pullout tests on the woven Geotex-6x6 geotextile are shown in table 17. The specimens broke at confining pressures of 11.3 psi and 13 psi. The breakage load of these specimens was about 6 kips/ft., which is less than the material tensile strength of 7.2 kips/ft. The results of pullout tests are shown in figures 64 and 65

**Table 17**  
**Field pullout test results on the Geotex-6x6 geotextile**

Test	No. of blocks	Overburden Pressure (psi)	Length (ft)	Pullout Resistance (Kips/ft)	Failure Mode
Wov6x6-A3	22.5	13	3	5.8	Breakage
Wov6x6-A4	22.5	13	4	5.9	Breakage
Wov6x6-B3	19.5	11.3	3	6	Breakage
Wov6x6-B4	19.5	11.3	4	6	Breakage
Wov6x6-C3	15.5	9	3	5.2	Pullout
Wov6x6-D3	10.5	6	3	5.1	Pullout

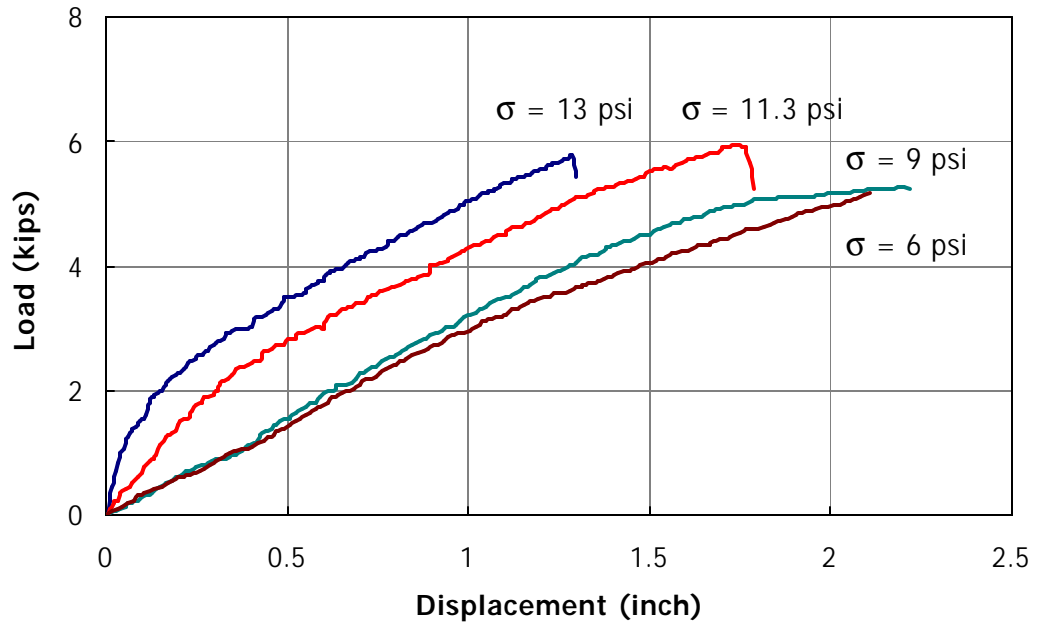


**Figure 64**  
Field pullout results on the Geotex-6x6 geotextile

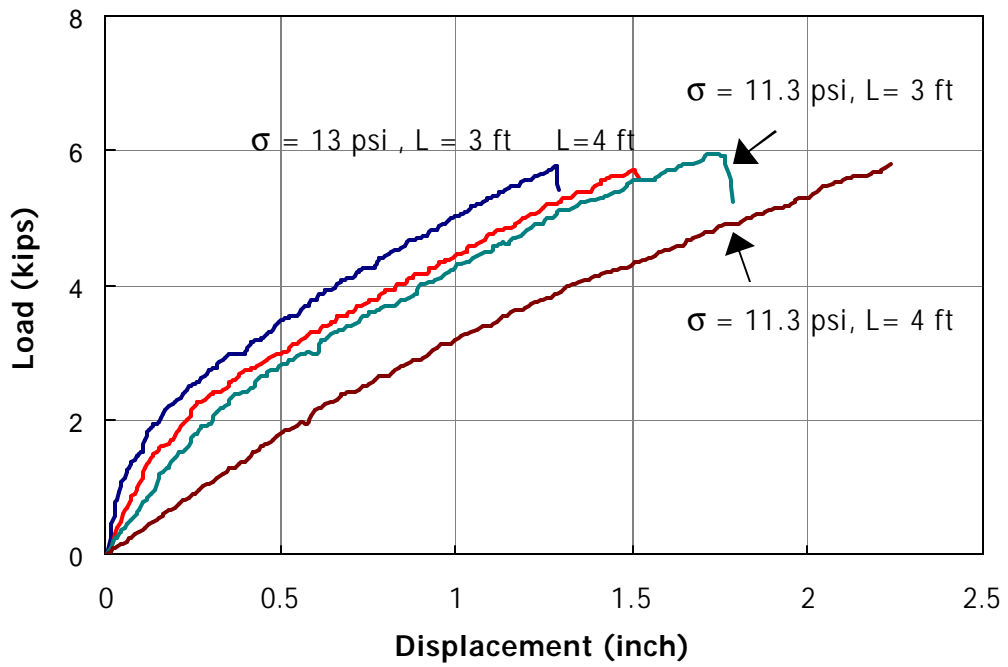


**Figure 65**  
Field pullout results on the Geotex-6x6 geotextile

## Pullout Tests on the Nonwoven Geotextile

### Field Pullout Tests

Only field pullout tests were performed on the nonwoven geotextile. Geotextile specimens of 3 ft. and 4 ft. lengths were tested at various confining pressure from 3 psi to 11 psi. A list of the pullout tests is shown in table 18. Figures 66 and 67 show the test results of the 3 ft. and 4 ft. lengths, respectively.

**Table 18**  
**Field pullout test results on the nonwoven geotextile**

Test	No. of blocks	Overburden Pressure (psi)	Length (ft)	Pullout Resistance (Kips/ft)	Failure Mode
NonWov-A3	20	11.5	3	2	Pullout
NonWov-A4	18	10.5	4	2.5	Pullout
NonWov-B3	14	8	3	1.7	Pullout
NonWov-B4	12	7	4	1.8	Pullout
NonWov-C3	11.5	6.6	3	1.3	Pullout
NonWov-D4	5.5	3.2	4	2.2	Pullout

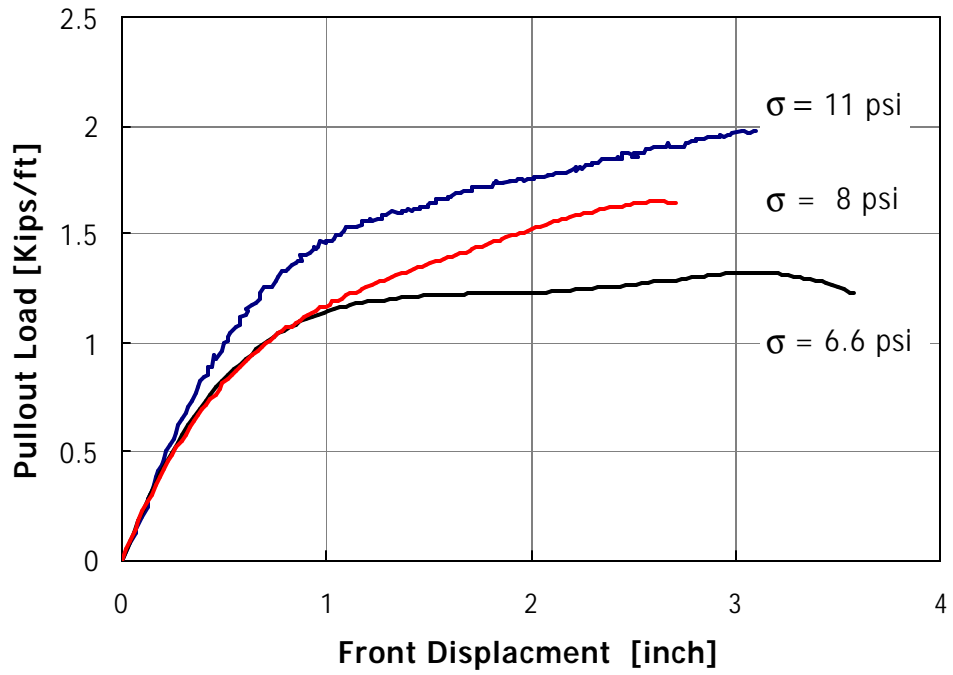


**Figure 66**  
Field pullout tests of the nonwoven of length 3 ft.

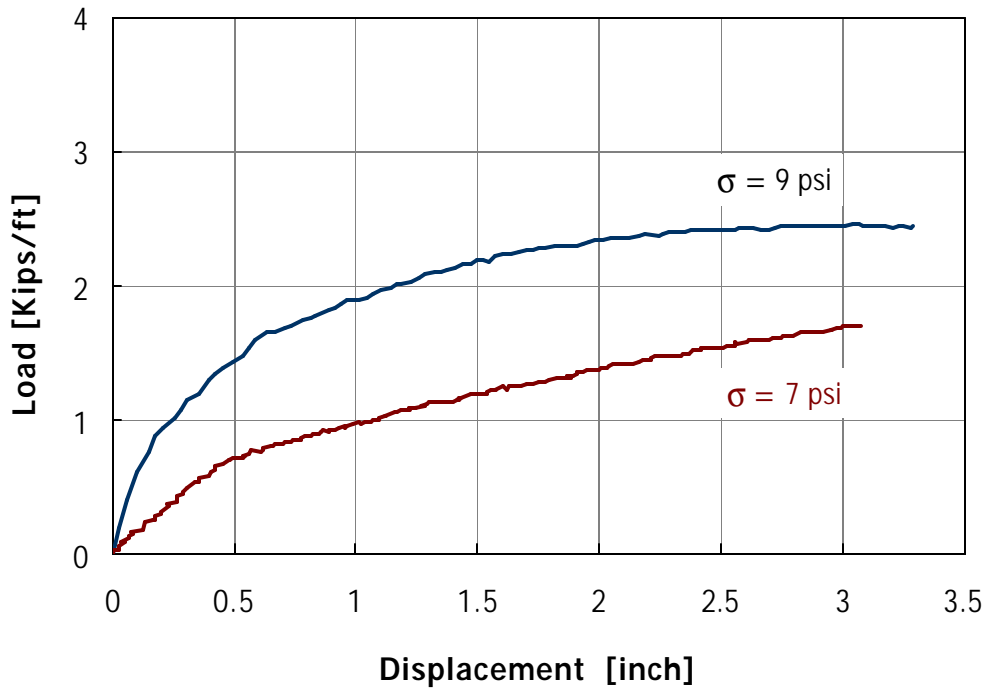


**Figure 67**  
Field pullout tests of the nonwoven of length 4 ft.

## Analysis of Pullout Test Results

### Evaluation of Pullout Coefficients

The pullout resistance of geosynthetics reinforcement equals the amount of shear strength along the length of the reinforcement and it is expressed in the form:

$$P_r = 2 t_a L_e \quad (3)$$

where  $P_r$  is the pullout resistance for unit width of the geosynthetics,  $t_a$  is the apparent shear strength at the interface, and  $L_e$  is the developed length of the reinforcement resisting the pullout force. Figure 68 shows a schematic of the forces in the geogrid specimen during pullout. The shear strength at the interface is calculated from the relationship:

$$t_a = s_v \tan d_a + C_a \quad (4)$$

where  $s_v$  is the normal stress at the reinforcement level,  $d_a$  is the apparent soil-reinforcement interface friction angle, and  $C_a$  is the apparent soil cohesion at the interface. Equations 3 and 4 result in an equation of the pullout resistance per unit width in the form:

$$P_r = 2 (s_v \tan d_a + C_a) L_e \quad (5)$$

Equation 5 can be written in terms of the soil shear strength parameters  $\phi$  and  $C$  in the form:

$$P_r = 2 C_i (s_v \tan j + C) L_e \quad (6)$$

where  $j$  is soil friction angle,  $C$  is soil cohesion, and the  $C_i$  term is the pullout coefficient of interaction:

$$C_i = \frac{s_v \cdot \tan d + C_a}{s_v \cdot \tan j + C} \quad (7)$$

The coefficient of interaction  $C_i$  is also known as the Interaction Factor and it is obtained from laboratory and field pullout tests. It usually ranges from 0.6 to 1.0 for geosynthetic reinforcement.

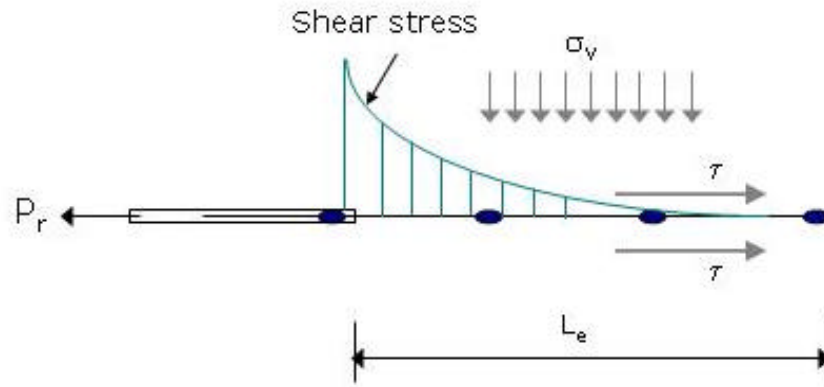


**Figure 68**  
**The mechanism of pullout in geogrid specimen**

The major concern of using equation 6 in the calculation of the geosynthetic pullout resistance pertains to the effect of the reinforcement extensibility on the pullout parameters. Inextensible reinforcement (such as metal strips) moves as a rigid member in the soil and develops a uniform shear strength distribution along its length. Meanwhile, the interface shear strength is not uniformly mobilized along the length of extensible geosynthetics. Accordingly, pullout resistance becomes a function of the specimen's length and extensibility. A correction factor, **a**, is introduced to account for such effect and the pullout equation is written in the form [6, 7]:

$$P_r = 2 F^* s'_v a L_e \quad (8)$$

where  $F^*$  = the pullout resistance factor. It is commonly taken as [6]:

$$F^* = 2/3 \tan j \quad \text{for geotextile reinforcement in granular soil}$$

$$F^* = 0.8 \tan j \quad \text{for geogrid reinforcement in granular soil}$$

And **a** = scale effect correction factor.

The scale effect correction factor **a** is a function of the nonlinearity of the pullout load along the length of the geosynthetic as shown in figure 68. For inextensible reinforcement, **a** is approximately 1.0 and it can be in the range of 0.6 to 0.8 for extensible reinforcement. In order to determine the scale effect, pullout resistance needs to be evaluated in tests with various reinforcement lengths.

Equation 8 can be used to estimate the pullout resistance of the geosynthetics providing that the coefficients  $F^*$  and  $\mathbf{a}$  are determined. Several empirical and theoretical methods have been proposed in order to determine these coefficients from pullout tests [25, 26].

The direct approach to determine the value of  $F^*$  coefficient is from direct shear tests with the geosynthetic specimen at the interface. The value of  $F^*$  can then be used with the results of the pullout test to calculate the coefficient  $\mathbf{a}$ .

The values of the pullout coefficients  $F^*$  and  $\mathbf{a}$  depend on the type of geosynthetic and its geometry, length, and confining pressure. The effect of these parameters is determined from the results of lab and field pullout tests.

### **Effect of Confining Pressure**

The results of laboratory and field pullout tests were used to calculate the coefficients  $F^*$  and  $\mathbf{a}$  for 3-ft.-long specimens and at various confining pressures. Equation 8 was used to determine the multiplier of the coefficients ( $F^* \cdot \mathbf{a}$ ) since both coefficients are a function of the reinforcement extensibility and geometry. The effect of confining pressures on the pullout coefficients is shown in figures 69 to 75 for the various types of geosynthetics in the testing program. The results show that an increase in confining pressure results in a decrease in the pullout coefficients. Flexible geogrids and geotextiles had comparable coefficients from field and lab results. The coefficient multiplier ( $F^* \cdot \mathbf{a}$ ) ranged from 0.4 to 0.7 for the flexible geogrids (Tensar UX-750 and Stratagrid-500) and the woven geotextiles. For the nonwoven geotextile, the coefficient was about 0.25 and was less dependent on the confining pressure. For the rigid geogrids (Tensar UX-1500 and Tensar UX-1700), the pullout coefficient multiplier ( $F^* \cdot \mathbf{a}$ ) was higher from field pullout results than from lab results.

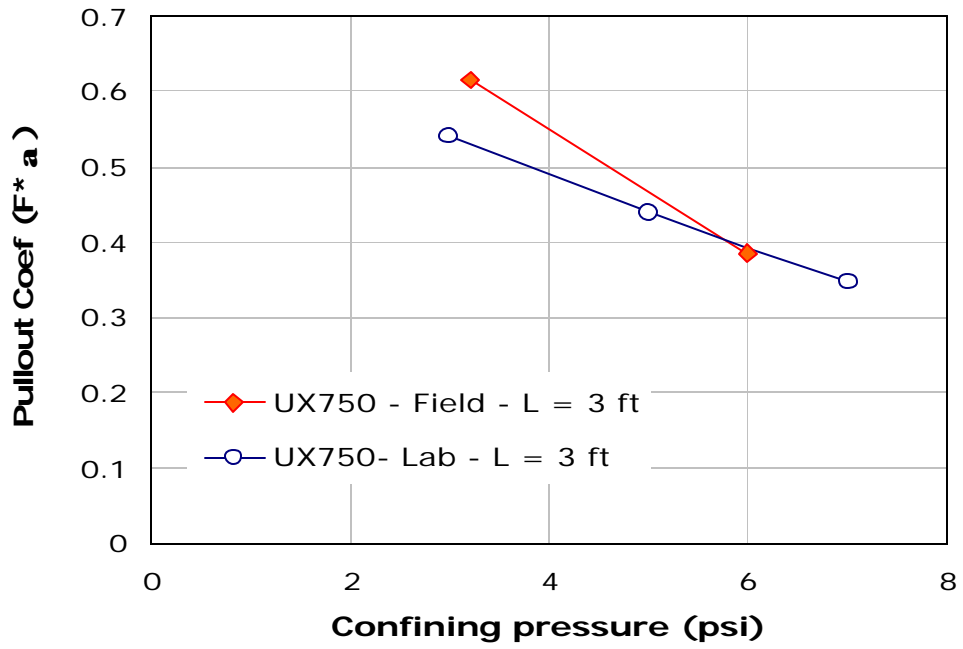


**Figure 69**  
**Pullout coefficient ( $F^*a$ ) for the Tensar UX-750**

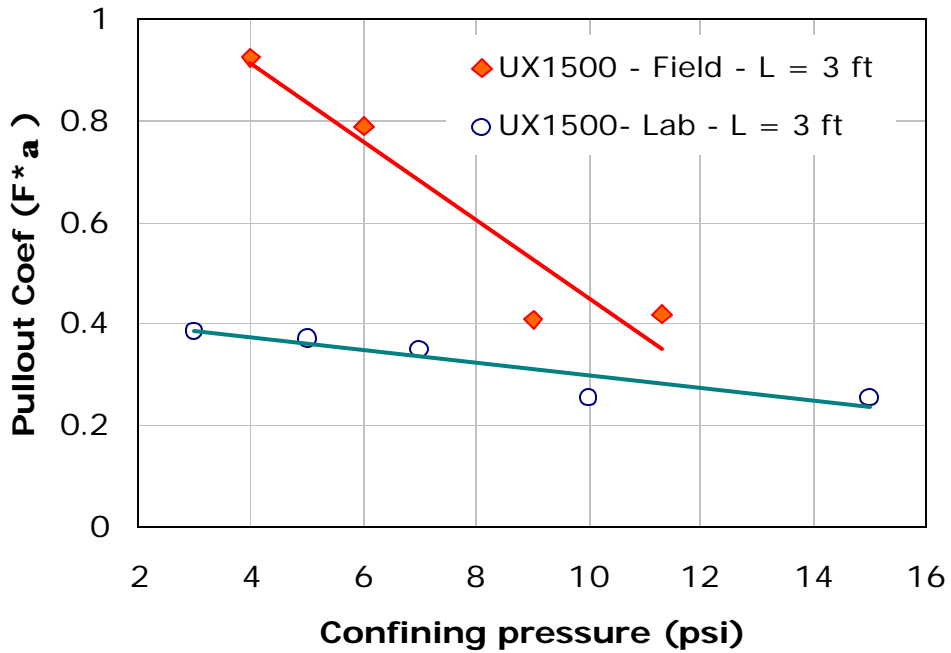


**Figure 70**  
**Pullout coefficient ( $F^*a$ ) for the Tensar UX-1500**

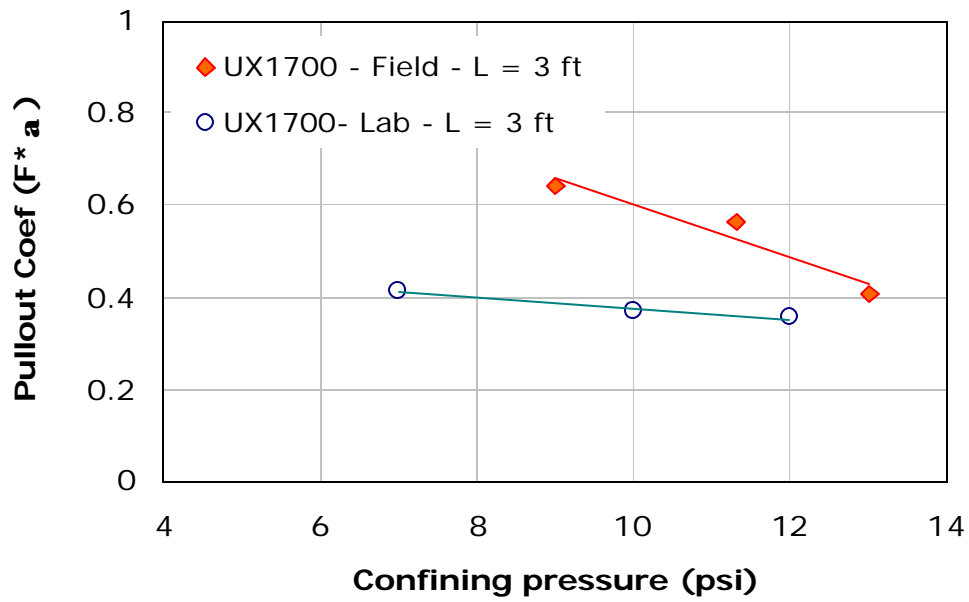


**Figure 71**  
**Pullout coefficient ( $F^*a$ ) for the Tensar UX-1700**

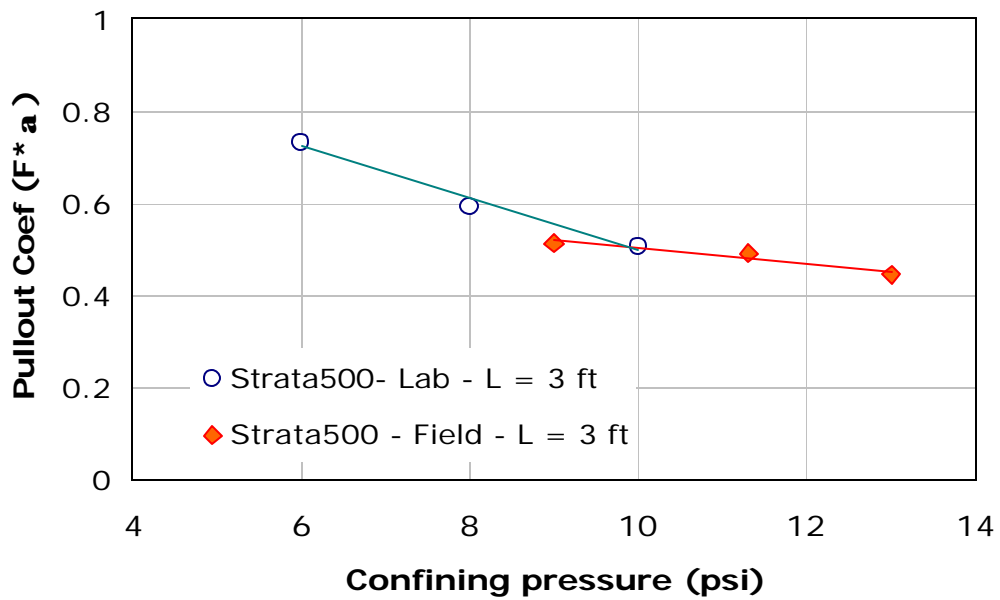


**Figure 72**  
**Pullout coefficient ( $F^*a$ ) for the Stratagrid-500**

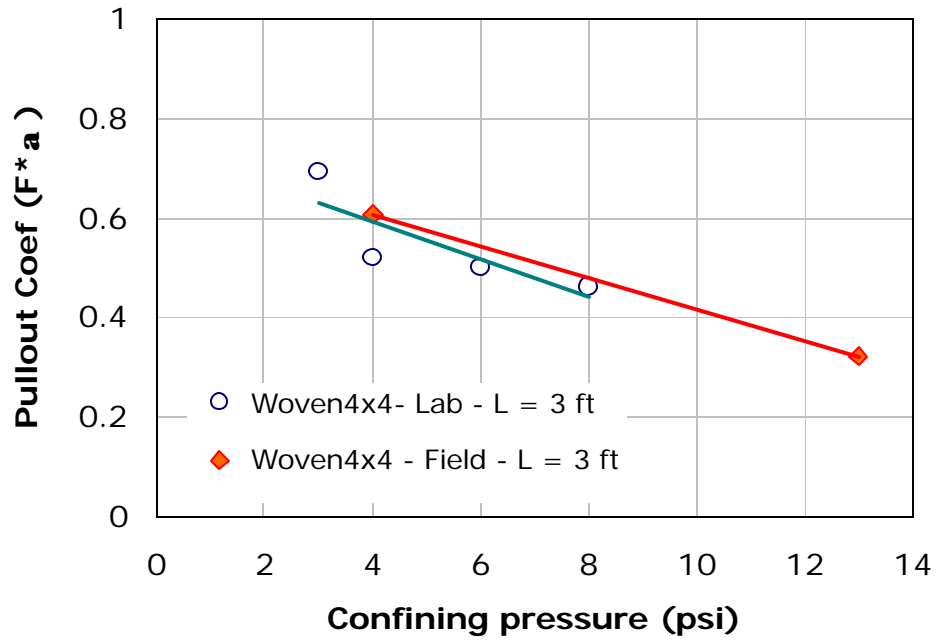


**Figure 73**  
**Pullout coefficient ( $F^*a$ ) for the woven Geotex 4 x4**

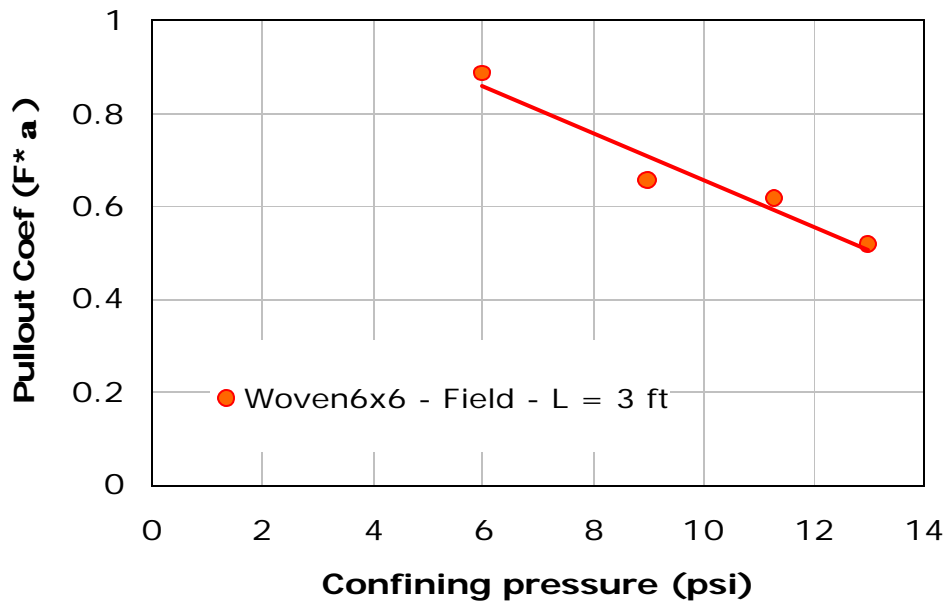


**Figure 74**  
**Pullout coefficient ( $F^*a$ ) for the woven Geotex 6x6**

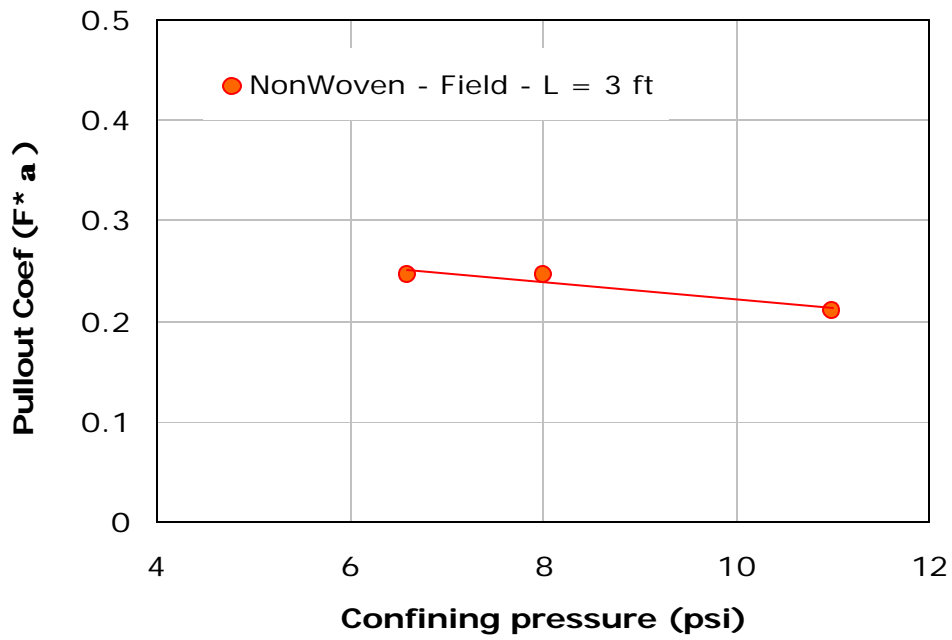


**Figure 75**  
**Pullout coefficient ( $F^* a$ ) for the nonwoven geotextile**

### **Effect of Specimen Length**

The results of field pullout tests at various specimen lengths were used to calculate the pullout coefficient multiplier ( $F^* a$ ) from equation 8. The results in figures 76 to 81 show the pullout coefficients for the various geosynthetic materials. An increase in the specimen length results in a decrease in the pullout coefficient.

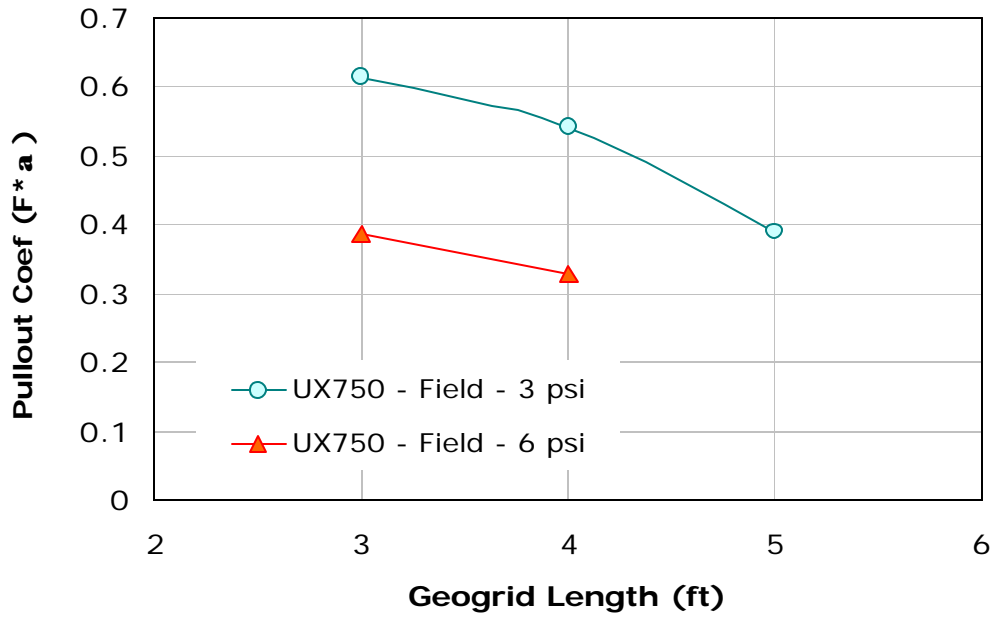


**Figure 76**  
**Pullout coefficient ( $F^*a$ ) for the UX-750**

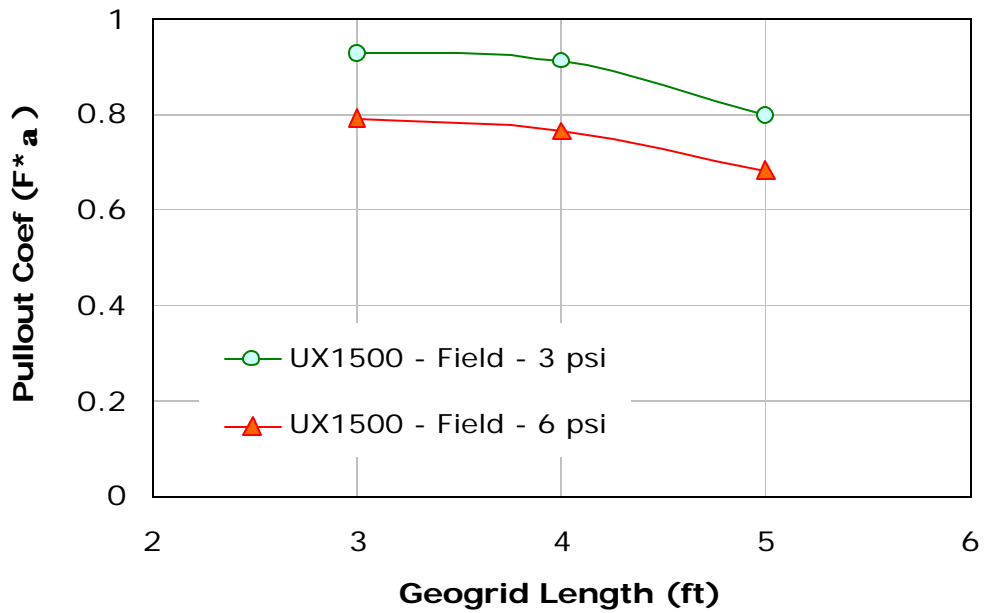


**Figure 77**  
**Pullout coefficient ( $F^*a$ ) for the UX-1500**

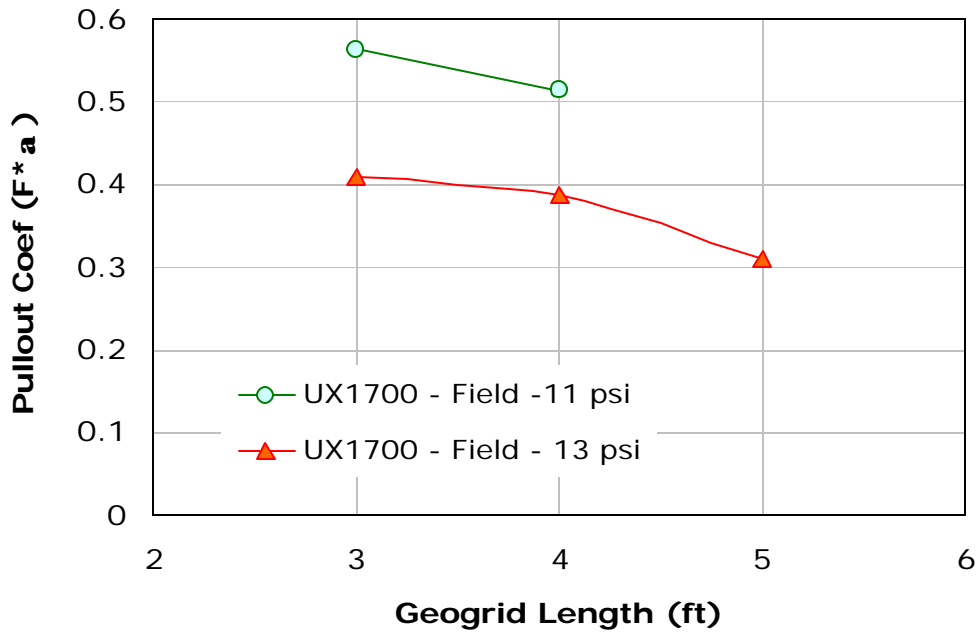


**Figure 78**  
 Pullout coefficient ( $F^*a$ ) for the UX-1700

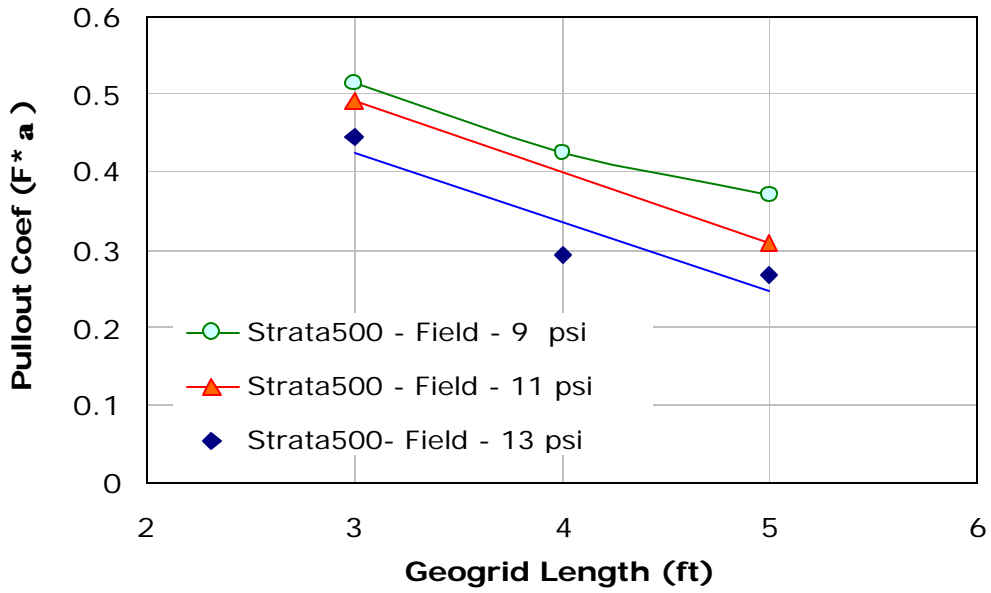


**Figure 79**  
 Pullout coefficient ( $F^*a$ ) for the Stratagrid-500

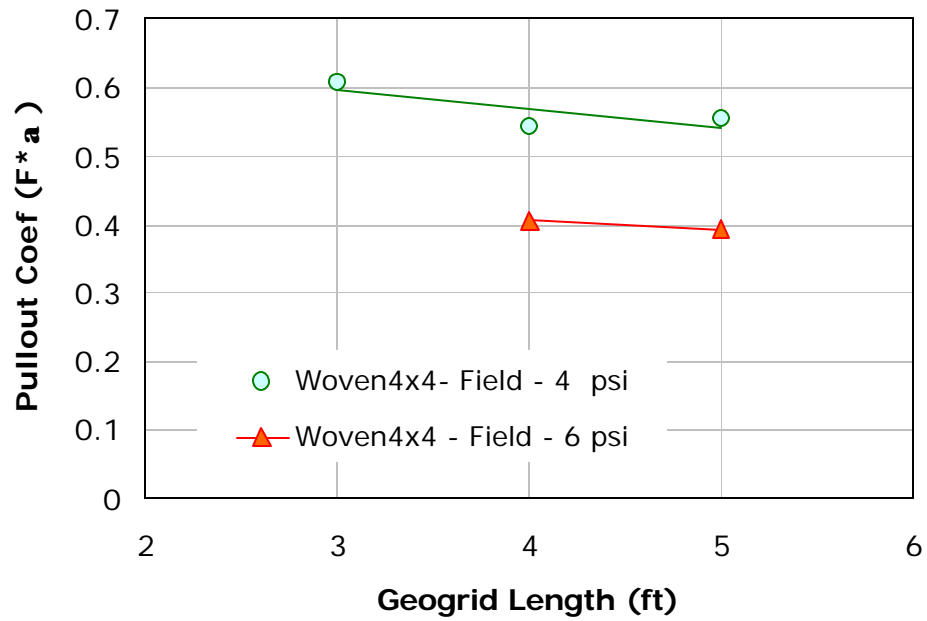


**Figure 80**  
**Pullout coefficient ( $F^*a$ ) for the woven Geotex 4x4**

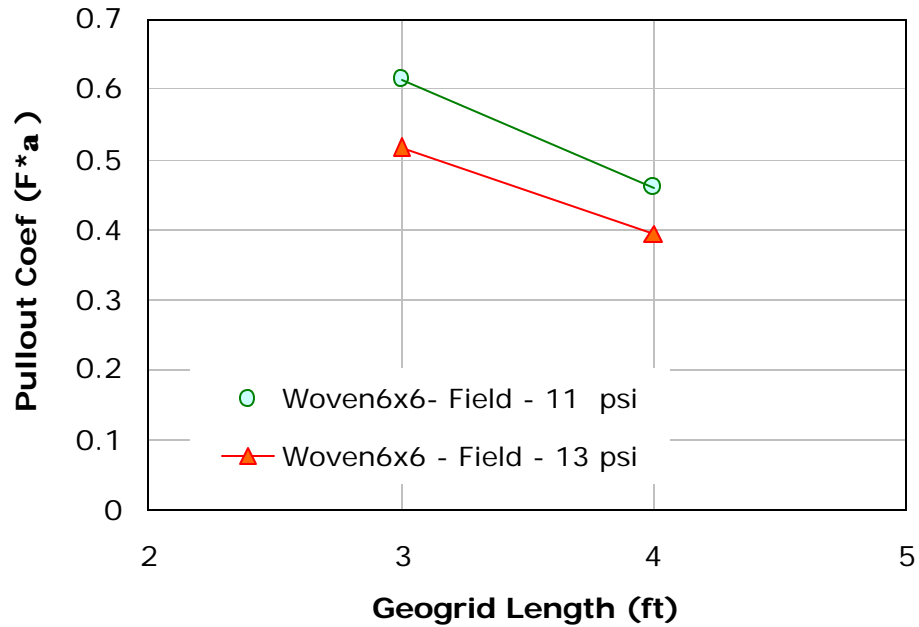


**Figure 81**  
**Pullout coefficient ( $F^*a$ ) for the woven Geotex 6x6**

### Effect of Reinforcement Extensibility

The confined extension modulus of the geogrid and geotextile specimens can be calculated at the front element at the early stages of pullout. Figure 82 shows a schematic of the first element of the geogrid specimen. Displacements are measured at the front ( $Displ_0$ ) and at the first cross-rib of the geogrid ( $Displ_1$ ). The movement at the first cross-rib indicates that the shear strength is mobilized along the full length of the first element and the confined modulus is calculated from the equation:

$$Et_{(conf.)} = \frac{(F_0 - F_1)/b}{(Displ_0 - Displ_1)/L_1} \quad (9)$$

where  $Et_{(conf.)}$  is the confined elastic modulus at the first element,  $F_0$  and  $Displ_0$  are the pullout load and displacement at the front, respectively,  $F_1$  and  $Displ_1$  are the load and displacement at the first cross-rib,  $b$  is the width of the element, and  $L_1$  is the length of the element. The load  $F_1$  was assumed zero when  $Displ_1$  is 0.1 in. This value insures that the shear strength is fully mobilized along the length of the first element.

The calculations of  $Et_{(conf.)}$  for the various types of geosynthetics are shown in figures 83 to 87. The figures show that the modulus at the first element is slightly higher than the unconfined modulus of the material and its value increases with increased confining pressure.

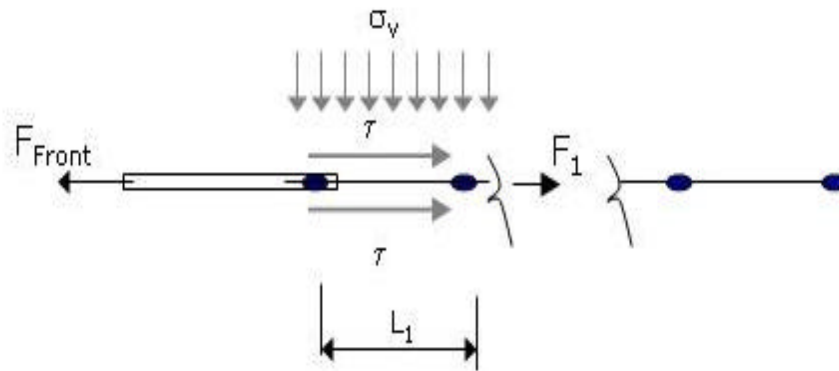


**Figure 82**  
**Schematic of the forces at the first element**

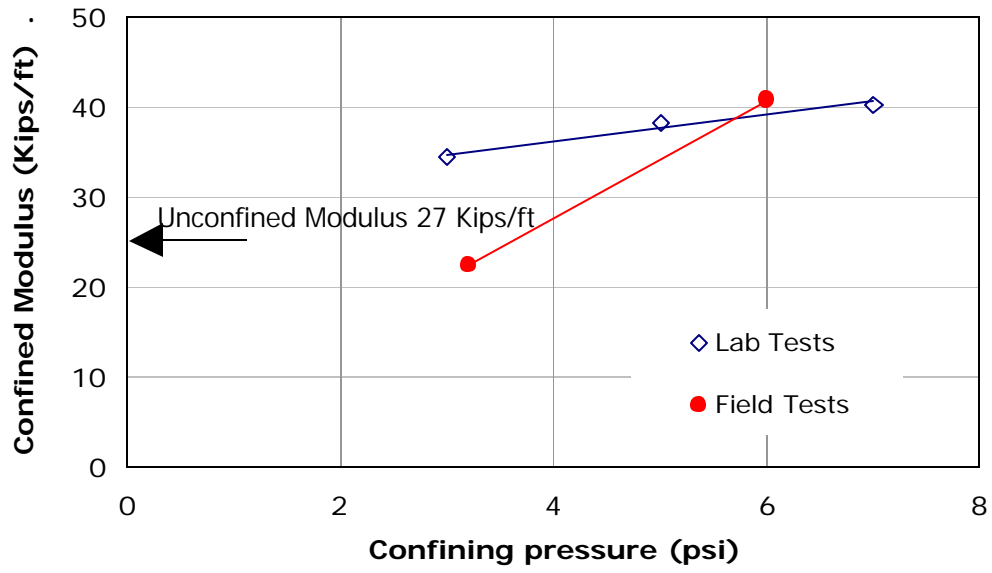


**Figure 83**  
**Confined extension modulus of the UX-750**

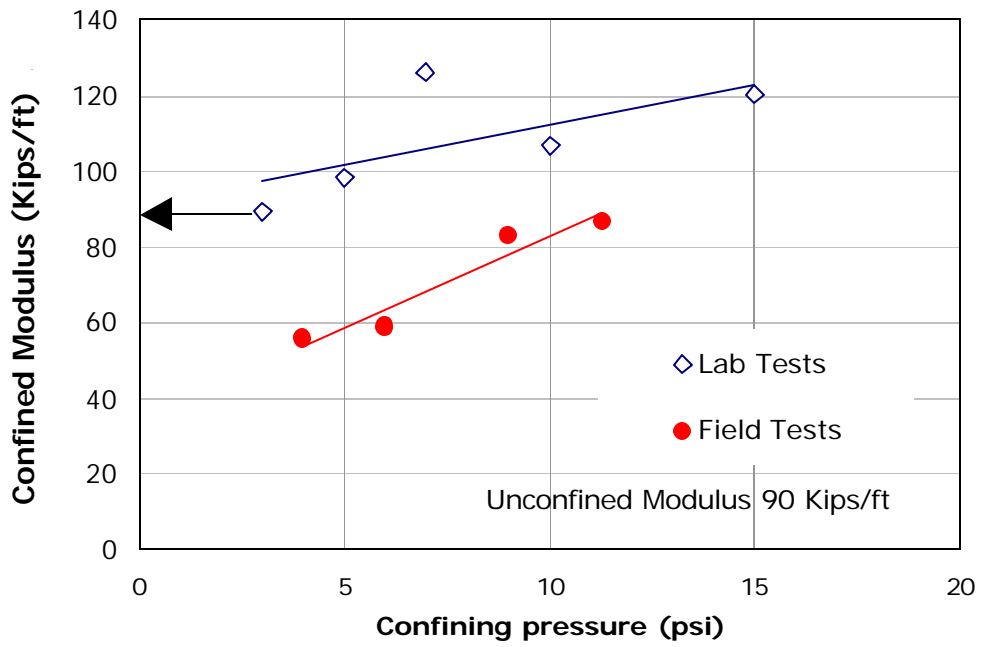


**Figure 84**  
**Confined extension modulus of the UX-1500**

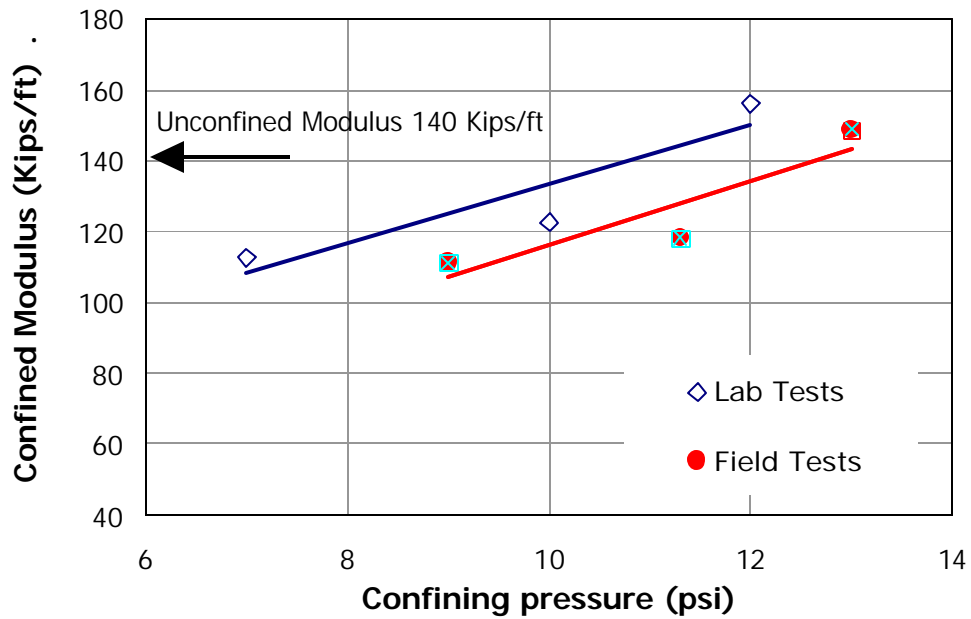


**Figure 85**  
**Confined extension modulus of the UX-1700**

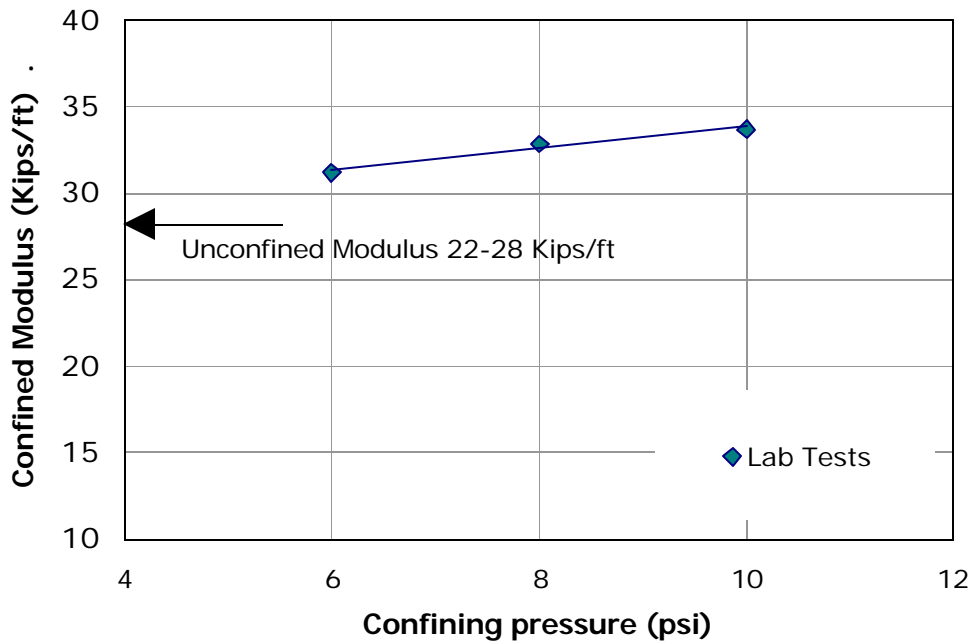


**Figure 86**  
**Confined extension modulus of the Stratagrid-500**

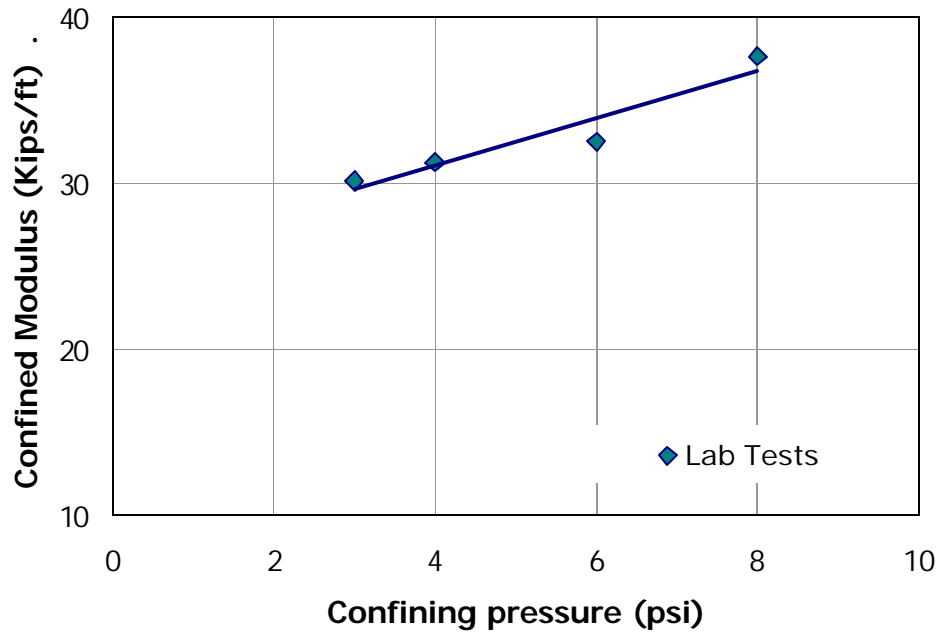


**Figure 87**  
**Confined extension modulus of the woven Geotex 4x4**



## CONCLUSIONS

The report presents the results of laboratory and field pullout tests on various types of geogrids and geotextiles. Laboratory pullout tests were carried out in a large pullout testing device. Field pullout tests were performed in a test section of the LTRC full-scale reinforced test wall. The testing program evaluated the effect of reinforcement type, length, and confining pressure on the pullout resistance.

Laboratory pullout tests were performed on 3-ft.-long x 1-ft.-wide specimens, while field tests were performed on specimens of 3 ft., 4 ft., and 5 ft. lengths with 1 ft. width. Field and lab test results were compared for the 3-ft. specimen length.

Field and lab pullout tests compared well for flexible geogrids and geotextiles (Tensar UX-750, Stratagrid-500, and Geotex-4x4). However, pullout results in the field were significantly higher than lab results for rigid geogrids (Tensar UX-1500 and UX-1700). Field test results on the rigid geogrids also showed that the strains at the front elements were higher and the pullout resistance was not fully mobilized along the whole length of the specimens.

Pullout tests were performed a few months after the construction of the wall. The consolidation of the silty clay soil underneath the wall and soil drying may have resulted in field density and moisture that are different from the lab values. Because rigid geogrids get a high percentage of their pullout resistance from the passive bearing resistance of their thick cross ribs in comparison to the thin geogrids, the effect of the changes in soil confinement and density between the lab and the field are more significant in the rigid geogrids.

Pullout tests in the field showed that longer specimens had higher pullout resistance. However, the effect of specimen length is not as significant as confining pressures. The increase of pullout load resulting from an increase in the specimen length was also insignificant at the early stages of the tests. This is due to the fact that shear strength progressively develops along the specimen length and the effect of specimen length is only recognized near the peak loads.

As the interface shear resistance is not uniform along the geosynthetics, pullout resistance becomes a function of specimen length and extensibility. The pullout coefficients  $F^*$  and  $\mathbf{a}$  are commonly used with equation 8 in order to account for the uniformity of the shear stress distribution and the scale effect of the specimen, respectively.

The direct approach to determine the value of  $F^*$  coefficient is from direct shear tests with the geosynthetic specimen at the interface. The value of  $F^*$  can then be used with the results of the pullout test to calculate the coefficient  $\mathbf{a}$ . However, the use of both parameters in the pullout equation does not necessitate their separation and the results of lab and field pullout tests were used to evaluate the combined effect of the  $(F^*\mathbf{a})$  parameters on the pullout resistance of the various geosynthetics.

The values of the pullout coefficient multiplier  $(F^*\mathbf{a})$  depend on the type of geosynthetic and its geometry, length, and confining pressure. The effect of these parameters was determined from the results of lab and field pullout tests. The coefficients decreased with the increase of confining pressure and specimen length, and they increased with the increase of reinforcement extensibility. Figures 69 to 87 can be used to estimate their values at various confining pressures and specimen lengths.

## RECOMMENDATIONS

Pullout tests can be used to determine the interface parameters of geogrids and geotextiles in cohesive soils. Laboratory pullout tests should be performed in testing conditions identical to the ones in the field since the results are highly dependent on soil confining pressure, density, moisture content, and geosynthetic types.

Laboratory pullout test results compared well with field pullout test results for flexible geogrids and geotextiles. Results of field tests were higher than lab tests for the rigid geogrids. This may be due to the effect of changes in soil confinement and density between the lab and the field.

The results can be used to determine the pullout coefficient of interaction  $F^*$  and the scale effect correction factor  $\alpha$ . These coefficients are used in the internal stability analysis of reinforced soil structures according to the FHWA design procedures.

The combined multiplier factor ( $F^* \alpha$ ) was used to incorporate the combined effect of reinforcement geometry and extensibility. The effect of soil confining pressure, geosynthetic length, and stiffness can be evaluated from figures 69 through 87 for the types of geogrids and geotextiles used in the testing program.



## REFERENCES

1. Farrag, K., and Morvant, M. *Evaluation of Interaction Properties of Geosynthetics in Cohesive Soils: LTRC Reinforced-Soil Test Wall*, Louisiana Transportation Research Center, Report Number 379, 2003.
2. Perkins, S., and Guelho, E., Soil-Geosynthetic Interface Strength and Stiffness Relationships from Pullout Tests,” *Geosynthetics International*, Vol. 6, No. 5, 1999, pp.321-346.
3. Yuan, Z., and Chua, K., “Analytical Model for Pullout of Soil Reinforcement,” *Transportation Research Board*, TRR No. 1330, pp.64-71.
4. Juran, I.; and Chen, C., “Soil-Geotextile Pullout Interaction Properties, Testing and Interpretation,” *Transportation Research Board*, TRR No. 1188, pp. 37-46.
5. Madhav, M.R.; Gurung, N.; and Iwao, Y., “A Theoretical Model for the Pullout Response of Geosynthetics Reinforcement,” *Geosynthetics International*, Vol. 5, No. 4, 1998, pp.399-424.
6. FHWA, *Mechanically Stabilized Earth Walls and Reinforced Soil Slopes, Design and Construction*, Federal Highway Administration, Report No. FHWA-SA-96-071, 1997.
7. FHWA, *Geosynthetics Design and Construction Guidelines*, Federal Highway Administration, Report No. FHWA HI-95-038, 1998.
8. Lafleur, J.; Sall, M.S., and Ducharme, A., “Frictional Characteristics of Geotextiles with Compacted Lateritic Gravels and Clays,” *Geosynthetics' 87*, New Orleans, 1987, pp. 205-215.
9. Brand, S.R., and Duffy, D.M., “Strength and Pull-out Testing of Geogrids,” *Geosynthetics' 87*, New Orleans, 1987, pp. 226-236.
10. Williams, N.D., and Houlihan, D.M., “Evaluation of the Interface Friction Properties between Geosynthetics and Soils,” *Geosynthetics' 87*, New Orleans, 1987, pp. 616-627.
11. Saxena, S.K., and Budiman, J.S., “Interface Response of Geotextiles,” *11th International Conference on Soil Mechanics and Foundation Engineering*, San Francisco, 1985, pp. 1801-1804.

12. Degoutte, G., and Mathieu, G., "Experimental Research of Friction Between Soil and Geomembranes or Geotextiles Using a 30x30 cm<sup>2</sup> Shear Box," *3rd International Conference on Geotextiles*, Vienna, 1986, pp. 1251-1255.
13. Fourie, A.B., and Fabian, K.J., "Laboratory Determination of Clay-Geotextile Interaction," *Geotextiles and Geomembranes*, Vol. 6, No. 4, 1987, pp. 275-294.
14. Richards, E.A.; Scott, J.D.; Bobey, L.W.; and Diyaljee, V., "Shear Resistance between Cohesive Soil and Geogrids," *Geosynthetics'89*, San Diego, 1989, pp. 489-500.
15. Bergado, D.T.; Bukkanasuta, A.; and Balasubramaniam, A., "Laboratory Pull-out Tests Using Bamboo and Polymer Geogrids Including a Case Study," *Geosynthetics and Geomembranes*, Vol. 5, 1987, pp. 153-189.
16. Ingold, T.S., "A Laboratory Simulation of Reinforced Clay Walls," *Geotechnique*, Vol. 31, No. 3, 1981, pp. 339-412.
17. Ingold, T.S., "A Laboratory Investigation of Geogrid Reinforcement in Clay," *Geotechnical Testing Journal*, ASTM, Vol. 6, No. 3, 1983, pp. 112-119.
18. Chang, J.; Hannon, J.B.; and Forsyth, R.A., "Pull Resistance and Interaction of Earthwork Reinforcement and Soil," *Transportation Research Record No. 640*, 1977, pp. 1-7.
19. Bergado, D.T.; Hardiyatimo, H.C.; Cisneros, C.B.; Chun, C.J.; Alfaro, M.C.; Balasubramaniam, A.; and Anderson, L.R., "Pull-out Resistance of Steel Geogrids with Weathered Clay as Backfill Material," *Geotechnical Testing Journal*, ASTM, Vol. 15, No. 1, (1992), pp. 33-46.
20. Bauer, G.E.; Halim, A.; and Shang, Q.; "Large-Scale Pullout Tests: Assessment of Procedure and Results," *Geosynthetics'91*, Atlanta, 1991, pp. 615-628.
21. Chua, K.M., Aspe, W., and De La Rocha, A., "Simulating Failures of Geosynthetics-Reinforced Earth Structures Under Saturated Conditions," *Geosynthetics'93*, Vancouver, 1993, pp. 417-430.
22. Farrag, K., and Griffin, P., "Pull-out Testing in Cohesive Soils, Geosynthetic Soil Reinforcement Testing Procedures," *ASTM STP No. 1190*, 1993, pp. 76-89.
23. Farrag, K., "Effect of Moisture Content on the Interaction Properties of Geosynthetics," *Geosynthetics'95 Conference*, Nashville, 1995, pp 1031-1041.

24. Farrag, K.; Juran, I.; and Acar, Y., "Pullout Testing Facility for Geosynthetics, Louisiana Transportation Research Center," *Report No. FHWA/LA-92-240*, 1992
25. Ochiai, H., Otani, J., Hayashic, S. and Hirai T., "The Pull-out Resistance of Geogrids in Reinforced Soil," *Geotextiles and Geomembranes*, Vol. 14, 1996, pp 19-42
26. Chen, R.H. and Lee, Y.S., "A Model for the Ultimate Pull-out Resistance of Geogrids," *Geosynthetics '98*, 1998, pp 721-724.

